Assessment of subclinical cardiac changes in structure and function by cardiovascular magnetic resonance

Peter Paranthaman Louis Swoboda

Submitted in accordance with the requirements for the degree of Doctor of Philosophy (PhD)

The University of Leeds

Division of Cardiovascular and Diabetes Research

Leeds Institute of Cardiovascular and Metabolic Medicine

School of Medicine

October 2015

Intellectual property and publication statements

The candidate confirms that the work submitted is his own, except where work which has formed part of jointly-authored publications has been included. The contribution of the candidate and the other authors to this work has been explicitly indicated below. The candidate confirms that appropriate credit has been given within the thesis where reference has been made to the work of others.

Chapter 1 includes content from the following peer-reviewed publication:

Swoboda PP, Plein S. Established and emerging cardiovascular magnetic resonance techniques for prognostication and guiding therapy in heart failure. Expert Rev Cardiovasc Ther. 2014 Jan;12(1):45-55.

Author contributions: Literature research, PPS; Guarantors of integrity of entire study PPS, SP; manuscript drafting or manuscript revision for important intellectual content, PPS, SP; approval of final version of submitted manuscript, PPS, SP.

Publications arising from this work

Papers

Swoboda PP, Plein S. Established and emerging cardiovascular magnetic resonance techniques for prognostication and guiding therapy in heart failure. Expert Rev Cardiovasc Ther. 2014 Jan;12(1):45-55.

Oral abstracts

Swoboda PP, McDiarmid AK, Erhayiem B, Dobson LE, Musa TA, Ripley DP, Garg P, Ajjan R, Greenwood JP and Plein S. Cardiovascular magnetic resonance assessment of left ventricular morphology to investigate the mechanisms of heart failure associated with Type 2 diabetes Diabetic Medicine 2015, 32 (Suppl. 1), 17-18

Swoboda PP, McDiarmid AK, Erhayiem B, Dobson LE, Musa TA, Ripley DP, Garg P, Ajjan R, Greenwood JP and Plein S. Cardiovascular magnetic resonance assessment of ventricular morphology to investigate the mechanisms of heart failure associated with type 2 diabetes Journal of Cardiovascular Magnetic Resonance 2015, 17(Suppl 1):O82 (3 February 2015)

Acknowledgements

Abstract

Background

The early identification of disease can benefit patients clinically and provide a powerful research tool. This thesis aims to identify subclinical cardiac change using cardiovascular magnetic resonance (CMR) in both disease and health and evaluate its diagnostic and prognostic uses.

Methods

We have prospectively recruited and conducted multi-parametric CMR in 50 patients with hypertrophic cardiomyopathy (HCM), 40 endurance athletes and 100 asymptomatic patients with type 2 diabetes mellitus.

Results

Study 1 and 2 evaluated CMR in the early diagnosis of HCM. Study 1 demonstrated the diagnostic accuracy of extracellular volume (ECV) mapping is superior to volumetric methods of differentiating HCM from athletic left ventricular (LV) hypertrophy. Study 2 demonstrated that ECV expansion could be detected prior to overt hypertrophy or impairment of contractile function in patients with HCM. Study 3 demonstrated that LV torsion is lower in endurance athletes than controls and is predominantly influenced by lactate threshold and intensity of training. Study 4 and 5 investigated the role of CMR in identifying patients with type 2 diabetes at risk of heart failure and silent myocardial infarction. Study 4 found that the increased risk of heart failure in patients with type 2 diabetes was mediated by ECV expansion and diffuse fibrosis. There was a high rate of silent myocardial infarction (17 %) which was unrelated to heart failure risk. In study 5 we developed a simple screening tool, using measures that can be carried out in a cardiology clinic, for the detection of silent myocardial infarction in type 2 diabetes.

Conclusions

CMR is able to detect subclinical change in both tissue characteristics and function of the heart. This can aid the early and appropriate diagnosis of disease and identify those at the highest risk of adverse outcomes.

Table of contents

Figures

Tables

Abbreviations

ACR	Albumin creatinine ratio
AUC	Area under the curve
CMR	Cardiovascular magnetic resonance
CPX	Cardiopulmonary exercise testing
DCM	Dilated cardiomyopathy
ECG	Electrocardiogram
ECV	Extracellular volume
EDSR	Early diastolic strain rate
EDV	End diastolic volume
EDVI	End diastolic volume indexed to BSA
EER	Endo-to-epicardial perfusion ratio
EF	Ejection fraction
eGFR	Estimated glomerular filtration rate
ESV	End systolic volume
FT	Feature tracking
GLS	Global longitudinal strain
HCM	Hypertrophic cardiomyopathy
HS-CRP	High sensitivity C reactive protein
HS-cTnT	High sensitivity cardiac troponin T
ICD	Implantable cardioverter-defibrillator
LDSR	Late diastolic strain rate
LGE	Late gadolinium enhancement
LT	Lactate threshold
LV	Left Ventricle
LVMI	Left ventricle mass indexed to BSA
LVOT	Left ventricle outflow tract
MACE	Major adverse cardiovascular events
MBF	Myocardial Blood Flow
MOLLI	Modified Look-Locker inversion recovery
NT-proBNP	Amino-terminal pro-brain natriuretic peptide

ROC   Receiver operating characteristic

RV   Right ventricle

SMI   Silent myocardial infarction

SPAMM   Spatial modulation of magnetization

SPECT   Single-photon emission computed tomography

SSFP   Steady-state free precession

SSR   Systolic strain rate

T1   T1 tissue relaxation time

TDI   Tissue Doppler imaging

VO$_2$max   Maximal oxygen uptake

1.   Introduction

Cardiovascular disease is the now the largest cause of death worldwide (Mortality and Causes of Death, 2015). Advancements in blood pressure control and smoking cessation are leading to improving primary prevention globally. However even if all international targets are met it is estimated that 5.7 million preventable cardiovascular deaths will occur each year (Roth et al., 2015).

Advances in primary prevention are imperative to reduce the burden of cardiovascular disease and will continue to be a fundamental method for reducing mortality. Screening for subclinical disease offers an additional method to identify those at the highest risk of mortality and offer targeted interventions (Berger et al., 2010). In order to justify focussing resources on screening for those at the highest risk the disease has to be important, have a latent period and have a suitable diagnostic test (Wilson and Jungner, 1968). Furthermore the disease has to be treatable in the early phases so disease progression or the risk of mortality can be reduced, Figure 1.1.

Risk of sudden death

| Predisposition | Asymptomatic phenotypic expression | Symptomatic phenotypic expression | Death |

- Genetic factors
- Lifestyle factors
- Screening for subclinical disease
- Medical intervention
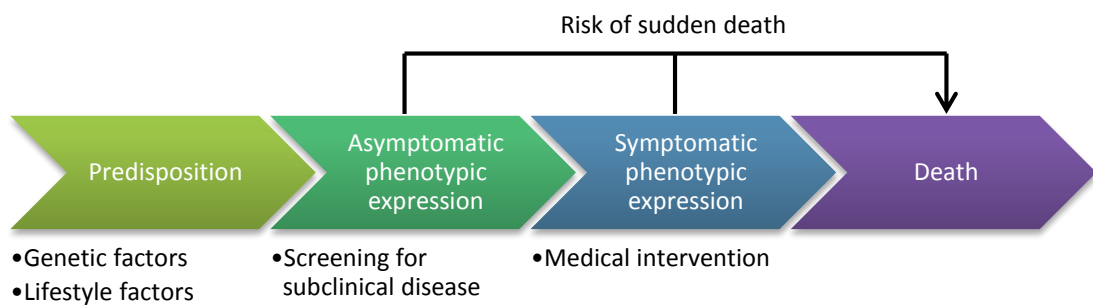
Figure 1.1 Schematic depicting the progression of cardiovascular disease from predisposition to death. For detection of subclinical disease in the asymptomatic prodrome to be beneficial it has to be possible to alter the risk of disease progression or mortality.

Cardiovascular magnetic resonance (CMR) has potential to be an important tool for the identification of subclinical cardiac disease. It is able to make accurate and reproducible assessment of ventricular morphology, tissue composition and function on both a global and regional level. There are many disease processes that

lead to alteration in the morphology, tissue characteristics and function of the heart. Identifying these changes early can ensure prompt diagnosis and timely intervention. The focus of this thesis is three important areas of cardiovascular medicine in which there are known to be morphological cardiac changes but identification of the diagnosis, particularly in the subclinical stage can be challenging. These are hypertrophic cardiomyopathy (HCM) and in particular how CMR can be used to diagnose it appropriately early in the disease progression; athletic remodelling of the heart which can be difficult to differentiate from HCM or dilated cardiomyopathy (DCM); and subclinical asymptomatic cardiac disease secondary to type 2 diabetes mellitus. The basic principles of CMR assessment of cardiac structure, function and tissue characterisation are discussed in detail before an appraisal of how each of these techniques can be applied to the areas investigated in this thesis.

1.1 CMR techniques used in the detection of subclinical change

A typical CMR study takes between 30 and 60 minutes and typically includes T1 weighted black blood images for assessment of anatomy, cine images in multiple planes for assessment of left ventricular (LV) and right ventricular (RV) volumes as well as late gadolinium enhancement (LGE) for delineation of scar and fibrosis (Figure 1.2). This basic protocol can be complemented with stress perfusion for ischaemia detection, T2-weighted imaging to detect myocardial oedema or T2* imaging for assessment of cardiac iron loading. Tissue tagging can be used for an assessment of regional or global strain and T1 mapping techniques can be used for assessment of the extracellular volume (ECV) fraction.
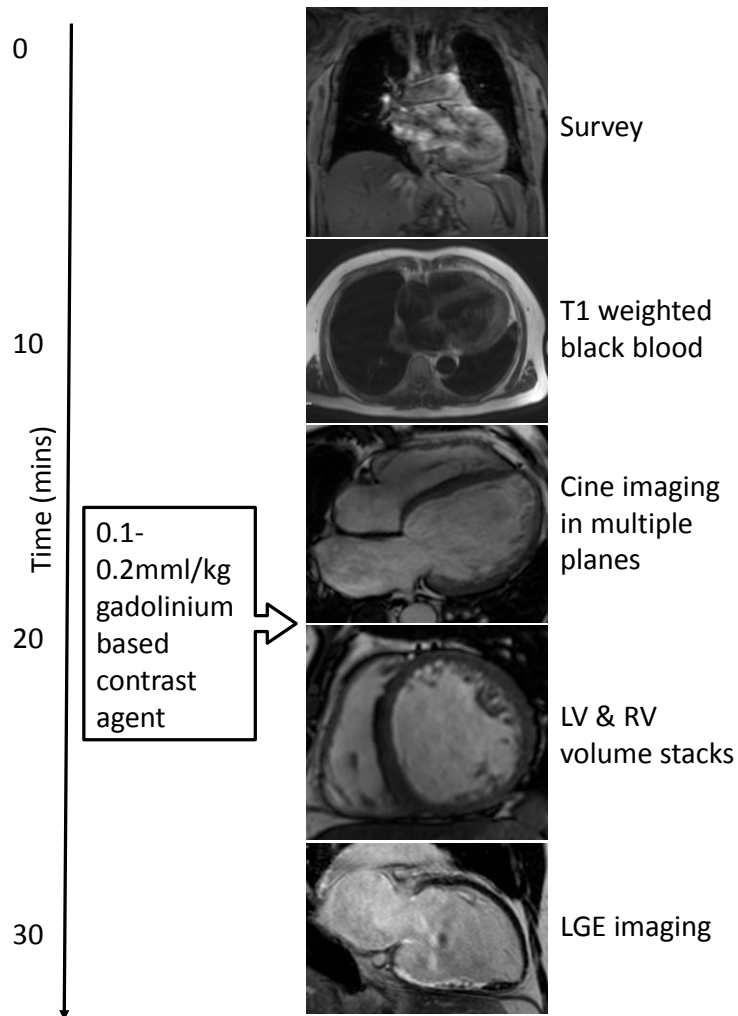
Figure 1.2 Typical flow chart of CMR protocol for the investigation of cardiomyopathy

1.1.1 Volumetric Analysis

Assessment of LV chamber volumes and ejection fraction (EF) forms the cornerstone of assessment of cardiac structure by CMR. Echocardiography is the most widely available and utilised non-invasive imaging modality for the assessment ventricular volumes. When suboptimal imaging quality does not allow for assessment of EF or more accurate assessment of EF is required, both American

(Yancy et al., 2013) and European (McMurray et al., 2012) guidelines recommend the use of CMR.

EF is usually measured by CMR with the acquisition of a two dimensional continuous stack of short axis gradient-echo cine images covering the length of the left ventricle (LV). The number of slices, and consequently the number of breath-holds, depends on the length of the ventricle and the chosen imaging parameters, in particular slice thickness and slice gap. In patients with poor breath-hold capacity, the acquisition can be shortened close to "real-time" with acceleration techniques (such as sensitivity encoding [SENSE], simultaneous acquisition of spatial harmonics [SMASH] and generalized autocalibrating partially parallel acquisitions [GRAPPA]), usually at the expense of signal-to-noise ratio, spatial or temporal resolution (Larkman and Nunes, 2007). The EF is typically calculated from these images by the "summation of discs" method (Utz et al., 1987). On each cine image within the stack, endocardial contours are drawn at end-systole and end-diastole. As the slice thickness is known, the volume of each disc can be calculated and by adding the volumes of each slice end-diastolic volume (EDV), end-systolic volume (ESV) and consequently EF can be calculated. This technique has been shown to be highly reproducible with interstudy reproducibility that is significantly better than two-dimensional echocardiography (Grothues et al., 2002). It has been estimated that to detect a 3% change in EF by echocardiography 87 patients are needed whereas only 11 patients are needed by CMR.

Measurement of EF by CMR can be used both to guide diagnosis and prognosis. It is well known that the degree of LV impairment is associated with adverse outcomes and increased mortality (Gradman et al., 1989; Unverferth et al., 1984). In the Candesartan in Heart Failure: Assessment of Reduction in Mortality and Morbidity (CHARM) study, each 10% decrease in EF below 45% was associated with a 39% increase in all-cause mortality (Solomon et al., 2005). For a more comprehensive assessment of prognosis, EF can also be incorporated as one of several factors in a risk score (Aaronson et al., 1997; Ketchum and Levy, 2011).

RV volumes and RV EF can also be calculated by CMR using the summation of discs method described above. Impaired RV function is associated with adverse outcomes in conditions that primarily affect the RV such as pulmonary arterial

hypertension and arrhythmogenic right ventricular cardiomyopathy (ARVC) (Valsangiacomo Buechel and Mertens, 2012) but also adds prognostic information in patients with heart failure. When assessed by CMR in patients with previous myocardial infarction (MI), RV EF <40% was associated with adverse outcomes independently of other factors including LV EF (Larose et al., 2007).

Atrial dimensions can be reproducibly measured by CMR using the summation of discs technique or from long axis cines (Maceira et al., 2010). Increased left atrial volume assessed by CMR has been shown to be a strong predictor of mortality in patients with heart failure (Gulati et al., 2013).

From the same continuous short axis LV stack used to measured EF LV mass can also be measured. Contours are drawn on the endocardial and epicardial borders at one point in the cardiac cycle, usually end diastole and the LV mass calculated using the summation of discs principle. It is possible in include or exclude papillary muscles with both techniques providing similar interobserver reproducibility (Han et al., 2009). Assessment of LV mass by this method has excellent interstudy reproducibility. It is estimated to detect a 10g change in LV mass using echocardiography 132 subjects would be needed compared with only 13 by CMR (Grothues et al., 2002).

Several cardiac diseases cause concentric remodelling of the LV which can be assessed by dividing LV mass by LV EDV. Concentric remodelling has been reported in diabetes and is associated with adverse outcomes (Heckbert et al., 2006; de Simone et al., 2008). This ratio has also been proposed as a method to differentiate athletic remodelling of the LV from HCM (Luijkx et al., 2013).

1.1.2 Tissue characterisation

The currently used gadolinium based CMR contrast agents are exclusively extracellular and can only passively enter damaged cells with a leaky cell membrane. These contrast agents therefore accumulate in areas with damaged cells and avascular extracellular regions. This phenomenon is exploited in LGE CMR imaging. LGE imaging involves administration of typically 0.1-0.2mmol/kg of a gadolinium based contrast agent. After a delay of 5-20 minutes the contrast agent is retained to a greater extent in areas of scar or fibrosis than in normal

myocardium. An inversion recovery sequence with an inversion time specified to null "normal" myocardium then displays scarred myocardium as bright when compared to the reference. The pattern of enhancement on LGE can aid in the diagnosis of the aetiology of asymptomatic disease with characteristic appearances of LGE in many conditions (Mahrholdt et al., 2005). For example, subendocardial or transmural LGE is seen in ischemic cardiomyopathy, mid wall LGE in dilated and hypertrophic cardiomyopathies, epicardial LGE in myocarditis and global subendocardial LGE in amyloidosis (see examples in Figure 1.3). The presence of enhancement on LGE imaging is shown to correspond well with discrete fibrosis on histology and confers an adverse prognosis in many cardiomyopathies (Ismail et al., 2012).
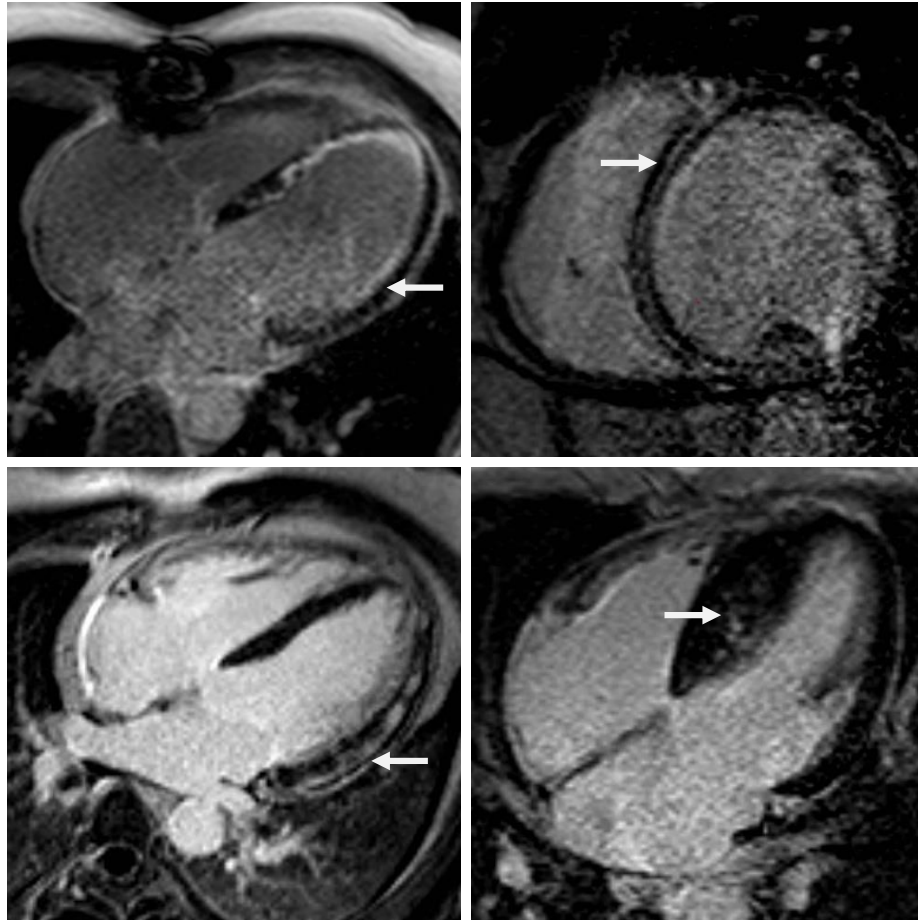
Figure 1.3 Typical distribution of LGE in various aetiologies of cardiomyopathy. Ischaemic cardiomyopathy (top left) near transmural infarction of the septum and apex and subendocardial infarction of the lateral wall (arrow), note the artefact secondary to sternomy wires. Dilated cardiomyopathy (top right) dilated ventricular chambers with midwall fibrosis (arrow). Myocarditis (bottom left) with subepicardial LGE of the lateral wall (arrow). Hypertrophic cardiomyopathy (bottom right) asymmetric septal hypertrophy with patchy midwall LGE within the hypertrophied septum (arrow).

Extracellular fibrosis is a common pathological finding in many aetiologies of heart failure. As described in the preceding section, CMR to assess LGE is a well-established method by which to assess and quantify the size and transmurality of discrete areas of fibrosis. However this process relies on nulling the healthy myocardium and on comparing the enhancement of healthy and diseased

myocardium qualitatively. When the myocardium is diffusely diseased, techniques that characterize the myocardium quantitatively provide additional insights into myocardial disease.

There has been renewed recent interest in methods that quantify the intrinsic T1 (Messroghli et al., 2004) and T2 (Verhaert et al., 2011) signal of the myocardium and create a map of their values. Native tissue maps alone can be used for tissue characterization or can be combined with post contrast acquisitions. Gadolinium-based contrast agents shorten in particular the T1 relaxation time and tissues with an expanded extracellular space due to fibrosis, infiltration or scar have a larger distribution volume for the extracellular contrast agent. In these tissues, the reduction in T1 relaxation time is therefore more pronounced than in normal tissue and is correlated with the extent of the extracellular space. Post-contrast myocardial T1 has been shown to significantly correlate with histological areas of fibrosis (Iles et al., 2008).

Post contrast T1 mapping makes assumptions about the kinetics of gadolinium contrast agents and the results can be influenced by renal function, haematocrit and body composition. These assumptions can be overcome by combining pre and post contrast T1 mapping of both myocardium and blood and correcting for the blood volume of distribution (1-haematocrit). From these data, maps of the ECV fraction can be calculated which show significant correlation with histological degree of fibrosis and volume of collagen in the myocardium (Flett et al., 2010). ECV is calculated using the formula:

$$ECV = (1 - Hct)\frac{R1(myo\ pre) - R1(myo\ post)}{R1(blood\ pre) - R1(blood\ post)} \qquad where\ R1 = 1/T1$$

Lengthened pre-contrast T1 times, shortened post-contrast T1 times and increased ECV have been reported in several cardiomyopathies including amyloidosis, DCM and HCM (Dass et al., 2012; Puntmann et al., 2013; Sado et al., 2012).

In the largest CMR study of ECV to date, T1 mapping was carried out in 793 patients at the time of CMR being done for clinical purposes (36% were for known or suspected cardiomyopathy, 35% for known or suspected IHD and 26% to

identify a substrate for arrhythmia) (Wong et al., 2012). Patients with HCM or amyloidosis were excluded. Over median follow up 0.8 years ECV related to all-cause mortality (hazard ratio 1.55 for every 3% increase in ECV). In multivariable regression analysis of this heterogeneous population only ECV, EF, age and extent of LGE (if there was previous infarction) were able to significantly predict mortality. By using a combination of LGE and T1 mapping it is possible to map out the entire left ventricle delineating both areas of extracellular matrix expansion and areas of scarring, infarction and replacement fibrosis. Both of these techniques can detect pathological changes in asymptomatic subjects and have the potential to be used as screening tools for the detection of subclinical disease.

1.1.3 Strain analysis

Ejection fraction is the most widely used and best validated measure of left ventricular function. It is also possible to measure contraction of myocardium by measurement of either regional or global strain. In cardiac terms strain is defined as the amount of myocardial fibre shortening in a given time divided by the precontraction length. The measurements of length are usually made at end-systole and end-diastole. By convention this number is negative if the fibre has shortened and positive if it has lengthened.

It is possible to measure strain by CMR using tissue tagging techniques where a selective radiofrequency saturation pulse prior to the acquisition is used to generate a tag line or grid in the myocardium that can be tracked throughout the cardiac cycle (Ibrahim el, 2011). Using either long or short axis tagged cines it is possible to measure myocardial strain in radial, circumferential or longitudinal directions. Tagged cines can also be used to measure twist and torsion of the left ventricle. The heart has a complex twisting motion where the base rotates clockwise in early systole and the apex rotates anticlockwise in later systole. These opposing directions of rotation at the apex and base generate maximal torsional force at end systole (Burns et al., 2008). LV twist is defined as apical minus basal rotation. Torsion takes into account the length and diameter of the ventricle allowing comparison of torsional forces between ventricles of different sizes (Young and Cowan, 2012). Both strain and torsion measured by CMR tagging

techniques have good interstudy reproducibility allowing measurement of serial global and regional function (Swoboda et al., 2013).

Feature tracking is a new post processing technique which allows for tracking of myocardial features from cine imaging throughout the cardiac cycle. This technique is analogous and provides similar results to speckle tracking, which is a well validated echocardiography measure of strain (Onishi et al., 2015). Feature tracking allows for quantification of strain without the need for the acquisition of tagged cine imaging. Results from reproducibility studies of feature tracking have proved very promising and it is reported to have similar reproducibility to strain measured by CMR tissue tagging (Moody et al., 2015).

Strain and torsion measured by CMR both provide important diagnostic and prognostic information and have been used to detect subclinical impairment of both regional and global cardiac function in a wide variety of conditions including HCM (Kramer et al., 1994), type 2 diabetes (Giannetta et al., 2012; Larghat et al., 2014), ischaemic, valvular and congenital heart disease (Ibrahim el, 2011).

1.2 CMR assessment of hypertrophic cardiomyopathy

HCM is commonly defined as a disease of hypertrophy of the left ventricle in the absence of another cardiac or systemic cause (Gersh et al., 2011). It is typically caused by autosomal dominant mutations of genes encoding sarcomeric proteins and myofilament elements (Bos et al., 2009). These mutations lead to micro- and macroscopic changes within the heart including cellular disarray, hypertrophy and interstitial fibrosis. When myocyte disarray is widespread it is a sensitive and specific marker for HCM (Hughes, 2004). These changes lead to hypertrophy that can affect the heart in a variety of patterns, and may affect any segment of the left ventricle (Klues et al., 1995). Although hypertrophy can be widespread, phenotypic expression within the same heart can be variable and less than half of the ventricle may be hypertrophied in as many as 50% of patients (Maron et al., 2009b).

At present the diagnosis of HCM is primarily made by the identification of one or more hypertrophied segments by a cardiac imaging modality (Gersh et al., 2011; Elliott et al., 2014). In the majority of cases this involves identification of a

segment ≥15mm by echocardiography. Increasingly CMR is used to confirm or make diagnosis of HCM when echocardiography is restricted by limited acoustic windows or the inability to assess all segments of the left ventricle. In addition to accurate measurement of segment thickness CMR is also able to make an assessment of the cellular composition and function of segments that are borderline in terms of being diagnostic for HCM. Furthermore CMR imaging is able to evaluate and exclude the possibility of alternative causes of hypertrophy such as aortic stenosis, amyloidosis, Fabry's disease or systemic hypertension.

1.2.1 Morphologic assessment

CMR cine imaging is able to make an accurate and reproducible assessment of the extent and location of hypertrophy when considering a diagnosis of HCM. It is reported that CMR detects hypertrophy in around 12% of patients with HCM that was not detected by echocardiography (Maron et al., 2009b). The areas where hypertrophy is most commonly detected by CMR but not echocardiography include the anterolateral wall, the inferior septum and the apex. Imaging the apex of the left ventricle can be notoriously difficult by echocardiography and it is quite possible for severe hypertrophy to be missed by this technique but detected by CMR (Moon et al., 2004b).

It is possible for echocardiography to overestimate the wall thickness in HCM because of difficulty planning the acquisitions exactly perpendicular to the long axis of the left ventricle, resulting in an oblique cut. The improved spatial resolution of CMR also allows for accurate delineation of endocardial borders and exclusion of structures such as the moderator band or false tendons from measurements. It is reported that these differences can lead to measurements of segment thickness being approximately 20% less when measured by CMR compared to echocardiography (Valente et al., 2013).

In addition to accurate and reproducible measurements of wall thickness CMR can also assess LV mass (usually by the summation of discs techniques outlined in 1.1.1). However LV mass has been shown to only correlate weakly to maximum

segment thickness which is a more powerful prognostic predictor (Olivotto et al., 2008).

CMR imaging can also detect diagnostic features of HCM that may be missed on echocardiography including apical aneurysm formation (Maron et al., 2008), thrombus formation, papillary muscle abnormalities and myocardial crypts (Germans et al., 2006). Myocardial Crypts are typically identified in the basal or mid inferior or inferoseptal walls of the LV and are thought to represent an early phenotypic manifestation of HCM. They are reported to be present in 70% of patients who have a HCM causing mutation without over hypertrophy but only 12% of genotype negative controls (Brouwer et al., 2012). Myocardial crypts can be difficult to detect using conventional echocardiography and offer a good example of how CMR is able to detect subclinical disease in otherwise asymptomatic carriers of a significant genetic mutation (Germans et al., 2006).

The left atrium is often dilated in HCM due to a combination of elevated filling pressures and mitral regurgitation due to systolic anterior motion of the anterior mitral valve leaflet. It is possible to measure left atrial volumes accurately and reproducibly by CMR (Maceira et al., 2010). However the mechanisms leading to LA dilatation occur late in the disease progression of HCM and left atrial dilatation although a powerful prognostic marker is a feature of advanced disease and less useful for the detection of subclinical disease (Nistri et al., 2006).

1.2.2 CMR tissue characterisation

Using CMR tissue characterisation techniques it is possible to detect and quantify myocyte disarray and replacement fibrosis, the histological hallmarks of HCM. Histological studies of patients who have died and undergone post mortem have revealed that myocyte disarray is an early feature of HCM and likely a direct consequence of dysfunction mutations of sarcomeric proteins. Replacement fibrosis and small vessel disease appear to occur later in the disease process and are attributed to factors unrelated to disarray including wall thickness, gender and even local autocrine factors (Varnava et al., 2000).

The presence of LGE is suggestive of replacement fibrosis and on necropsy there is a strong linear correlation between the extent of LGE within a particular segment

and the amount of collagen measured histologically (Moon et al., 2004c). Small intramural coronary arteriole dysplasia has been suggested to cause replacement fibrosis by local ischaemia (Maron et al., 1986). The degree of small intramural coronary arteriole dysplasia on histological specimens after surgical myomectomy has been demonstrated to correlate with the extent of LGE on pre-operative CMR (Kwon et al., 2009).

CMR studies have also shown a correlation between the extent of LGE and the degree of hypertrophy, with some studies suggesting that hypertrophy occurs prior to the development of fibrosis (Choudhury et al., 2002; Moon et al., 2005). Studies using serial CMR have shown that replacement fibrosis is an ongoing dynamic characteristic of the disease process in HCM. Once replacement fibrosis detected by the presence of LGE it is associated with both progressive development of further replacement fibrosis and LV dilatation and adverse remodelling (Todiere et al., 2012; Moon et al., 2003).

Mechanistically it seems very plausible that replacement fibrosis detected by CMR could act as a substrate for malignant tachyarrhythmia. However studies that have investigated the prognostic potential of LGE in predicted sudden cardiac death or appropriate implantable cardioverter-defibrillator (ICD) therapy have given mixed results. This has largely been because of the low event rates and high prevalence of LGE. However all studies have shown that the presence of LGE is a marker with more advanced disease and is therefore associated with increased mortality and heart failure (Green et al., 2012). In the largest study to date, 1293 patients with HCM were followed up for 3.3 years. The presence of LGE was associated with malignant arrhythmia (Chan et al., 2014). However the event rate of malignant arrhythmia was low (around 1% per year) and the presence of LGE was more strongly associated with heart failure outcomes than arrhythmic outcomes.

With T1 and ECV mapping it is now possible to detect phenotypic expression of HCM prior to the onset of overt hypertrophy or replacement fibrosis. Cellular disarray and extracellular matrix expansion occur early in the disease process and can be detected by using quantitative T1 and ECV mapping techniques. Results demonstrate good correlation with histological fibrosis quantification from specimens taken at the time of surgical myomectomy (Flett et al., 2010). One study

has attempted to validate post contrast T1 mapping in HCM hearts explanted at the time of transplant and did report a correlation between the degree of fibrosis histologically and post contrast T1 time (Iles et al., 2015). Unfortunately in this study ECV (which is better validated than post-contrast T1 time) was not calculated, the sample size was small (4 HCM necropsy specimens) and there was a long interval between the CMR and surgical explant (median 546 days).

Myocyte disarray and collagen deposition are early features of HCM and can be detected histologically or biochemically in genotype positive subjects prior to the onset of hypertrophy (Varnava et al., 2001; Ho et al., 2010). It has been reported that ECV expansion can also be detected in the same cohort, adding further support to the hypothesis that ECV mapping is able to detect early phenotypic expression of HCM (Ho et al., 2013).

1.2.3 CMR assessment of regional function

Studies, predominantly using echocardiography speckle tracking to measure regional and global strain have demonstrated that impaired contractility is related to the extent of hypertrophy and the presence of replacement fibrosis detected by LGE (Urbano-Moral et al., 2014; Popovic et al., 2008). Current guidelines therefore recommend that strain imaging could be used to investigate unexplained left ventricular hypertrophy that is not diagnostic of HCM (Gersh et al., 2011; Elliott et al., 2014).

CMR tissue tagging is an alternative method to echocardiography for the assessment of regional strain and is highly reproducible in this setting (Shehata et al., 2009; Swoboda et al., 2013). Using CMR tissue tagging it is reported that significant heterogeneity in contractile function can be detected in different regions of the heart depending upon the extent of phenotypic expression in that region (Kramer et al., 1994). It was subsequently confirmed that the presence of LGE strongly correlated with impaired strain detected by tissue tagging (Kim et al., 2008).

One recent study has used CMR feature tracking to investigate regional strain in subjects under the age of 20 with HCM. They report that regional strain is most impaired in areas of hypertrophy or replacement fibrosis detected as LGE (Smith et

al., 2014). These findings are in keeping with previous echocardiography and CMR tagging studies.

1.2.4 Diastolic dysfunction and LV outflow tract obstruction

In addition to the CMR techniques that have been discussed other diagnostic features of HCM can be detected during a routine CMR examination. HCM is associated with impaired relaxation of the left ventricle which can be detected as diastolic dysfunction on Doppler echocardiography. Whilst it is possible to make an assessment of LV filling pattern and longitudinal function by CMR using cine imaging, phase velocity flow mapping, tissue tagging and feature tracking none of these techniques have been validated to the same extent as echocardiographic assessment of diastolic dysfunction. In addition the temporal resolution is higher when assessed by echocardiography, which is an important consideration when measuring diastolic function.

LV outflow tract (LVOT) obstruction is another diagnostic feature of HCM that is present in approximately one third of patients. Conventionally this assessment has been carried out by Doppler echocardiography. It is possible to make an assessment of flow obstruction using phase velocity flow mapping during a routine CMR examination. However alignment of the imaging plane can be difficult, intravoxel dephasing and signal loss due to phase offset errors can lead to errors in quantification and it can only be measured at rest. A significant proportion of patients with HCM only have LVOT obstruction during exercise, termed dynamic outflow tract obstruction. Technically it is much easier to make an assessment of dynamic outflow tract obstruction during echocardiography than CMR.

It is possible to make an assessment of both LV diastolic function and LV outflow tract obstruction during a routine CMR examination. However results from echocardiography appear to be more reproducible, easier to acquire and are better validated. Furthermore they both tend to be a consequence of significant hypertrophy or replacement fibrosis and therefore occur later in the disease process. For these reasons these techniques are not routinely used for the assessment of subclinical disease in HCM.

From one CMR examination it is now possible to make an accurate assessment of the expression of HCM phenotype by measuring myocardial hypertrophy, myocyte disarray and collagen deposition (with ECV mapping) and replacement fibrosis (LGE). During the same examination the functional consequences of these changes in tissues characteristic can be assessed (using either tissue tagging or feature tracking). Additional techniques to assess diastolic function or LVOT obstruction can also be added if required. Using these techniques it is possible to detect subclinical features of HCM in an otherwise asymptomatic subject.

1.3 Subclinical cardiac changes in endurance athletes

1.3.1 Change in cardiac morphology in trained athletes

It is well recognised that athletic training leads to ventricular remodelling, specifically increases in LV EDV and RV EDV and LV mass (Maron and Pelliccia, 2006). These structural changes are most frequently seen in athletes who undergo prolonged periods of endurance training (Utomi et al., 2013) and are typically subclinical with no associated symptoms. The increase in LV mass occurs as early as 6 months after commencement of endurance training (Arbab-Zadeh et al., 2014) and may be accompanied by an increase in LV EDV resulting in a typical phenotype of eccentric remodelling referred to as "athlete's heart" (Maron, 2003; Utomi et al., 2013).

CMR volumetric assessment of LV EDV and mass is established to be accurate and reproducible (Grothues et al., 2002) and is therefore an ideal tool for the quantification of the cardiac structural changes that can be detected in athletes.

Although athlete's heart has a fairly well established phenotype in certain cases the extent of LV hypertrophy can overlap into the pathological range. In these cases it is important to exclude a diagnosis of HCM. Although rare (Basavarajaiah et al., 2008), HCM is the leading cause of sudden cardiac death in young athletes (Maron et al., 2009a). Current guidelines advise that patients with HCM should avoid competitive sport and it is therefore imperative that HCM and physiological remodelling are correctly distinguished in an athlete with LV hypertrophy (Gersh et al., 2011; Elliott et al., 2014).

Several imaging parameters have been previously proposed to distinguish between physiological LVH and HCM including: EDV/LV mass (Luijkx et al., 2013), left atrial remodelling (Pelliccia et al., 2005), changes in strain pattern (Vinereanu et al., 2001), maximal oxygen consumption during cardiopulmonary exercise testing (Sharma et al., 2000) or composite assessments of multiple imaging findings (Caselli et al., 2014).

In subjects with very localised and asymmetric hypertrophy, the differentiation between the two entities can be straight-forward. However, when myocardial thickness is borderline or more widespread, it can be challenging to exclude a diagnosis of HCM in athletes (Basavarajaiah et al., 2008; Rawlins et al., 2010). Establishing the correct diagnosis may then require the athlete to undergo a period of detraining, which is challenging in elite athletes (Pelliccia et al., 2002).

Some endurance athletes display a cardiac phenotype of dilated left ventricle and low normal ejection fraction which can be difficult to differentiate clinically from early dilated cardiomyopathy (Abergel et al., 2004). This is usually less challenging than excluding HCM however in certain circumstances detraining can be necessitated too.

In certain situations it can be difficult to differentiate physiological athletic RV dilatation from pathological arrhythmogenic right ventricular cardiomyopathy. It has been postulated that imaging during exercise may be able to differentiate the two pathologies better than other methods; RV function improves if there is physiological RV dilatation whereas it does not in patients with pathological dilatation associated with cardiomyopathy (La Gerche et al., 2015).

1.3.2 Change in strain in trained athletes

Although less well established than changes in volumetric parameters, there is also evidence for changes in functional parameters in the hearts of trained athletes. Endurance athletes have reduced ejection fraction, circumferential and longitudinal strain of both the left and right ventricles compared to healthy controls (Caselli et al., 2015; Nottin et al., 2008). It has also been reported that athletes have decreased LV twist and torsion when compared to sedentary controls (Nottin et al., 2008). Several echocardiography studies using techniques

including tissue Doppler imaging and speckle tracking have been used to investigate left ventricular torsion in athletes. Contrasting findings have been reported including decreased apical rotation and LV torsion in athletes with high levels of aerobic fitness (Stohr et al., 2012) no effect of high intensity exercise on LV torsion (Stewart et al., 2015), or even an increase in LV torsion (Weiner et al., 2010). The inconsistent results that have been reported may in part reflect different sport and training techniques, research methodology used and also the difficulty in positioning the apical and basal slices in echocardiography studies, which is based upon anatomical landmarks with a degree of subjectivity.

Conflicting findings have been reported when echocardiographic assessment of diastolic function has been used with some studies reporting augmented relaxation of both ventricles in endurance athletes (Caselli et al., 2015; Baggish et al., 2008) and others reporting no difference from controls (Pluim et al., 2000).

1.3.3 Tissue characterisation in trained athletes

In addition to the physiological subclinical changes that can be detected by CMR in athletes it is also possible to detect subclinical pathological change. One study reported the presence of LGE in 6 lifelong athletes over the age of 50 (N=12). 4/6 had non-specific LGE, 1/6 had a previous myocarditis pattern and 1/6 had a subendocardial pattern suggestive of previous MI (Wilson et al., 2011). Another study reported a prevalence of non-ischaemic pattern LGE in 2/95 asymptomatic athletes (Mangold et al., 2013). One recent case series has attempted to establish the prognostic significance of non-ischaemic LGE detected on routine screening in asymptomatic athletes (Schnell et al., 2015). On following up 7 athletes with sub-epicardial lateral LGE suggestive of previous myocarditis over three years 5/7 had symptomatic ventricular arrhythmias and 1/7 had progressive LV dysfunction. This study was small and the nature of the ventricular arrhythmia variable, ranging from exercise induced couplets to ventricular tachycardia requiring ICD implantation, however it does suggest that non-ischaemic LGE in athletes may be a prognostically significant pathological finding.

1.4 Detection of subclinical heart failure in diabetes

The mechanisms that lead from chronic hyperglycaemia to heart failure are complex and are thought to involve altered substrate metabolism, impaired calcium handling, increased reactive oxygen species and microvascular advanced glycation end product deposition (Boudina and Abel, 2007; Seferovic and Paulus, 2015). It is possible to detect the consequences of many of these pathways using cardiac imaging in the subclinical phase of disease. Changes in cardiac morphology, function and microscopic structure can all be detected in type 2 diabetes before the onset of heart failure symptoms. Many of these features have been associated with adverse outcomes.

1.4.1 Changes in cardiac morphology

Several studies have demonstrated that type 2 diabetes is associated with increased LV mass and concentric remodelling of the left ventricle independently of blood pressure. Original studies were carried out using echocardiography and demonstrated that diabetes was associated with increased LV wall thickness and LV mass (Galderisi et al., 1991; Devereux et al., 2000). Echocardiographic assessment of LV mass is dependent on image quality and echocardiographic windows. CMR assessment of LV dimensions is not hampered by these issues and consequently the assessment of LV mass by this technique is significantly more reproducible (Grothues et al., 2002).

CMR data of 4869 patients from the large observational MESA (Multiethnic study of atherosclerosis) study (Heckbert et al., 2006) demonstrated that diabetes is associated with an increase in LV mass. After regression analysis for multiple risk factors including BMI and systolic blood pressure diabetes was associated with a 3.5g greater LV mass (95% confidence interval 1.2-5.8g).

In large population studies not specifically restricted to patients with type 2 diabetes increased LV mass predicted the onset of heart failure after correction for other risk factors such as blood pressure and coronary disease (de Simone et al., 2008; Bluemke et al., 2008). However no studies to date have been carried out investigating the association between LV mass and heart failure in low risk patients with diabetes.

1.4.2 Changes in cardiac function

As many as 75% of asymptomatic patients with type 2 diabetes have abnormal parameters of diastolic function measured by conventional Doppler and tissue Doppler (TDI) echocardiography (Poirier et al., 2001; Boyer et al., 2004). In addition impaired peak longitudinal systolic velocity measured by TDI (Kosmala et al., 2004) and by speckle tracking (Ng et al., 2009) has also been reported in patients with type 2 diabetes. It is possible to measure strain in three dimensions using CMR tissue tagging. Using this technique both circumferential strain and longitudinal strain are reported to be impaired in type 2 diabetes (Fonseca et al., 2004).

TDI echocardiography provides prognostic information in patients with type 2 diabetes. E/E' ratio measured by TDI is a relatively simple measurement and is a well validated non-invasive measure of left ventricular filling pressure (Ommen et al., 2000). A retrospective study of 1760 patient with diabetes by From et al identified 23% of patients with elevated E/E' and therefore diastolic dysfunction (From et al., 2010). Over 5 years follow up the cumulative proportion of those who developed heart failure was 36.9% in those with elevated E/E' compared to 16.8% in those with normal E/E'. Age, hypertension, coronary artery disease and ejection fraction were stronger predictors of heart failure development than diastolic dysfunction but even after adjusting for these factors E/E' was a strong predictor of the development of heart failure. These findings were not replicated in a recent prospectively recruited study of 305 patients with type 2 diabetes without history of coronary artery disease (Poulsen et al., 2013) who all underwent single-photon emission computed tomography (SPECT) and TDI echocardiography. They found that age, hypertension, E/E' and left atrial volume but not ischaemia on SPECT were predictors of a composite of cardiovascular events or mortality. However on multivariable regression analysis left atrial volume and ejection fraction were the only independent predictors of cardiovascular events or mortality. Measuring E' by TDI during exercise can provide incremental evidence about diastolic function which appears to have prognostic information. E', representing passive filling of the left ventricle, normally increases during exercise. It is reported that that this

response can be impaired in diabetes and has been associated with increased mortality and heart failure admissions on follow up (Kim et al., 2011).

The prognostic significance of systolic strain parameters in type 2 diabetes has also been studied. Impaired global longitudinal strain measured by speckle tracking echocardiography was associated with increased mortality and hospitalisation (Holland et al., 2015). Although not specifically studied in diabetes impaired global circumferential strain measured by CMR tagging has been shown to be associated with subsequent development of heart failure (Choi et al., 2013).

Measurement of diastolic dysfunction by echocardiography is a comparatively cheap screening tool that does not involve exposure to ionising radiation. There is some conflicting data that suggests diastolic dysfunction may predict the onset of heart failure in type 2 diabetes. However diastolic dysfunction is a prevalent finding and has significant interactions with other risk factors such as age, blood pressure and presence of coronary disease. Furthermore randomised studies of interventions have failed to demonstrate an improvement in E/E' with intervention (van der Meer et al., 2009; Ofstad et al., 2014).

Left ventricular torsion is a measure of the wringing motion of the heart calculated from the basal clockwise rotation and apical anticlockwise rotation. It can be measured by speckle tracking echocardiography or tagged CMR images. A paradoxical increase in left ventricular torsion has been reported in diabetes (Chung et al., 2006) and is thought to be due to small vessel ischaemia, subendocardial myofibre dysfunction and compensatory increased subepicardial myofibre contraction (Larghat et al., 2014). It was demonstrated in a randomised study of sildenafil, a phosphodiesterase type 5 inhibitor, in patients with diabetes that these changes could be overcome and torsion normalised (Giannetta et al., 2012). However it remains to be established whether torsion is associated with increased heart failure or mortality on long term follow up.

1.4.3 Changes in myocardial tissue characteristics

ECV fraction has been demonstrated to be increased in asymptomatic patients with type 2 diabetes and also associated with impaired diastolic strain detected by TDI echocardiography (Jellis et al., 2011; Ng et al., 2012). A recent study by Wong

et al followed up 231 patients with type 2 diabetes who had clinically indicated CMR for a median duration of 1.3 years (Wong et al., 2013). They found those with a higher ECV were at higher risk of heart failure admission or death (hazard ratio 1.52 per 3% increase in ECV). However it should be noted that in the study of Wong *et al* the patients were recruited from clinical scans they were not asymptomatic and in fact had a high rate of prior coronary revascularisation (33%) and prior myocardial infarction (11%).

ECV holds real promise as a potential screening tool for identifying those at highest risk of heart failure. However the prognostic value of ECV in asymptomatic patients and whether ECV can be altered by any intervention remains to be established.

Magnetic resonance spectroscopy is able to measure the concentration of metabolites within the heart non-invasively without the use of ionising radiation. Studies have shown that patients with type 2 diabetes have increased cardiac triglyceride content, termed steatosis (McGavock et al., 2007). Furthermore cardiac steatosis in type 2 diabetes is associated with impaired function measured by both systolic and diastolic strain measured by TDI and speckle tracking echocardiography (Rijzewijk et al., 2008; Ng et al., 2010). However it remains to be established whether this process can be reversed and whether it is independently associated with adverse prognosis.

1.4.4 Changes in microvascular function

Silent ischaemia due to epicardial coronary artery stenosis can be detected by several techniques including nuclear imaging, stress echocardiography and first pass perfusion CMR (see 1.5.4). SPECT measures relative blood flow and is therefore not able to detect abnormalities in the microvasculature. Conversely, positron emission tomography (PET) allows the non-invasive quantification of absolute myocardial blood flow at rest and during pharmacological vasodilator stress. Comparing the blood flow at rest and stress allows the calculation of coronary flow reserve (CFR). In the absence of coronary disease impairment of CFR reflects microvascular dysfunction.

Impaired CFR detected by PET is has been reported in asymptomatic patients with type 2 diabetes without known coronary disease (Nahser et al., 1995) and is shown

to correspond with degree of hyperglycaemia measured by Hba1c rather than insulin resistance (Yokoyama et al., 1998). Patients with impaired CFR measured by PET are reported to also have increased ECV measured by CMR (Rao et al., 2013). Studies have shown that abnormalities in myocardial blood flow detected by PET can also be reversed by interventions including pioglitazone (Naoumova et al., 2007) and spironolactone (Garg et al., 2015). There is also evidence that CFR impairment in type 2 diabetes is associated with excess cardiovascular risk. Murthy *et* followed up 1172 patients with diabetes after a clinically indicated PET scan for a median duration of 1.4 years (Murthy et al., 2012). Those with CFR below the median had an adjusted hazard ratio of 3.2 for cardiac death compared to those with CFR above the median. Diabetic patients without coronary artery disease but impaired CFR had a comparable event rate to diabetic patients with coronary artery disease. However these patients were not asymptomatic with 47.2% having the test because of chest pain and had a high rate of prior revascularisation (45.6%) and prior myocardial infarction (36.1%).

Coronary blood flow during stress is impaired in patients with type 2 diabetes independent of epicardial coronary artery disease. These changes can be reversed by medical therapy and appear to be associated with adverse outcomes (Murthy et al., 2012; Garg et al., 2015). Cardiac PET however is not widely available and involves exposure to ionising radiation. It is possible to measure CFR with other techniques including stress first pass perfusion CMR (Ibrahim et al., 2002) and stress echocardiography (Cortigiani et al., 2007). However these techniques can be challenging and do not have as broad an evidence base as CFR measured by PET.

1.5 Asymptomatic ischaemic heart disease in diabetes

1.5.1 Myocardial infarction

MI is the single largest cause of mortality in type 2 diabetes. Electrocardiogram (ECG) remains the most important diagnostic test in acute MI and is used to prioritise which patients should receive urgent reperfusion therapy. In patients with chest pain but ECG changes non-diagnostic of acute MI imaging modalities can

be used to detect acute changes in structure and function that may help confirm or rule out a diagnosis of MI. The presence of acute myocardial infarction can be confirmed by urgent echocardiography demonstrating wall motion abnormality. The diagnostic and prognostic accuracy can be improved further by the addition of strain imaging, intravenous contrast, physiological or pharmacological stress (Shah et al., 2013). The presence of a perfusion defect on resting SPECT is an alternative method to confirm the diagnosis (Udelson et al., 2002). CMR can detect the presence of acute MI by wall motion abnormality or perfusion defect and is also able to detect the presence of oedema using T2 weighted imaging or scar imaging by LGE (Cury et al., 2008). Finally using CT coronary imaging it is possible to exclude acute coronary stenosis with high negative predictive value (Hulten et al., 2013).

After the acute phase of MI chronic changes such as scarring, fibrosis, associated wall motion abnormalities and perfusion defects can be detected. Therefore the techniques most commonly used to detect chronic MI include ECG, echocardiography, nuclear techniques and CMR.

Chronic MI can be diagnosed by 12 lead ECG according to the presence of Q waves. Although a good screening test, the sensitivity to detect chronic MI is reported to be only 33% (Jaarsma et al., 2013). The prevalence of silent MI by the presence of Q waves in patients with newly diagnosed type 2 diabetes in UKPDS was reported to be 17% (Davis et al., 2013). The adjusted hazard ratio for all cause mortality of diabetic patients with silent MI by Q waves compared to those without over 17 years follow up was 1.31. The mortality of diabetic patients with silent MI detected by Q waves is reported to be similar to patients with recognised MI (Davis et al., 2004).

Silent MI can also be assessed by SPECT by intravenous injection of a gamma emitting radioisotope during rest and stress (either exercise induced or pharmacological). An area of myocardium that has decreased tracer uptake at both rest and stress is deemed non-reversible and has been shown to correspond to areas of prior myocardial infarction (Zellweger et al., 2002). The prevalence of silent MI assessed using this technique was reported to be 28.5% in patients with type 2 diabetes undergoing SPECT for clinical purposes (Arenja et al., 2013).

Currently the best validated method for the presence and extent of silent MI is the LGE technique measured by CMR. Kwong et al first reported a prevalence of 28% of silent MI using LGE imaging in symptomatic patients without prior MI type 2 diabetes undergoing CMR (Kwong et al., 2006). Schelbert *et al* reported a prevalence of 21% of silent MI of diabetic patients enrolled in the ICELAND MI study who underwent CMR between 2004 and 2007 (Schelbert et al., 2012). However patients in both studies were not necessarily asymptomatic and in ICELAND MI 28% of those with silent MI had prior coronary revascularisation. In both of these studies the presence of silent MI in diabetes was associated with significant morbidity and mortality. Kwong et al reported that over 17 months follow up the presence of silent MI in patients with diabetes was associated with increased mortality (hazard ratio 3.72, P<0.001) and major adverse cardiovascular events (MACE) (HR3.61, P=0.007)(Kwong et al., 2006). Schelbert et al reported that that over 6.4 years follow up the mortality of all patients with silent MI was similar to those with recognised MI (28% vs 33%, P=0.40) (Schelbert et al., 2012).

Asymptomatic patients with type 2 diabetes have increased risk of silent myocardial infarction compared to normoglycaemic patients. The exact prevalence of silent MI In type 2 diabetes varies according to imaging modality and the extent of symptoms patients had within the study. However whichever imaging modality is used it is clear that those with silent MI are at increased risk or mortality and morbidity. At present the LGE technique is favoured for the detection of silent MI given its improved sensitivity compared to ECG, echocardiography and SPECT (Ibrahim et al., 2007) without the need for ionising radiation.

1.5.2 Plaque Imaging

Most imaging methods can only detect MI, silent or recognised, after the event. Although the risk of future MI is highest in those with previous MI, it may also be possible to predict the likelihood of future MI directly with imaging. Molecular imaging techniques with radiolabelled molecules have been used to detect the pathological components of unstable coronary plaques. 18F-fluorodeoxyglucose (18F-FDG) PET can to identify high risk plaques in large arteries (Langer et al., 2008). However this technique is unable to identify unstable plaque in the

coronary vessels as it is hampered by myocardial activity (Dweck et al., 2012). 18F-sodium fluoride (18F-NaF) is able to overcome this issue and identify localised ruptured and unstable plaque particularly when combined with anatomical CT imaging (Joshi et al., 2014).

Cross sectional imaging techniques are also reported to be able to identify high risk plaque according to its anatomical features. Plaques with positive remodelling and low attenuation identified by CT coronary angiography are at significantly higher risk of myocardial infarction over 3.9 years follow up (Motoyama et al., 2015). Non contrast CMR coronary imaging is able to identify plaques with increased T1 weighted signal, a marker of increased tissue water content and potentially plaque instability (Hoshi et al., 2015). After a year treatment with high dose statin therapy there was a significant decrease in the intensity of the coronary signal suggesting plaque stabilisation (Noguchi et al., 2015).

The prognostic utility of imaging techniques to identify unstable coronary plaque in low risk and asymptomatic patients (particularly those with diabetes) has not yet been established and requires significant expertise for acquisition and post processing. It is likely however that in the near future these techniques will be important to identify patients with diabetes at the highest risk of acute coronary events for inclusion in clinical trials.

1.5.4 Stable Coronary Artery Disease

It is possible to detect stable coronary artery disease either by detecting the stenosis itself by anatomical imaging of the coronary tree (usually by CT, CMR or invasive angiography) or by detecting the inducible ischaemia that occurs as a consequence of the stenosis. Testing for ischaemia typically involves the administration of pharmacological or physiological stress and then imaging to detect either decreased uptake of contrast (SPECT, PET or CMR first pass perfusion) or wall motion abnormality as a consequence of ischaemia (stress echocardiography).

Patients with diabetes and significant inducible ischaemia have increased mortality. It is reported that in patients with diabetes undergoing SPECT for clinical

purposes that mortality and non-fatal MI increase from 1-2% for those with normal MPS to 7% for those with moderate to severe inducible ischaemia (Kang et al., 1999). Furthermore the high event rate associated with significant inducible cardiac ischaemia appears to be independent of the presence or absence of symptoms (Zellweger et al., 2004).

However randomising asymptomatic diabetic patients to screening with SPECT in Detection of Silent Myocardial Ischemia in Asymptomatic Diabetics (DIAD) study did not alter their mortality (Young et al., 2009). 1123 patients with type 2 diabetes were randomised to investigation by SPECT screening or not. 113/522 patients (22%) in the SPECT arm had silent ischemia (Wackers et al., 2004). Although the prevalence of ischaemia was high the reported cardiovascular event rate was very low (0.6% per year) leading the authors to suggest that routine SPECT could not be recommended in patients with type 2 diabetes (Young et al., 2009). These recommendations have been repeated in European guidelines (Perrone-Filardi et al., 2011).

Similarly to DIAD the utility of screening asymptomatic diabetic patients for coronary artery disease using CT coronary angiography has been tested in the FACTOR 64 trial (Muhlestein et al., 2014). 900 patients were randomised to either CT or standard care. 76/336 patients who underwent CT coronary angiography had moderate or severe coronary stenosis which resulted in 25 coronary revascularisation procedures. However despite the intervention there was no difference in the primary outcome a composite of all-cause mortality, nonfatal MI, or unstable angina requiring hospitalization over 3 to 5 years follow up between CT guided or standard care (6.2% vs 7.6%, P=0.38).

Despite the high prevalence of stable coronary artery disease detected in asymptomatic patients with type 2 diabetes by SPECT or CT the associated mortality appears to be low. Two high quality landmark trials (DIAD and FACTOR 64) using different imaging modalities have both shown that intervening upon silent stable coronary artery disease in this population does not appear to alter long term outcomes. Although it is possible to detect silent stable coronary artery disease in asymptomatic patients with type 2 diabetes, it is associated with only modest increase in mortality which does not appear to be altered by intervention.

Therefore screening for subclinical stable coronary artery disease cannot be recommended.

1.6 Aims of thesis

Using CMR imaging it is possible to detect subclinical cardiac change in both disease and health. This has several potential applications in both clinical cardiology and research. Detection of subclinical change in asymptomatic subjects allows for the identification of disease prior to the onset of symptoms. For patients this facilitates early diagnosis and treatment, which has the potential to improve outcomes. Certain imaging parameters that can be detected in asymptomatic patients have been independently associated with increased mortality. By specifically recruiting patients to studies who display subclinical pathology on imaging it may be possible to increase the event rate and even decrease the required sample size. Depending upon the parameter chosen it may also be possible to monitor the progression of subclinical disease. This could potentially be used clinically or as a surrogate end point in research.

The subsequent chapters each have a specific aim with individual introduction, methods, results and discussion:

Study 1: To establish whether T1 and ECV mapping can distinguish athletic cardiac remodelling from HCM

Study 2: To investigate whether regional strain impairment in HCM is an early or late feature of HCM

Study 3: To study the three dimensional changes in strain parameters in highly trained endurance athletes and their relationship with aerobic capacity

Study 4: To identify whether increased risk of heart failure in patients with type 2 diabetes is mediated by focal or diffuse cardiac fibrosis

Study 5: To establish which parameters might be useful in screening for silent myocardial infarction in patients with type 2 diabetes

2 . Study 1- CMR to differentiate hypertrophic cardiomyopathy from athlete's heart

2.1 Abstract

Background

Athletes who train regularly can develop left ventricular (LV) hypertrophy, which can be difficult to differentiate from hypertrophic cardiomyopathy (HCM), the leading cause of sudden cardiac death in young athletes. Cardiovascular magnetic resonance (CMR) T1 and extracellular volume (ECV) mapping provide quantitative assessment of myocardial composition. We hypothesised that ECV could differentiate athletic from pathological hypertrophy, in particular in subjects with indeterminate segment thickness.

Methods

50 HCM patients, 40 athletes and 35 volunteers underwent 3.0T CMR including 5b(3s)3b Modified Look-Locker Inversion (MOLLI) T1 maps before and 15 minutes after administration of 0.15mmol/kg intravenous gadobutrol. Native T1 and ECV were measured for each segment of each subject.

Results

Native T1 and ECV of the thickest segment were significantly lower in athletes than HCM (1175.5±37.3ms vs 1261.1±52.3ms and 22.2±3.5% vs 32.8 ±9.0%, P<0.001 for both). On receiver operator curve analysis the area under the curve (AUC) to differentiate HCM from athlete for native T1 was 0.91 and ECV 0.95 (P<0.001). The maximal segment thickness overlapped between HCM and athletes in 26 individuals (13 athletes and 13 HCM). The AUC of ECV, native T1 and EDV/LV mass to differentiate between athletes and HCM in these indeterminate subjects were 0.99, 0.95, and 0.82 respectively, P<0.001 for all. The optimal cut-off to diagnose HCM was ECV>22.5% (sensitivity 100%, specificity 92%), native T1>1190.4 (sensitivity 100%, specificity 77%). In these subjects diagnostic accuracy of ECV was

significantly better than EDV/LV mass or the presence of LGE, P=0.03 and P<0.001, respectively.

Conclusions

T1 mapping and ECV measurement by CMR can be used to distinguish HCM and athletic remodelling with high diagnostic accuracy and has a potential role in the exclusion of HCM in athletes presenting with intermediate left ventricular wall thickness.

2.2 Introduction

Athletes who train and compete regularly develop changes in cardiac morphology and function, most notably an increase in LV mass (Maron and Pelliccia, 2006). This increase in LV mass occurs as early as 6 months after commencement of endurance training (Arbab-Zadeh et al., 2014) and may be accompanied by an increase in LV end-diastolic volume (LVEDV) resulting in a typical phenotype of eccentric remodelling referred to as "athlete's heart" (Maron, 2003; Utomi et al., 2013). An important differential diagnosis of athlete's heart is HCM. Although rare (Basavarajaiah et al., 2008), HCM is the leading cause of sudden cardiac death in young athletes (Maron et al., 2009a). Current guidelines advise that patients with HCM should avoid competitive sport and it is therefore imperative that HCM and physiological remodelling are correctly distinguished in an athlete with LV hypertrophy (Gersh et al., 2011; Elliott et al., 2014). Several imaging parameters have been reported to differentiate athletic from pathological hypertrophic remodelling (Pelliccia et al., 1991; Pelliccia et al., 2012; Luijkx et al., 2013). In subjects with very localised and asymmetric hypertrophy, the differentiation between the two entities can be straight-forward. However, when myocardial thickness is borderline or more widespread, it can be challenging to exclude a diagnosis of HCM in athletes (Basavarajaiah et al., 2008; Rawlins et al., 2010). Establishing the correct diagnosis may then require the athlete to undergo a period of detraining, which is challenging in elite athletes (Pelliccia et al., 2002).

CMR is increasingly used to aid in the differential diagnosis of LV hypertrophy because it provides more accurate measurements of LV thickness than echocardiography (Valente et al., 2013) and permits detection of focal scar according to the presence of LGE (Maron et al., 2009b). While LGE imaging appears to have merits in risk stratification, it is a qualitative technique, and detection of pathology requires a contrast between normal and abnormal tissue, limiting application in diffuse myocardial change. In contrast, T1 mapping provides quantitative assessment of myocardial composition and diffuse fibrotic change, by measuring either the native T1 alone or myocardial ECV from both native and post contrast T1 mapping (Flett et al., 2010). ECV in HCM has been shown to be

increased even in segments that do not have scar on LGE (Kellman et al., 2012). This elevation in ECV is thought to be related to myocardial disarray, the pathological hallmark of HCM (Sheppard, 2012). We hypothesised that athlete's heart, conversely, is characterised by myocyte hypertrophy without ECV expansion and therefore, that T1and ECV mapping can differentiate between HCM and athlete's heart. We specifically investigated the ability of the CMR methods to differentiate between the entities in those subjects with borderline myocardial thickness.

2.3 Methods

2.3.1 Enrolment Criteria

40 athletes, 50 patients with HCM and 35 volunteers were enrolled in the study. Patients under the age of 65 with HCM were recruited from the Inherited Cardiovascular Conditions Service at Leeds General Infirmary, Leeds, UK. The diagnosis of HCM was made independently by clinicians in keeping with current guidelines and based upon imaging, ECG, exercise testing, family history and genetic testing if possible (Elliott et al., 2014; Gersh et al., 2011). We specifically identified patients with definite HCM but maximum segment thickness <15mm. Exclusion criteria were previous surgical myomectomy, previous septal ablation, atrial fibrillation, previous myocardial infarction, uncontrolled hypertension, permanent pacemaker, defibrillator or other contraindication to CMR. Of the 40 athletes, 11 were runners, 13 were triathletes and 16 were cyclists. These sports were chosen as they are reported to lead to cardiac remodelling to differing extents (Maron and Pelliccia, 2006; Utomi et al., 2013). All athletes trained more than 6 hours a week, competed at local or national level and were under the age of 45. Athletes underwent cardio-pulmonary exercise testing to ensure high fitness levels. They had a mean VO$_2$max of 58.3 ± 9.0 ml/min/kg, a similar level to that associated with athletic cardiac remodelling previously (Arbab-Zadeh et al., 2014; Sharma et al., 2000). The 35 healthy volunteers exercised less than three hours per week. No athletes or controls had any other medical conditions or took any regular

medication. The study was conducted in accordance with the declaration of Helsinki and was approved by the local ethics committee (14/YH/0126). All subjects gave informed written consent.

2.3.2 CMR protocol

All subjects underwent identical CMR protocol performed on a 3.0 Tesla Philips Achieva TX system (Philips, Best, The Netherlands) equipped with a 32 channel cardiac phased array receiver coil. A full blood count, including haematocrit was measured at the time of intravenous cannulation. The cardiac long and short axes were determined using standard scout views. Basal, mid and apical pre-contrast (native) T1 maps were generated using a validated MOLLI protocol (Kellman et al., 2013) (ECG triggered 5b(3s)3b MOLLI scheme with voxel size of 1.98 x 1.98 mm^2, slice thickness 10mm) and were planned using the 3 of 5 method (Messroghli et al., 2005). Left ventricular volumes were obtained from cine imaging covering the entire LV in the short axis: balanced SSFP, voxel size 1.2 x 1.2mm^2, slice thickness 10mm with no gap, 50 cardiac phases. Left atrial (LA) volumes were obtained from cine imaging covering the entire heart in the transverse axis: balanced SSFP, voxel size 1.2 x 1.2mm^2, slice thickness 6mm with no gap, 50 cardiac phases. 0.15mmol/Kg Gadovist (Bayer Schering) was delivered by power injector (Medrad Inc, Warrendale, Pennsylvania, USA) as a single bolus via a cannula placed in the ante-cubital fossa followed by 20ml saline flush. Two-dimensional LGE imaging with whole heart coverage was performed seven to ten minutes following contrast administration and a Look Locker TI scout. Post contrast T1 maps were performed using the same MOLLI scheme fifteen minutes after contrast administration.

2.3.3 CMR interpretation

Analysis was carried out using standard software (cvi42, Circle CVI, Canada) by two physicians blinded to clinical and exercise data (BE & AKM). LV mass, end diastolic volumes (EDV), end systolic volume (ESV) and LV ejection fraction (EF) were measured from short axis cine images. LA volume was measured from the transverse image in atrial end diastole. Native and post contrast T1 relaxation time of myocardium and blood pool were measured from the scanner generated T1

maps by contouring a region of interest in each segment of the American Heart Association (AHA) model (Cerqueira et al., 2002). ECV was calculated from native and post contrast T1 times of myocardium and blood pool and haematocrit as previously reported (Flett et al., 2010). Segment thickness was measured from diastolic SSFP cine images with corresponding slice location to the T1 maps. The thickest maximal thickness athlete segment was 13.8mm the thinnest maximal thickness HCM segment was 10.6mm. Segments that fell in this overlapping range were therefore defined as indeterminate in this cohort (Valente et al., 2013). The presence of LGE in each AHA segment was reported by 2 physicians experienced in CMR interpretation.

2.3.4 Statistical analysis

Continuous variables were expressed as means ± SD. Categorical variables were expressed as N (%). Shapiro-Wilk test was used to test normality and depending on the result analysis of variance (ANOVA) and Kruskal Wallis test were used to compare means of athletes, HCMs and controls. Mann Whitney U test was used to compare athletes and HCMs. Pearson's correlation coefficient and Spearman's rank correlation were used for linear correlations as appropriate.

Receiver operating characteristic (ROC) analysis was used to determine the diagnostic accuracy of native T1, ECV, LV mass and EDV/LV mass on a per subject and per segment analysis. The diagnostic accuracy is expressed as area under the ROC curves (AUC) and 95% confidence interval. Nested models were used to assess the additive value when combining native T1, ECV and EDV/LV mass. AUCs were compared by using validated methods described by DeLong et al (DeLong et al., 1988). Optimal sensitivity and specificity were calculated using Youden index. Reclassification tables were constructed using decile cut-offs from which net reclassification index (NRI) was calculated to assess the incremental value of native T1 and ECV over EDV/LV mass (Pencina et al., 2008). ROC and NRI analysis was repeated in subjects who were defined as indeterminate. P<0.05 was considered statistically significant.
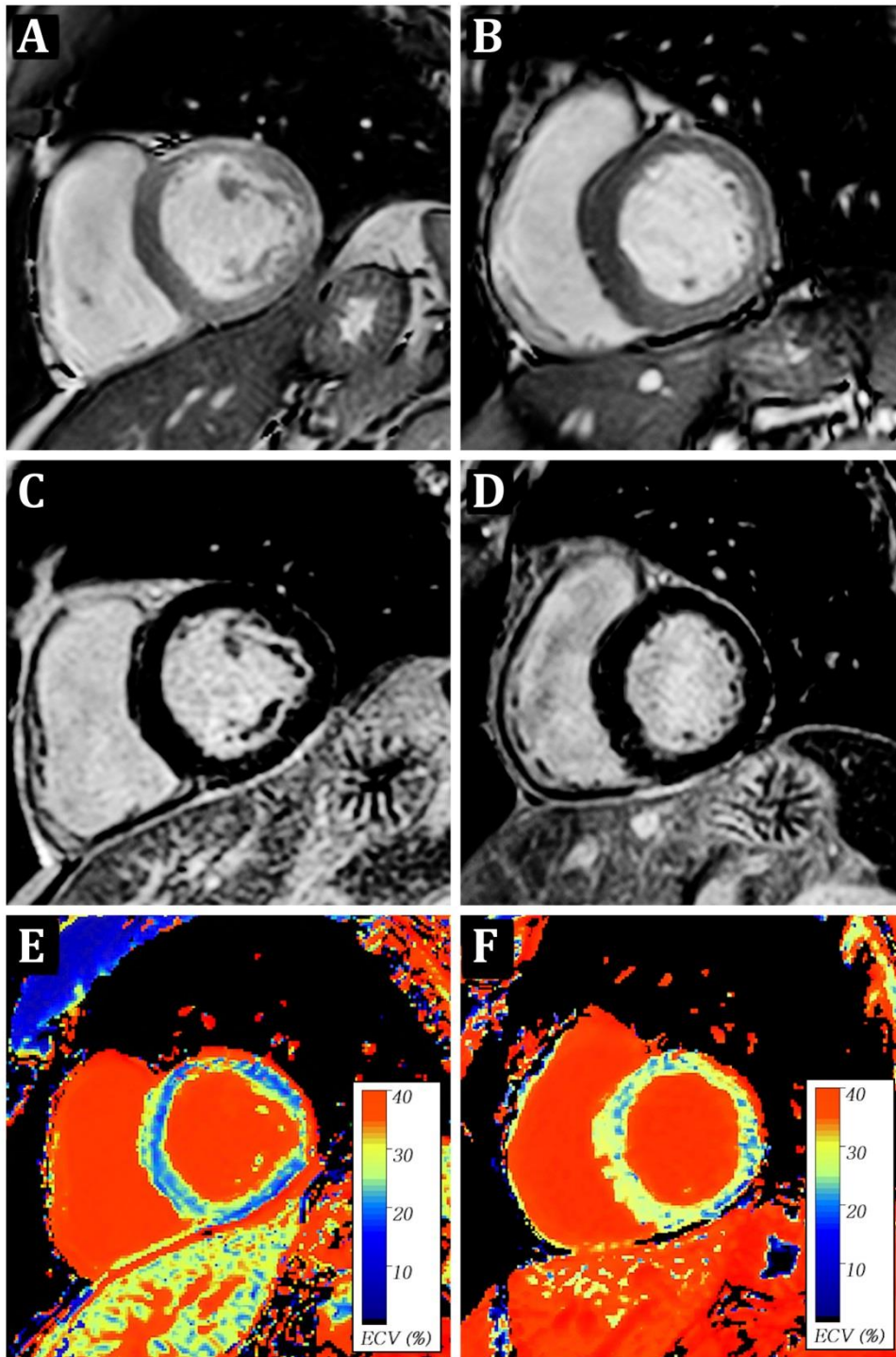
Figure 2.1 CMR images comparing a healthy athlete (left) and patient with HCM (right). On SSFP cine imaging both the athlete (A) and HCM patient (B) had a maximal end diastolic septal thickness of 13mm and EDV/LV mass of 1.6. On LGE imaging neither the athlete (C) or HCM (D) had any focal scarring or fibrosis. On ECV mapping the septal ECV of the athlete (E) was 22% and HCM (F) was 30%. Using the cut-off of 22.5% only ECV identified both subjects correctly.

2.4 Results

Baseline characteristics are shown in Table 2.1. Weight and BMI were lower in athletes than controls and HCMs (P=0.02 and P<0.01 respectively). CMR findings of LV EDV, ESV, EF, LV mass, EDV/LV mass, maximal segment thickness, LVOT obstruction, native T1 and ECV in the three groups are shown in Figures 2.1 & 2.2 and Table 2.2. The range of maximum segment thicknesses was 6.4-10.8mm, 7.0-13.8mm and 10.6-28.0mm in control, athlete and HCM respectively.

	Athlete	Control	HCM	P value
N	40	35	50	NA
Male gender, n (%)	32 (80)	27 (77)	37 (74)	0.80
Age, years	31.3 ± 6.9	36.2 ± 11.7	46.9 ± 11.7	<0.001
Height, cm	178.5±8.2	174.6±13.0	171.2 ± 9.0	<0.01
Weight, kg	72.3±9.8	80.2±12.6	81.7±14.6	<0.001
Body mass index, kg/m^2	22.6±2.2	26.6±5.6	27.7±3.7	<0.001
Systolic blood pressure, mmHg	119.3±8.2	117.8±12.5	125.5±17.6	0.05
Diastolic blood pressure, mmHg	69.0±9.3	65.4±11.9	74.5±12.5	<0.01
Heart rate	54.9±6.8	61.9±8.0	60.6±10.2	<0.001
FH of HCM, n (%)	0	0	19 (38)	<0.001
Hours training per week	11.7±4.7			NA
Number of years training at >6 hours per week	8.7±5.9			NA

Table 2.1 Subject characteristics. FH, family history; HCM, hypertrophic cardiomyopathy

45/50 HCM patients had maximal segment thickness measured by echocardiography prior to CMR (5 had apical HCM where segment thickness could not be assessed accurately by echocardiography). Maximum segment thickness by echocardiography was on average 2.2mm thicker than by CMR (19.8±4.9mm vs 17.6±3.9mm, P=0.001).
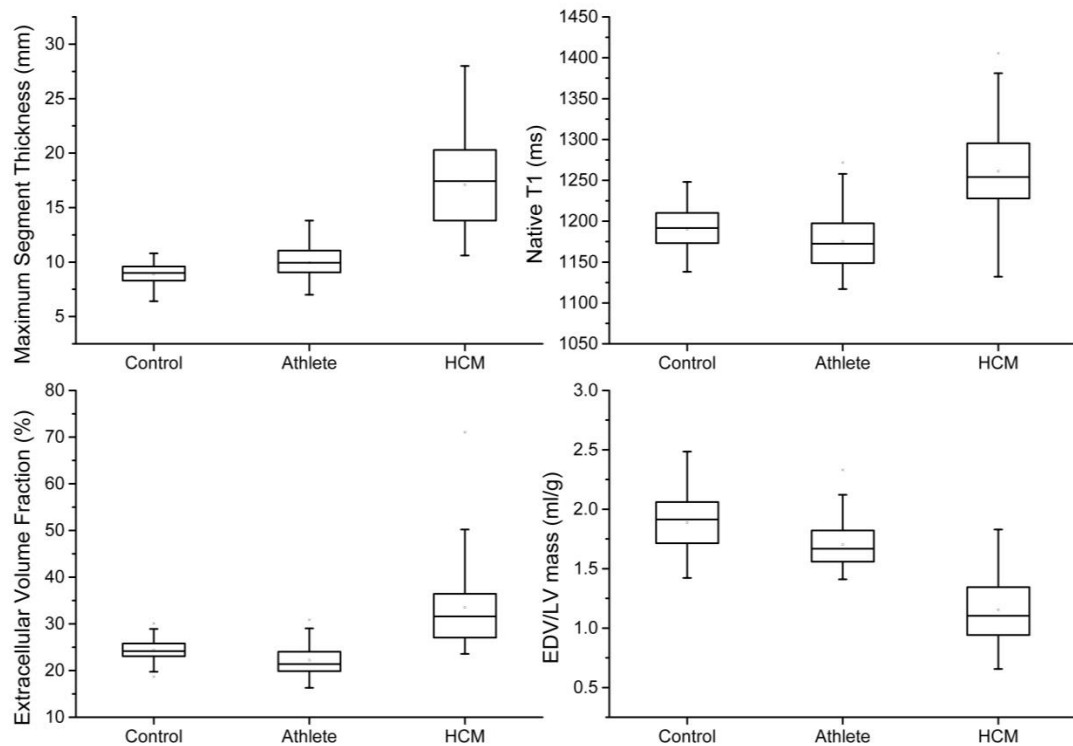
Figure 2.2 Box and whisker plots showing maximum segment thickness, native T1, ECV and EDV/LVM for athletes, controls and HCMs showing median (line), mean (small square), interquartile range (box) and outliers (whiskers).

Native T1 and ECV of the thickest segment were both significantly lower in athletes than HCMs (1175.5.8 ±37.3ms vs 1261.1±52.3ms and 22.2±3.5% vs 32.8 ±9.0%, P<0.001 for both). LV mass and LVMI were not significantly different between athlete and HCM (P=0.46 and P=0.97 respectively). LV EDV and LV EDVI were higher in athletes (219.4±34.3ml vs 155.0±32.2ml and 115.1±14.3ml/m^2 vs 78.7±13.13ml/m^2, P<0.001 for both) and EF lower (56.0 ± 4.5% vs 62.3 ± 5.9%, P<0.001). EDV/LV mass was higher in athletes than HCMs (1.7±0.2ml/g vs

1.2±0.3ml/g, P<0.001). Two (5.8%) athletes had subepicardial lateral LGE in a myocarditis pattern, no controls had LGE and 35 (70%) HCMs had LGE.

Native T1 and ECV of the thickest segment were both significantly lower in athletes than controls (1175.5±37.3 vs 1195.9±42.7ms, P=0.049 and 22.2±3.5% vs 24.4±2.8%, P=0.004).
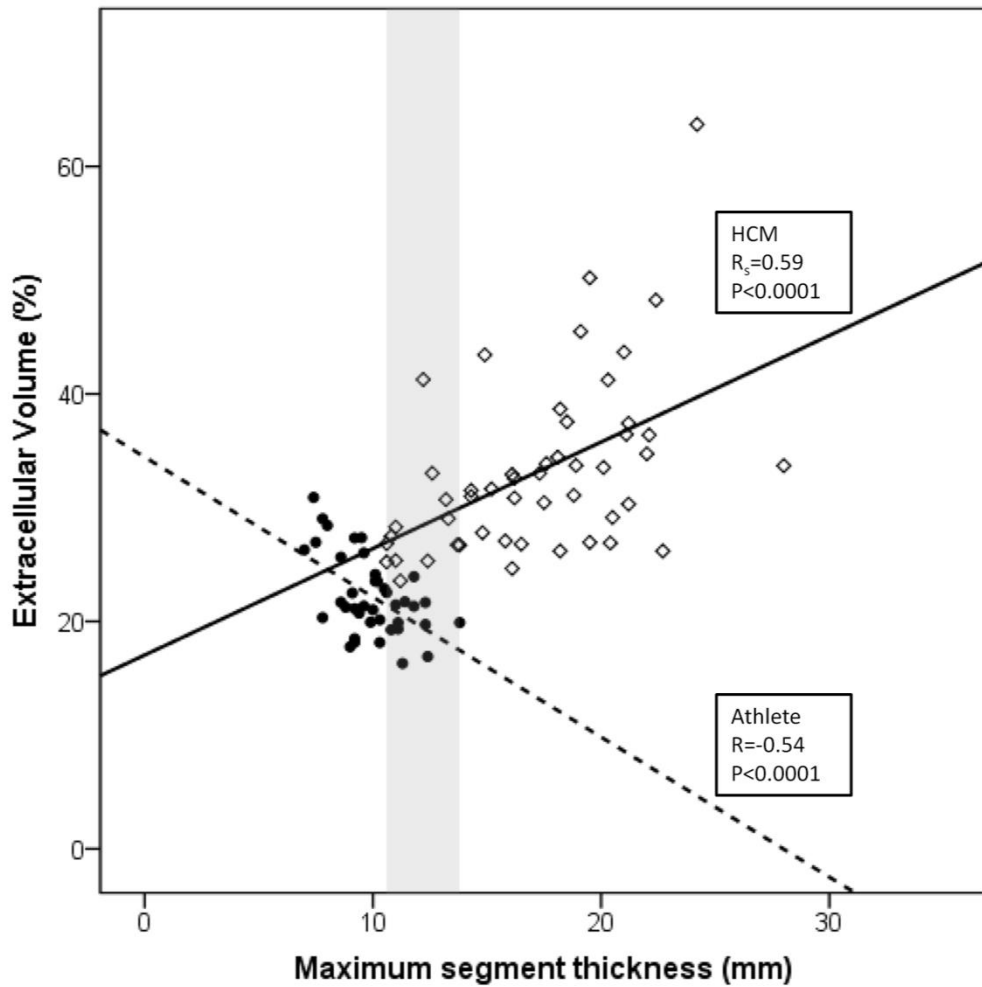
Figure 2.3 Scatter plot showing maximal segmental thickness and corresponding ECV of the same segment. HCMs are hollow diamonds with solid trend line and athletes are filled circles with a dashed line. They grey area highlights the indeterminate zone between the thinnest maximal thickness HCM segment (10.6mm) and thickest maximal thickness athlete segment (13.8mm).

	Athlete	Control	HCM	P value
LV EDV, ml	219.4±34.3	183.5±32.3	155.0±32.2	<0.001
LV EDV indexed to BSA, ml/m^2	115.1±14.3	92.6±14.3	78.7±13.1	<0.001
LV ESV, ml	96.6±19.0	79.2±18.3	59.1±17.7	<0.001
LV Ejection Fraction, %	56.0±4.5	57.1±4.4	62.3±5.9	<0.001
LV Mass, g	130.7±25.3	99.1±22.0	143.2 ± 50.1	<0.001
LV Mass indexed to BSA, g/m^2	68.7±10.6	50.0±9.6	72.8 ± 26.3	<0.001
LV EDV/ LV mass, ml/g	1.7±0.2	1.9±0.3	1.2±0.3	<0.001
Left atrial volume, ml	100.0±17.2	88.1±19.2	116.6±28.9	<0.001
LAV indexed to BSA, ml/m^2	53.1±8.1	44.4±7.8	59.3±13.5	<0.001
Maximal segment thickness, mm	9.9±1.5	8.9±1.2	17.1±4.0	<0.001
LGE, n (%)	1 (2.9)	0 (0)	35 (70)	<0.001
LVOT obstruction, n (%)	0	0	11 (22)	<0.001
LVOT gradient, mmHg	0	0	68.5 ± 40.0	NA
Thickest segment native T1, ms	1175.5±37.3	1195.9±2.7	1261.1±2.3	<0.001
Thickest segment ECV, %	22.2±3.5	24.4±2.8	32.8±9.0	<0.001

Table 2.2 CMR findings. BSA, body surface area; ECV, extracellular volume; EDV, end diastolic volume; ESV, end systolic volume; LAV, left atrial volume; LGE, late gadolinium enhancement; LV, left ventricle; LVOT, left ventricular outflow tract

In athletes there were significant negative correlations between ECV and maximum segment thickness(r=-0.54, P<0.001), LV mass (r=-0.48, P<0.01) and LVMI (-0.42, P<0.01), see Figure 2.3. In controls there were significant negative correlations between ECV and maximum segment thickness(r=-0.45, P<0.01), LV mass (r=-0.42, P=0.01) and LVMI (-0.34, P=0.046). In HCMs there was a significant positive correlations between ECV and maximum segment thickness (r_s=0.51, P<0.001) but no correlation with LV mass (P=0.42) or LVMI (P=0.34). For athletes, controls and HCM there were no significant correlations between native T1 and maximum segment thickness, LV mass or LVMI.

2.4.1 Diagnostic performance

To detect the 50 HCMs from the 40 athletes the diagnostic accuracy (AUC) of maximal segment thickness, native T1, ECV and EDV/LV mass were 0.962 [0.899-0.991], 0.914 [0.836-0.963], 0.945 [0.876-0.982] and 0.944 [0.875-0.982] respectively, P<0.001 for all. There was no significant difference between AUCs, Figure 2.4. In this cohort the optimal cut-offs to diagnose HCM were maximal segment thickness>12.4mm (sensitivity 84%, specificity 98%), ECV >24.1% (sensitivity 98%, specificity 78%), native T1 >1207.8ms (sensitivity 90%, specificity 83%) and EDV/LV mass ≤1.36ml/g (sensitivity 78%, specificity 100%).

We identified 26 indeterminate subjects (13 athlete and 13 HCMs) whose maximum segment thickness fell in the overlapping range of 10.6-13.8mm, Table 2.3. AUCs for native T1, ECV, and EDV/LV mass were 0.953 [0.790-1.000], 0.994 [0.857-1.000], and 0.793 [0.590-0.925] respectively P<0.001 for all, Figure 2.5. AUC for maximal segment thickness was not significant 0.553 (0.124-0.747) P=0.46. The diagnostic accuracy of ECV was significantly better than EDV/LV mass (P=0.03). Native T1 was not significantly better than EDV/LV mass (P=0.08). The difference between ECV and native T1 was not significant (P=0.29). Native T1 and ECV were better than segment thickness (P<0.001 for both). EDV/LV mass was not significantly better than segment thickness (P=0.1). In patients with indeterminate maximal segment thickness the optimal cut-offs to diagnose HCM were ECV>22.5%

(sensitivity 100%, specificity 92%), native T1>1190.4 (sensitivity 100%, specificity 77%).

We also identified 15 subjects with maximum segment thickness of 12-15mm (Elliott et al., 2014; Gersh et al., 2011) (4 athletes and 11 HCMs). AUCs were; native T1 0.977[0.909-1.000] P=0.006 and ECV 1.000[1.000-1.000] P=0.006. AUCs for EDV/LV mass 0.818 [0.599-1.000] P=0.07 and segment thickness 0.761 [0.488-1.00] P=0.13 were not significant. Differences between AUCs were not significant.

	Athlete	HCM	P value
N	13	13	NA
Male gender; n (%)	13 (100)	8 (74)	0.80
Age, years	35.3±5.7	44.0±12.2	0.03
LV EDV indexed to BSA, ml/m^2	117.7±17.3	81.4±12.9	<0.001
LV Mass indexed to BSA, g/m^2	73.6±11.7	62.2±24.1	0.03
LV EDV/ LV mass, ml/g	1.6±0.2	1.4±0.3	0.01
LAV indexed to BSA, ml/m^2	55.9±8.7	48.5±7.8	0.03
LGE (%)	1 (8)	6 (46)	0.03
LVOT obstruction (%)	0	0	NA
Thickest segment native T1, ms	1166.1±35.7	1249.8±42.6	<0.001
Thickest segment ECV, %	20.3±2.1	28.4 ±4.6	<0.001
FH of HCM; N (%)	0	5 (38)	0.04

Table 2.3 Characteristics of 26 subjects in the indeterminate range of maximal segment thickness 10.6-13.8mm. BSA, body surface area; ECV, extracellular volume; EDV, end diastolic volume; ESV, end systolic volume; LAV, left atrial volume; LGE, late gadolinium enhancement; LV, left ventricle; LVOT, left ventricular outflow tract

2.4.2 Combinations of Native T1, ECV and EDV/LV mass

When the results of native T1 and ECV were combined with EDV/LV mass there were further improvements in the diagnostic accuracy. AUCs for the nested models were EDV/LV mass + native T1 0.979 [0.954-1.000] and EDV/LV mass + ECV 0.996 [0.989-1.000] (P<0.001 vs EDV/LV mass for both). In indeterminate subjects AUCs for nested models were EDV/LV mass + native T1 0.911 [0.798-1.000] and EDV/LV mass + ECV 0.994 [0.975-1000] (P<0.001 vs EDV/LV mass for both).

2.4.3 Net Reclassification Index

When native T1 was added to EDV/LV mass 14 HCMs (28%) were re-classified correctly and 2 (4%) re-classified incorrectly. 19 (47.5%) athletes were reclassified correctly and 5 (12.5%) incorrectly (NRI=0.59, P<0.001). When ECV was added to EDV/LV mass 16 HCMs (32%) were re-classified correctly and 2 (4%) re-classified incorrectly. 21 (52.5%) athletes were reclassified correctly and 3 (7.5%) incorrectly (NRI=0.73, P<0.001).

In indeterminate subjects when native T1 was added to EDV/LV mass 6 HCMs (46%) were re-classified correctly and 1 (7.7%) re-classified incorrectly. 7 (54%) athletes were reclassified correctly and 1 (8%) incorrectly (NRI=0.85, P=0.005). When ECV was added to EDV/LV mass 7 HCMs (54%) were re-classified correctly and 2 (15%) re-classified incorrectly. 9 (69.2%) athletes were reclassified correctly and 0 (0%) incorrectly (NRI=1.08, P=0.001).
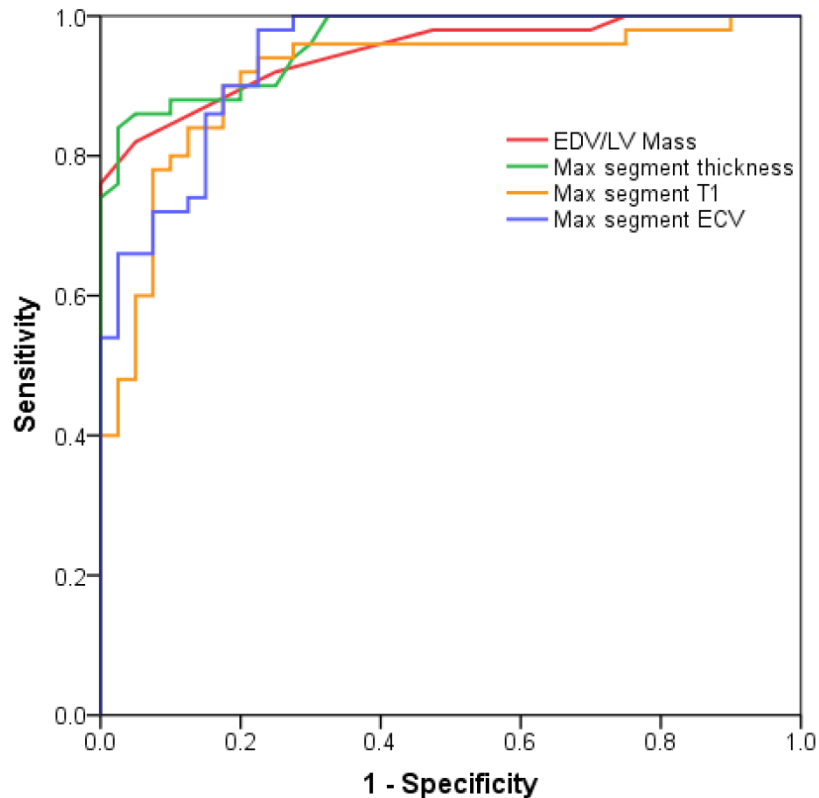
Figure 2.4 Receiver operator characteristic curves for maximal segment thickness, native T1, ECV and EDV/LV mass for the detection of HCM against athletes. AUCs were 0.96, 0.91, 0.95 and 0.94 respectively P<0.001 for all. There was no significant difference between each of the measures.

2.4.4 Segmental Analysis

For segmental analysis, 640 athlete segments and 800 HCM segments were available. Of these, there were 23 athlete segments and 128 HCM segments in the indeterminate wall thickness range of 10.6-13.8mm. There were 123 HCM segments and no athlete segments >13.8mm. Native T1 and ECV were analysable for 149/151 of all indeterminate segments. The AUCs for ECV, native T1 and segment thickness to detect HCM segments against athlete segments in the indeterminate wall thickness diagnostic range were 0.90, 0.86, and 0.74 respectively (P<0.001 for all, Figure 3.5). The diagnostic accuracy of ECV was superior to segment thickness (P= 0.03). The differences between native T1 and segment thickness, and native T1 and ECV were non-significant (P=0.06 and P=0.32 respectively).

2.4.5 Late Gadolinium Enhancement

2/40 athletes and 35/50 HCMs had LGE. Therefore the sensitivity and specificity of LGE on a per patient basis to diagnose HCM were 70% and 95% respectively. The AUC of LGE to diagnose HCM correctly was 0.825[0.731-0.897] P<0.001. The AUC of segment ECV was significantly better than LGE (P=0.002) although the difference between native T1 and LGE was non-significant (P=0.08). Of the 26 subjects with indeterminate maximal segment thickness 1/13 (8%) athletes and 6/13 (46%) HCMs had LGE. The AUC of LGE to diagnose HCM in these subjects was 0.692[0.482-0.857] P=0.02 and was significantly worse than the AUC of native T1 and ECV (P<0.001 for both).

24/151 indeterminate HCM segments had LGE and 1/23 indeterminate athlete segments had LGE. T1 maps were degraded by artefact in 2 HCM segments from the same patient and could not be analysed. When ROC analysis was performed on the 147 remaining LGE -ve segments of indeterminate wall thickness AUCs of ECV, native T1 and segment thickness remained significant (0.89, 0.86, 0.74 respectively, P<0.001 for all).
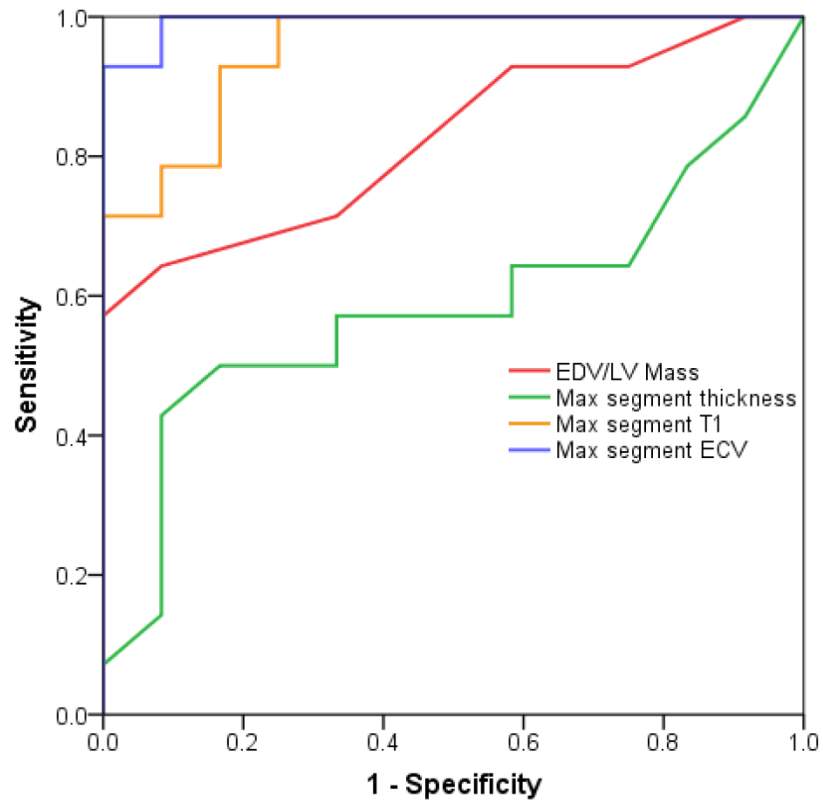
Figure 2.5 Receiver operator characteristic curves for native T1, ECV and EDV/LV mass for the detection of HCM against athletes of the 26 subject (13 HCM and 13 HCM) in with indeterminate maximal segment thickness. AUCs were 0.95, 0.99 and 0.82 respectively P<0.0001 for all. AUC for maximal segment thickness was 0.553 P=0.46. The diagnostic accuracy of ECV was significantly better than EDV/LV mass (P=0.03). EDV/LV mass was not significantly better than segment thickness (P=0.1).

2.5 Discussion

In this study we have demonstrated that ECV measured by CMR T1 mapping is lower in athletes than in patients with HCM and this difference can be utilised to distinguish athlete's heart from HCM, in particular in subjects with indeterminate maximal wall thickness, where the differential diagnosis between the two entities is most challenging. In these intermediate subjects, ECV was 20.3±2.1% in athletes and 28.4±4.6% in HCMs, permitting accurate distinction. Furthermore we have demonstrated that ECV is lower in athletes than healthy controls and that in both athletes and controls there is a strong negative correlation between ECV and LV mass suggesting that the increase in LV mass in healthy myocardium is mediated

by cellular hypertrophy rather than extracellular expansion. ECV was a better discriminator between athlete's heart and HCM than EDV/LV mass or the presence of LGE.

HCM is characterised by macroscopic and microscopic cardiac changes. Macroscopic changes are typified by differing patterns of LV hypertrophy, including asymmetric septal, concentric or apical hypertrophy and mitral valve abnormalities. Microscopic change is characterised by expansion of the extracellular space secondary to fibrosis and myocyte disarray (Varnava et al., 2001), with the development of replacement fibrosis as the disease progresses. Current non-invasive imaging techniques rely upon the identification of gross cardiac abnormalities to confirm the diagnosis of HCM but do not interrogate microscopic change and change in tissue composition.

A CMR protocol including assessment of cardiac morphology, scar with LGE imaging and myocardial tissue composition using T1 mapping and ECV calculation can provide a comprehensive assessment of both macroscopic and microscopic change associated with HCM. Several imaging parameters have been previously proposed to distinguish between physiological LVH and HCM including: left atrial remodelling (Pelliccia et al., 2005), changes in strain pattern (Vinereanu et al., 2001), maximal oxygen consumption during cardiopulmonary exercise testing (Sharma et al., 2000) or composite assessments of multiple imaging findings (Caselli et al., 2014). Of these EDV/LV mass has been reported to be one of the best CMR discriminatory methods (Luijkx et al., 2013). In this study, to differentiate HCM from athletic remodelling native T1 and ECV performed as well as EDV/LV mass and maximum segment thickness in all patients and significantly better when segment thickness fell in the indeterminate zone. Therefore both native T1 and ECV have incremental value over established parameters. Furthermore we have demonstrated that in patients with indeterminate maximal segment thickness, a cut-off of 1190ms for native T1 or 22.5% for ECV was able to identify all patients with HCM correctly.

We have also demonstrated that segmental wall thickness correlates with ECV in HCM with an inverse correlation seen in athletic adaptation. It is widely recognised that in HCM that ECV correlates with histological (Flett et al., 2010; Iles et al., 2015)

and cellular markers of fibrosis (Fang et al., 2013). The divergent finding that with increasing hypertrophy ECV decreases in athletes but increases in HCM provides a mechanistic explanation as to why ECV has high diagnostic accuracy and performs better than maximum segment thickness or EDV/LV mass in subjects with indeterminate hypertrophy.

Myocyte disarray and fibrosis are the earliest pathological changes seen in HCM. Therefore changes in ECV can be detected before the development of hypertrophy. Left atrial dilatation, LVOT obstruction and replacement fibrosis (detectable as LGE) occur much later in the disease process and these parameters are therefore less useful in subjects with indeterminate maximal segment thickness.

On analysis of indeterminate subjects and segments ECV performed better than native T1 for the diagnosis of HCM. However measurement of native T1 still has merits that would support its use in this clinical application. Its measurement does not require intravenous cannulation, administration of contrast, or a blood sample to measure haematocrit. The major shortcoming of native T1 is that it varies significantly between field strengths, scanner vendor and technique used to measure it (Raman et al., 2013). Use of native T1 maps in clinical practice requires validation for the specific pulse sequence and field strength used (Moon et al., 2013) . ECV on the other hand is less dependent on imaging platforms and field strengths (Raman et al., 2013) but does require the administration of a gadolinium based contrast agent.

In our study 70% of HCM patients had abnormal LGE consistent with the reported prevalence of 40 to 80% (Chan et al., 2014; Rudolph et al., 2009). The high specificity (97.5%) of LGE in diagnosing HCM indicates that it is useful for confirming the diagnosis. In our study ECV still had a high diagnostic accuracy even in segments without focal scar on LGE. Therefore ECV is useful in differentiating athlete's heart from the significant proportion of HCM that does not have LGE.

2.6 Limitations

All athletes were white and it remains to be established if our findings are applicable to other racial groups. The athletes in this study trained predominantly in endurance sports and had a high aerobic capacity (mean VO_2max 58.3 ± 9.0

ml/kg/min) and whether our findings are applicable to non-endurance athletes is not known. However there is conflicting evidence about whether non-endurance training leads to cardiac remodelling (Utomi et al., 2013; Maron and Pelliccia, 2006).

The indeterminate zone from our population was 10.6-13.8mm which is less than the 12-15mm termed indeterminate in current guidelines (Gersh et al., 2011; Elliott et al., 2014). However we have measured segment thickness only from the same slice as the T1 maps to ensure they are from identical tissue. In our cohort maximum thickness measured by echocardiography was 2.2mm greater and it is likely that our indeterminate zone corresponds to 12-15mm measured from anywhere in the LV.

There are still controversies about which is the most robust pulse sequence for measurement of myocardial T1 relaxation time. The dose of contrast, the number and timings of acquisitions also need to be considered. ECV was marginally lower in our healthy controls than in other published work which may reflect differences in vendor, field strength, pulse sequence, contrast regime and number of T1 measurements after contrast administration (Kellman et al., 2012; Dabir et al., 2014). At present it is therefore recommended that each site establish normal values considering these variables (Moon et al., 2013) prior to the clinical use of ECV in the athlete with unexplained LV hypertrophy.

2.7 Conclusions

As LV hypertrophy increases ECV decreases in athletes but increases in HCM. Based on this divergent finding ECV can be used distinguish HCM and athletic remodelling with high diagnostic accuracy, in particular in subjects with indeterminate maximal segmental wall thickness. CMR using T1 mapping thus has a potential role in the exclusion of HCM in athletes presenting with left ventricular hypertrophy, but requires further validation in larger and more varied patient populations.

3. Study 2- Regional contractile dysfunction in hypertrophic cardiomyopathy is associated with extent of hypertrophy rather than diffuse fibrosis

3.1 Abstract

Introduction

At present the diagnosis of hypertrophic cardiomyopathy (HCM) is made when one or more segment measure ≥15mm using cardiac imaging. International guidelines recommend the use of strain imaging in borderline cases. Using cardiovascular magnetic resonance (CMR) extracellular volume (ECV) mapping techniques it is possible to detect early phenotypic manifestation of HCM, such as extracellular matrix expansion, which can occur before overt hypertrophy. It is unknown whether strain impairment occurs early in the disease process when there is ECV expansion with overt hypertrophy.

Methods

50 patients with HCM underwent CMR studies at 3.0T including cine imaging in multiple planes, T1 mapping for calculation of ECV and late gadolinium enhancement (LGE) imaging. For each segment of the American Heart Association (AHA) model of each subject segment thickness, the presence of LGE and strain by feature tracking were measured.

Results

Circumferential strain by feature tracking (Ecc-FT) was lower in segments with ECV expansion (-17.0±10.3 vs -19.9±8.4%, N=783 P<0.001). However in segments <15mm Ecc-FT was not significantly different between those with and without ECV expansion (19.7±9.2 vs -20.6±7.9%, N=684, P=0.43). In segments <15mm Ecc-FT was significantly lower in those with LGE (-12.9±8.2 vs -20.9±8.1%, N=684, P<0.001) There were significant correlations between Ecc-FT and both segment thickness and ECV (R_s=0.616 and 0.176 P<0.001 for both). However on multivariable linear

regression only segment thickness had a significant association with Ecc-FT (beta=-0.54, p<0.001).

Conclusion

Regional strain impairment is predominantly associated with the degree of hypertrophy and replacement fibrosis assessed by the presence of LGE. In non-hypertrophied segments strain is not significantly impaired by the presence of interstitial fibrosis detected by ECV expansion on T1 mapping. Therefore the presence of interstitial fibrosis may be a more useful method than impairment of strain of identifying HCM in subjects with borderline LV hypertrophy.

3.1 Introduction

HCM is commonly defined as a disease of hypertrophy of the LV in the absence of another cardiac or systemic cause (Gersh et al., 2011). It is typically caused by autosomal dominant mutations of genes encoding sarcomeric proteins and myofilament elements (Bos et al., 2009). These mutations lead to micro- and macroscopic changes within the heart including cellular disarray, hypertrophy and interstitial fibrosis. When myocyte disarray is widespread it is a sensitive and specific marker for HCM (Hughes, 2004). These changes lead to hypertrophy that can affect the heart in a variety of patterns, and may affect any segment of the LV (Klues et al., 1995). Although hypertrophy can be widespread, phenotypic expression within the same heart can be variable and less than half of the ventricle may be hypertrophied in as many as 50% of patients (Maron et al., 2009b).

At present the diagnosis of HCM is primarily made by the identification of one or more hypertrophied segments by a cardiac imaging modality (Gersh et al., 2011; Elliott et al., 2014). In the majority of cases this involves identification of a segment ≥15mm by echocardiography. Increasingly CMR is used to confirm or make diagnosis of HCM when echocardiography is restricted by limited acoustic windows or the inability to assess all segments of the left ventricle.

In addition to accurate volumetric measurement, CMR may also make an assessment of microscopic expression of the HCM phenotype. Cellular disarray and extracellular matrix expansion occur early in the disease process and can be detected by using quantitative T1 and ECV mapping; techniques which demonstrate good correlation with histology specifically in HCM (Flett et al., 2010; White et al., 2013). ECV expansion can be detected in genotype positive patients prior to the onset of overt hypertrophy (Ho et al., 2013). Replacement fibrosis occurs later in the disease process and is detected as the presence of LGE. Replacement fibrosis is progressive over the course of the disease (Todiere et al., 2012) and its presence is associated with an adverse prognosis (Chan et al., 2014).

Studies, predominantly using echocardiography speckle tracking to measure regional and global strain have demonstrated that impaired contractility is related

to the extent of hypertrophy and the presence of replacement fibrosis detected by LGE (Urbano-Moral et al., 2014; Popovic et al., 2008). Current guidelines therefore recommend that strain imaging could be used to investigate unexplained left ventricular hypertrophy that is not diagnostic of HCM (Gersh et al., 2011; Elliott et al., 2014). An alternative method to echocardiography for the assessment of regional strain is CMR tagging which is highly reproducible in this setting (Shehata et al., 2009; Swoboda et al., 2013). More recently, post processing feature tracking of cine CMR images allows quantification of strain without the need for acquisition of tagged images. Strain measured by feature tracking and tissue tagging are reported to show good agreement (Moody et al., 2015).

Current evidence suggests that regional function assessed by strain imaging may be impaired later in the disease process of HCM when there is overt hypertrophy and replacement fibrosis. It is unknown whether impairment of contractile function occurs earlier in the disease process when there is myocyte disarray and extracellular matrix expansion in the absence of overt hypertrophy.

We hypothesised that ECV expansion occurs prior to impairment of contractile function in the pathogenic process. We therefore assessed contractile function in segments with early (non-hypertrophied with ECV expansion) and late (hypertrophied with replacement fibrosis) phenotypic expression to establish whether impairment of systolic function is an early or late feature of HCM.

3.2 Methods

3.2.1 Enrolment Criteria

 50 patients with HCM under the age of 65 with HCM were prospectively recruited from the Inherited Cardiovascular Conditions Service at Leeds General Infirmary, Leeds, UK. The diagnosis of HCM was made independently by clinicians in keeping with current guidelines and based upon imaging including CMR, ECG, exercise testing, family history and genetic testing if possible (Elliott et al., 2014; Gersh et al., 2011). Exclusion criteria were previous surgical myomectomy, previous septal ablation, atrial fibrillation, previous myocardial infarction, uncontrolled

hypertension, permanent pacemaker, defibrillator or other contraindication to CMR. 35 healthy controls who had no existing medical conditions were also recruited to establish the normal range of ECV using the CMR protocol. The study was conducted in accordance with the declaration of Helsinki and was approved by the local ethics committee (14/YH/0126). All subjects gave informed written consent.

3.2.2 CMR protocol

All subjects underwent an identical CMR protocol performed on a 3.0 Tesla Philips Achieva TX system (Philips, Best, The Netherlands) equipped with a 32 channel cardiac phased array receiver coil. A full blood count, including haematocrit was measured at the time of intravenous cannulation. The cardiac long and short axes were determined using standard scout views. Basal, mid and apical pre-contrast (native) short axis T1 maps were generated using a validated MOLLI protocol (Kellman et al., 2013) (ECG triggered 5b(3s)3b MOLLI scheme with voxel size of 1.98 x 1.98 mm^2, slice thickness 10mm) and were planned using the 3 of 5 method (Messroghli et al., 2005). Tissue tagging using a spatial modulation of magnetization (SPAMM) pulse sequence (spatial resolution 1.51x1.57x10mm^3, tag separation 7 mm, ≥18 phases, typical TR/TE 5.8/3.5 ms, flip angle 10°, typical temporal resolution 55ms) was acquired in the same three short axis slices in 34/50 patients. Left ventricular volumes were obtained from cine imaging covering the entire LV in the short axis: balanced SSFP, voxel size 1.2 x 1.2mm^2, slice thickness 10mm with no gap, 50 cardiac phases. Left atrial (LA) volumes were obtained from cine imaging covering the entire heart in the transverse axis: balanced SSFP, voxel size 1.2 x 1.2mm^2, slice thickness 6mm with no gap, 50 cardiac phases. 0.15mmol/Kg Gadovist (Bayer Schering) was delivered by power injector (Medrad Inc, Warrendale, Pennsylvania, USA) as a single bolus via a cannula placed in the ante-cubital fossa followed by 20ml saline flush. Typical parameters were TR/TE 3.5/2.0 ms, flip angle 25°, acquired spatial resolution 1.54x1.76x10mm^3 and performed in 10-12 short axis slices with ≥3 long axis orientations and phase-swapped acquisitions if indicated. Post contrast T1

mapping was carried out in the same three slices exactly 15 minutes following last contrast injection (as above).

3.2.3 CMR interpretation

Analysis was carried out using CVI42 (Circle Cardiovascular Imaging Inc. Calgary, Canada) and inTag (v1.0, CREATIS lab, Lyon, France) by two physicians blinded to clinical data. LV mass, EDV, ESV and LV EF were measured from short axis cine images. Native and post contrast T1 relaxation time of myocardium and blood pool were measured from the scanner generated T1 maps by contouring a region of interest in each segment of the American Heart Association (AHA) model (Cerqueira et al., 2002). ECV was calculated from native and post contrast T1 times of myocardium and blood pool and haematocrit as previously reported (Flett et al., 2010). Segment thickness was measured for each AHA segment from end-diastolic SSFP cine images corresponding to the T1 maps. Feature tracking analysis was carried out on the same images by drawing endocardial and epicardial contours and circumferential (Ecc-FT) and radial (Err-FT) strain calculated for each AHA segment.

For tagging analysis endocardial and epicardial contours were drawn on the short axis SPAMM sequences. Peak circumferential strain was measured for each segment of the AHA model. Strain was measured in the mid-myocardial layer which has previously been reported to be the most reproducible (Swoboda et al., 2013).

Segments were defined as hypertrophied if the maximal thickness was ≥15mm in keeping with current guidelines (Gersh et al., 2011; Elliott et al., 2014). The normal range for ECV derived from healthy volunteers was 24.4±2.8%. Therefore segments that were >30% (+2SD from the normal range) were defined as having extracellular expansion. Replacement fibrosis was defined as the presence of LGE reported by 2 physicians experienced in CMR interpretation for each segment for a corresponding slice to T1 maps. All analyses were carried out blinded to the results of strain analysis.

3.2.3 Statistical analysis

Continuous variables were expressed as means ± SD. Categorical variables were expressed as N (%). Shapiro-Wilk test was used to test normality then unpaired T test or Mann Whitney U test used as appropriate. Spearman's rank correlation was used for linear correlations. Univariable analyses were performed to identify predictors of strain. Variables with a probability value <0.1 in the univariable analysis were included in a multivariable linear regression analysis. P<0.05 was considered statistically significant.
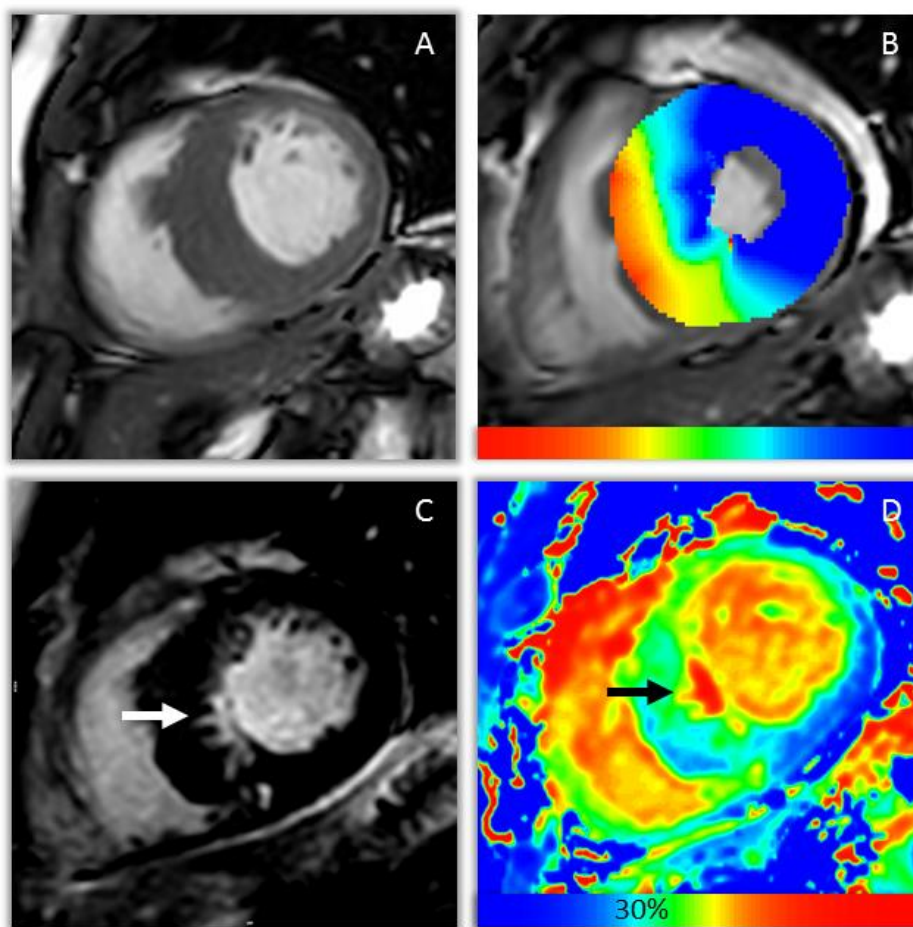
Figure 3.1 CMR images from a patient with asymmetric septal HCM. A- SSFP imaging of the basal septum showing gross hypertrophy (>15mm) in anteroseptum and inferoseptum. All other segments are less than 15mm. B- Radial strain map derived from feature tracking of the same slice, shown in systole. Colour scale ranges from akinetic (red) to >20% strain (blue). C- Late gadolinium enhancement imaging showing a discrete area of replacement fibrosis in inferoseptum (white

arrow). D- ECV map ranging from 0 (blue) to 100% (red). The transition point of 30% above which is defined as extracellular expansion is cyan. Note the replacement fibrosis seen on LGE imaging (black arrow) and the non-hypertrophied anterior and anterolateral walls have marked ECV expansion (35-45%) yet have normal radial strain on FT imaging.

3.3 Results

Patient characteristics are shown in Table 3.1. The distribution of hypertrophy was asymmetrical septal 36 (72%), concentric 5 (10%), mid cavity 4 (8%), apical 3 (6%) and isolated lateral 2 (4%). An example of cine imaging, strain, LGE and ECV mapping from an identical slice of one patient is shown in Figure 3.1. Maximum segment thickness, ECV, the presence of LGE and circumferential and radial strain findings are shown in Table 3.2. Segment thickness, LGE and tissue tagging could be analysed in all available segments. ECV could not be analysed in 43/800 segments because of artefact. Ecc-FT could not be analysed in 17/800 and Err-FT in 12/800 because of either artefact or poor tracking of myocardial features.

There were 99 hypertrophied segments (>15mm) and 701 non-hypertrophied segments. Ecc-FT (-8.5±8.6 vs -20.3±8.3%, N=783, P<0.001), Err-FT (15.2±12.8 vs 45.0±27.2%, N=788, P<0.001) and Ecc-SPAMM (-11.1±4.8 vs -20.4±8.1%, N=544, P<0.001) were all lower in hypertrophied segments than non-hypertrophied segments.

There were 296 segments with extracellular expansion (ECV>30%) and 504 without extracellular expansion. Ecc-FT (-17.0±10.3 vs -19.9±8.4%, N=783, P<0.001), Err-FT (38.0±29.4 vs 43.2±26.4%, N=788, P=0.001) and Ecc-SPAMM (-17.3±8.7 vs -20.7±7.9%, N=544, P<0.001) were all lower in those with extracellular expansion than those without.

There were 107 segments with replacement fibrosis (LGE +ve) and 693 without replacement fibrosis. Ecc-FT (-10.6±8.5 vs -20.1±8.7%, N=783, P<0.001), Err-FT (18.7±15.5 vs 44.8±27.5%, N=788, P<0.001) and Ecc-SPAMM (-11.1±4.7 vs -20.5±8.1%, N=544, P<0.001) were all lower in those with replacement fibrosis than in those without.

N	50	FH of HCM, n (%)	19 (38)
Male gender, n (%)	37 (74)	**CMR findings**	
Age, years	46.9±11.7	LV EDV, ml/m^2	78.7 ± 13.1
Height, cm	171.2±9.0	LV EF, %	62.3 ± 5.9
Weight, kg	81.7±14.6	LV Mass, g/m2	72.8 ± 26.3
Body mass index, kg/m^2	27.7±3.7	LAV, ml/m^2	59.3 ± 13.5
Systolic blood pressure, mmHg	125.5±17.6	LGE, n (%)	35 (70)
Diastolic blood pressure, mmHg	74.5±12.5	**Medications**	
Heart rate	60.6±10.2	Beta blocker, n (%)	24 (48)
Echocardiography		CC blocker, n (%)	8 (16)
LVOT obstruction, n (%)	11 (22)	Disopyramide, n (%)	4 (8)
LVOT gradient, mmHg	68.5 ± 40.0	Diuretic, n (%)	2 (4)

Table 3.1 Patient characteristics and CMR findings. CC, calcium channel; EDV, end diastolic volume indexed to body surface area; EF, ejection fraction; FH, family history; LAV, left atrial volume indexed to body surface area; LGE, late gadolinium enhancement; LV, left ventricle; LVOT, left ventricular outflow tract

3.3.1 Linear correlation and regression

There were significant correlations between segment thickness and Ecc-FT, Err-FT and Ecc-SPAMM (R_s=0.616, -0.617 and 0.458 respectively, P<0.001 for all). There were significant but weaker correlations between ECV and Ecc-FT, Err-FT and Ecc-SPAMM (R_s=0.176, -0.165 and 0.195 respectively P<0.001 for all). There was also a significant correlation between segment thickness and ECV (R_s= 0.244, P<0.001) which is shown with radial strain in Figure 3.2.

On univariable linear regression analysis segment thickness, ECV and the presence of LGE all had significant associations with Ecc-FT, Err-FT and Ecc-SPAMM and were all included in multivariable analysis (Table 3.3). Only segment thickness had a significant multi-variate association with Ecc-FT and Err-FT (beta=-0.540 and 0.584 respectively, P<0.001 for both). Both segment thickness (beta=0.437, P<0.001) and LGE (beta=0.136, P=0.002) had significant associations with Ecc-SPAMM.
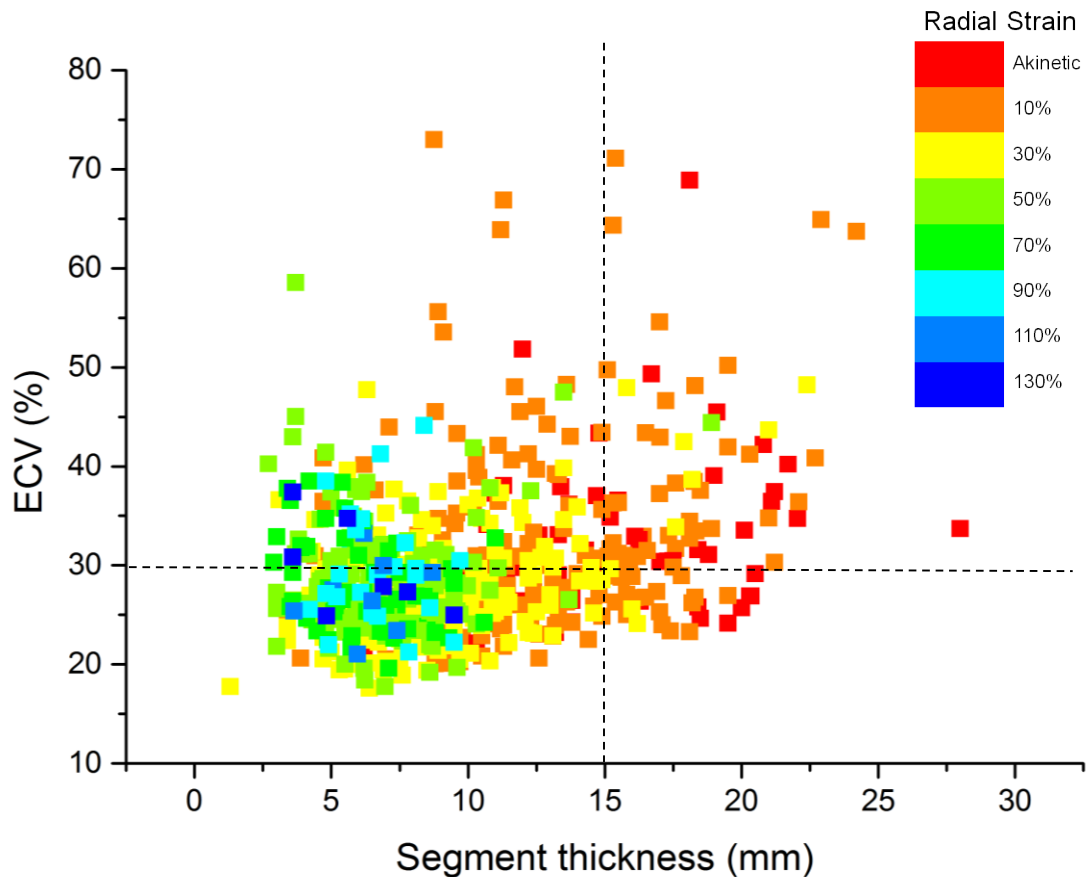
Figure 3.2 Scatter plot showing segment thickness (mm) and extracellular volume fraction (%) and radial strain (%) of each segment. Radial strain is represented as a colour scale ranging from akinetic (red) to hyperdynamic (blue). The upper left quadrant shows patients with phenotypic expression of HCM manifested as ECV expansion without hypertrophy. A significant proportion of segments in this quadrant have normal strain.

3.3.2 Analysis according to cellular composition of each segment

We examined strain in segments without overt hypertrophy according to the presence of early disease extracellular matrix expansion (ECV>30%) or later disease demonstrated by replacement fibrosis (LGE +ve).

Of the 701 segments of <15mm thickness, 474 had ECV<30% and 227 had ECV >30%. Ecc-FT (-19.7±9.2 vs -20.6±7.9%, N=684, P=0.43) and Err-FT (45.0±29.2 vs 44.9±26.1%, N=689, P=0.81) in non-hypertrophied segments were not significantly different in segments with ECV >30% compared to those with ECV<30% (Figure 3.3). Ecc-SPAMM however was significantly lower in non-hypertrophied segments with ECV>30% (-18.8±8.7 vs -21.1±7.8%, N=496, P=0.003).

Of the 701 segments of <15mm thickness 651 were LGE-ve and 50 LGE +ve. Ecc-FT (-12.9±8.2 vs-20.9±8.1%, N=684, P<0.001), Err-FT (23.3±16.0 vs 46.7±27.2, N=689, P<0.001) and Ecc-SPAMM (-11.9±4.9 vs -20.9±8.0, N=496, P<0.001) were all lower in non-hypertrophied segments with LGE compared to those without (Figure 3.3).

Of the 681 segments without replacement fibrosis (LGE -ve) 42 segments were >15mm, 192 were <15mm with ECV>30% and 459 were <15mm with ECV<30%. Comparing the non-hypertrophied segments (<15mm) there was no significant difference according to whether ECV was more or less than 30% Ecc-FT (-21.2±8.5 vs -20.8±7.9%, N=634, P=0.43), Err-FT (49.3±29.0 vs 45.5±26.3%, N=639, P=0.81) and Ecc-SPAMM (-19.7±8.8 vs -21.4 ±7.6, N=467, P=0.053).
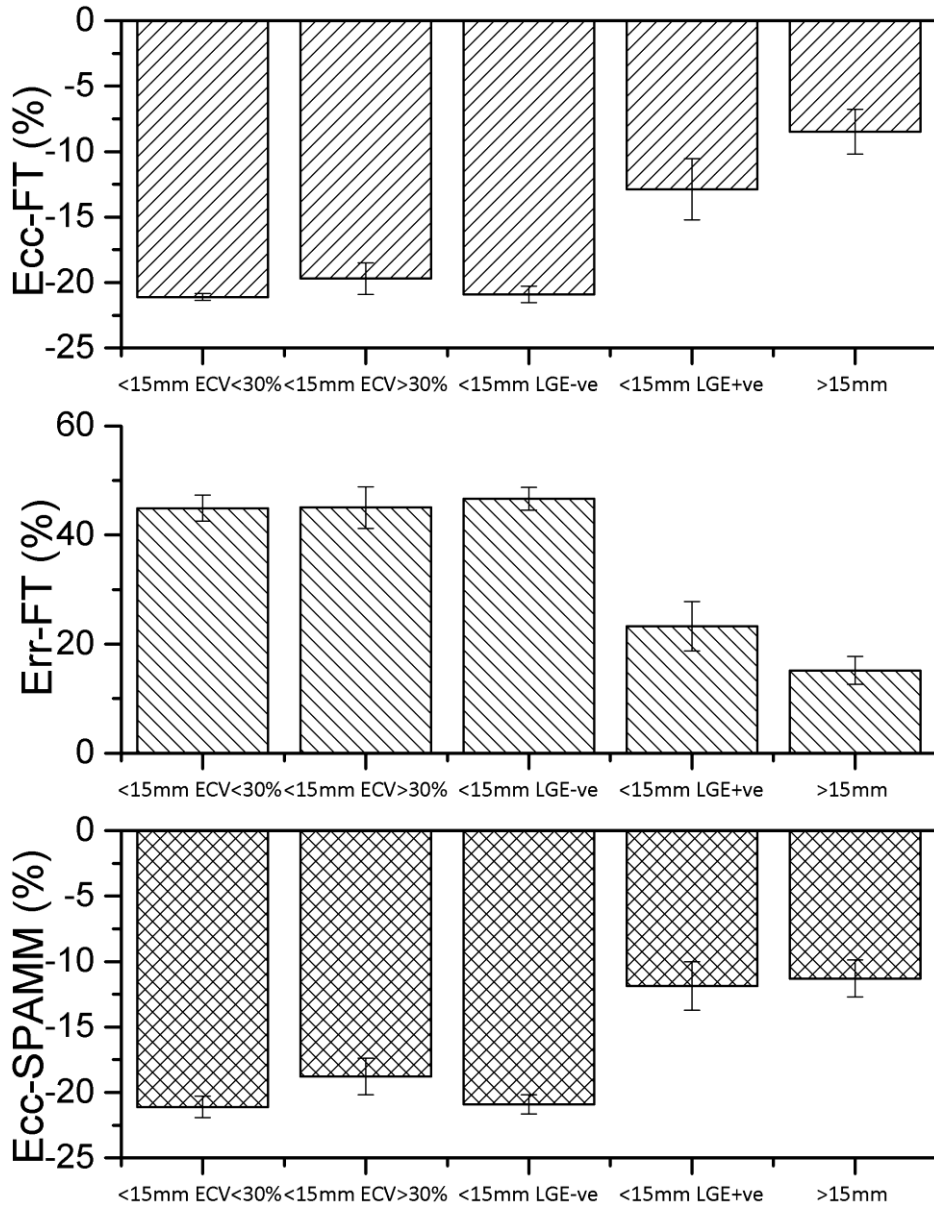
Figure 3.3 Circumferential and radial strain in hypertrophied segments and non-hypertrophied segments split into those with extracellular expansion (ECV>30%) and replacement fibrosis (LGE +ve) displayed as mean ± 95% confidence intervals. In non-hypertrophied segments strain was impaired in those with replacement fibrosis but not those with ECV expansion.

		Thickness (mm)	ECV (%)	LGE (N)	Ecc-FT (%)	Err-FT (%)	Ecc-SPAMM (%)
Base	**Anterior**	8.9±3.3, 50	29.1±7.6, 49	4, 50	-21.7±7.4, 50	48.6±28.3, 50	-21.1±7.4, 34
	Anteroseptum	14.9±3.8, 50	32.9±9.9, 50	20, 50	-10.7±7.9, 50	18.3±12.5, 50	-13.3±4.3, 34
	Inferoseptum	14.6±4.8, 50	30.3±5.3, 50	16, 50	-6.8±8.9, 48	11.3±12.2, 48	-14.3±4.7, 34
	Inferior	8.1±2.7, 50	26.5±3.7, 48	1, 50	-16.0±10.1, 49	34.4±22.4, 50	-19.8±6.1, 34
	Inferolateral	7.0±2.2, 50	27.0±4.6, 46	1, 50	-25.0±6.1, 48	58.5±25.9, 48	-27.1±7.8, 34
	Anterolateral	7.4±2.6, 50	25.5±3.5, 45	1, 50	-26.2±6.7, 48	69.2±35.0, 49	-27.6±6.8, 34
Mid LV	**Anterior**	8.4±3.2, 50	32.1±9.4, 43	5, 50	-20.1±10.5, 50	46.3±27.4, 50	-21.9±8.9, 34
	Anteroseptum	11.9±3.9, 50	33.0±9.1, 50	11, 50	-18.0±5.4, 50	33.5±15.7, 50	-14.1±5.5, 34
	Inferoseptum	12.9±4.2, 50	31.1±6.2, 49	16, 50	-13.0±8.6, 49	23.3±18.3, 49	-14.1±5.5, 34
	Inferior	8.3±2.9, 50	26.5±5.1, 48	3, 50	-17.4±6.2, 49	32.9±19.2, 49	-17.4±4.9, 34
	Inferolateral	7.1±2.7, 50	26.4±4.9, 48	1, 50	-23.5±5.6, 48	50.8±20.4, 50	-26.9±7.4, 34
	Anterolateral	8.1±2.6, 50	27.0±4.9, 45	1, 50	-22.3±8.7, 47	52.7±27.2, 50	-22.0±5.5, 34
Apex	**Anterior**	8.6±4.5, 50	34.0±10.2, 46	7, 50	-20.1±7.7, 49	44.9±27.9, 49	-19.7±9.6, 34
	Septum	9.2±4.0, 50	31.4±7.0, 47	9, 50	-20.7±6.4, 48	44.2±22.3, 48	-15.2±7.5, 34
	Inferior	7.3±3.3, 50	28.7±7.2, 47	7, 50	-19.8±8.9, 50	44.4±27.1, 50	-16.9±8.8, 34
	Lateral	8.3±3.5, 50	28.6±5.8, 47	4, 50	-20.3±8.5, 50	45.8±26.5, 50	-21.7±8.0, 34

Table 3.2 Mean ± SD followed by number of segments analysed segment thickness, extracellular volume (ECV), circumferential strain measured by feature tracking (Ecc-FT), radial strain measured by feature tracking (Err-FT) and circumferential strain measured by tissue tagging (Ecc-SPAMM) for each segment of the American Heart Association model. The number of segments that display replacement fibrosis on late gadolinium enhancement (LGE) is reported followed by the number of segments analysed.

			Segment thickness	Extracellular volume	LGE
Ecc-FT	Univariable	Beta	0.608	0.205	0.352
		P value	<0.001	<0.001	.001
	Multivariable	Beta	**0.584**	-0.008	0.58
		P value	**<0.001**	0.80	0.10
Err-FT	Univariable	Beta	-0.554	-0.165	-0.323
		P value	<0.001	<0.001	<0.001
	Multivariable	Beta	**-0.540**	0.038	-0.065
		P value	**<0.001**	0.27	0.08
Ecc-SPAMM	Univariable	Beta	0.471	0.163	0.335
		P value	<0.001	<0.001	<0.001
	Multivariable	Beta	**0.437**	0.014	**0.136**
		P value	**<0.001**	0.72	**0.002**

Table 3.3 Univariable and multivariable linear regression to evaluate which out of segment thickness, ECV and LGE have a significant association with impairment of segmental strain

3.4 Discussion

We have demonstrated that the main predictors of impairment of regional strain in HCM are degree of LV hypertrophy and presence of replacement fibrosis, which are both later features of HCM. Myocyte disarray and extracellular matrix expansion which can be detected by CMR as increased ECV earlier in the disease process do not appear to cause significant impairment of regional strain.

Myocyte disarray and collagen deposition are early features in the phenotypic expression of HCM and can be detected histologically or biochemically in subjects without overt hypertrophy (Varnava et al., 2001; Ho et al., 2010). Using CMR ECV mapping we have identified 296/800 segments with clear extracellular matrix expansion in the absence of overt hypertrophy. This is in keeping with pathological studies that have demonstrated that the extent of myocyte disarray has no correlation with segment thickness (Maron et al., 1992) and CMR studies that have shown ECV expansion in genotype positive patients without overt expression of a hypertrophied phenotype (Ho et al., 2013).

Our novel finding that contraction in non-hypertrophied segments is not significantly influenced by the presence of extracellular matrix expansion suggests that contractile dysfunction is a later process in the phenotypic expression of HCM. We have also reported that segmental strain is predominantly associated with segment thickness and the presence of replacement fibrosis assessed by the presence of LGE. These findings corroborate previous studies that have shown a relationship between degree of hypertrophy and presence of LGE and strain measured by speckle tracking echocardiography (Urbano-Moral et al., 2014; Popovic et al., 2008) and feature tracking by CMR (Smith et al., 2014). Dhillon et al measured longitudinal strain by feature tracking echocardiography in subjects with HCM undergoing surgical myomectomy, also reporting histological findings and in vitro contractility of the surgically excised myocardium. They found that the degree of histological fibrosis correlated with both strain measured by echocardiography and in vitro (Dhillon et al., 2014). However strain was measured in segments with severe hypertrophy causing LVOT obstruction and more than half of the specimens studied displayed small intramural coronary arteriole dysplasia which is known to correspond strongly with focal LGE detected by CMR (Kwon et al., 2009). Therefore the subjects studied were at the severe end of the hypertrophic spectrum and not directly comparable with our subjects and segments with a wide range of phenotypic presentations.

Current international guidelines advocate the use of strain imaging to investigate patients with unexplained LV hypertrophy but without a clear diagnosis of HCM (Gersh et al., 2011; Elliott et al., 2014). Our novel finding that CMR strain measurements are not able to identify those non-hypertrophied segments with interstitial fibrosis suggests that it is of limited use early in the disease process before the onset of overt hypertrophy and replacement fibrosis. Given that it is able to identify disease before impairment of strain we would advocate that it should be used more widely and preferentially over measurement of strain in the investigation of possible HCM.

3.5 Limitations

Our definition of 30% for ECV expansion was derived from 2SD above an age and sex matched normal range. ECV does not appear to be influenced by aging in healthy controls (Dabir et al., 2014) but may increase in patients with cardiac disease as they age (Ugander et al., 2012). ECV is influenced by pulse sequence, dose of contrast, number and timings of acquisitions. At present if ECV expansion is to be used to detect early HCM it is recommended that each centre derive their own normal range considering these variables and potentially a range of healthy controls of different ages (Moon et al., 2013).

We have only measured strain from short axis measurements specifically because the strength of the segmental analysis that we have carried out is based on the fact that T1 maps, SSFP cines and LGE acquisitions can all be carried out in the identical short axis plane. Comparing strain from long axis cines to ECV from short axis maps would add an unacceptable degree of error.

3.6 Conclusions

Regional strain impairment measured by feature tracking and SPAMM is predominantly associated with the degree of hypertrophy and replacement fibrosis assessed by the presence of LGE. In non-hypertrophied segments strain is not significantly impaired by the presence of interstitial fibrosis. Therefore the presence of interstitial fibrosis (defined as ECV>30% in this cohort) may be a more useful method than impairment of strain for identification of HCM in subjects with borderline LV hypertrophy.

4. Study 3- Changes in cardiac strain parameters in highly trained athletes

4.1 Abstract

Background

Athletic training leads to remodelling of both left and right ventricles with increased myocardial mass and cavity dilatation. Changes in cardiac strain parameters are less well established. In this study we investigated the relationship in trained athletes between cardiovascular magnetic resonance (CMR) derived strain parameters of cardiac function and aerobic capacity that has not previously been investigated.

Methods

35 endurance athletes and 35 age and sex matched sedentary controls underwent CMR at 3.0T including cine imaging in multiple planes and tissue tagging by spatial modulation of magnetization (SPAMM). CMR data were analysed quantitatively reporting circumferential strain and torsion from tagged images and left and right ventricular longitudinal strain from feature tracking of cine images. Athletes underwent a standard ramp-incremental step-exercise protocol to estimate lactate threshold (LT) aerobic capacity (VO_{2max}).

Results

LV circumferential strain at all levels, LV twist and torsion, LV late diastolic longitudinal strain rate, RV peak longitudinal strain and RV early and late diastolic longitudinal strain rate were all lower in athletes than controls. On multivariable linear regression only LV torsion (beta=-0.37, P=0.03) had a significant association

with LT. Only age (beta=-0.36, P=0.01), sex (beta=0.38, P=0.04) and RV longitudinal late diastolic strain rate (beta=-0.39, P=0.02) had a significant association with VO_{2max}.

Conclusions

The cohort of endurance athletes in this study had lower LV circumferential strain, LV torsion and biventricular diastolic strain rates than sedentary controls. The linear association between LT and LV torsion has potential applications in clinical cardiology and sports science including differentiation of athletic remodelling from early dilated cardiomyopathy.

4.2 Introduction

It is well recognised that athletic training leads to ventricular remodelling, specifically increases in left and right ventricular end diastolic volume (LVEDV & RVEDV) and left ventricular mass (LVM) (Maron and Pelliccia, 2006; Arbab-Zadeh et al., 2014). These structural changes are most frequently seen in athletes who undergo prolonged periods of endurance training (Utomi et al., 2013).

Although less well established, there is also evidence for changes in functional parameters in the hearts of trained athletes. Endurance athletes have reduced ejection fraction, circumferential and longitudinal strain of both the left and right ventricles compared to healthy controls (Caselli et al., 2015; Nottin et al., 2008). The heart has a complex twisting motion where the base rotates clockwise in early systole and the apex rotates anticlockwise in later systole. These opposing directions of rotation at the apex and base generate maximal torsional force at end systole (Burns et al., 2008). It has been reported that athletes have decreased LV twist and torsion when compared to sedentary controls (Nottin et al., 2008).

Both strain and torsion parameters can be measured using CMR tagging techniques (Ibrahim el, 2011). CMR tagging is considered to be the gold standard for measurement of myocardial strain and torsion (Shehata et al., 2009; Young and Cowan, 2012). More recently, post processing feature tracking to track the features of cine sequences through the cardiac cycle has been proposed for quantification of strain without the need for acquisition of tagged cines (Moody et al., 2015). Previous studies have shown good agreement between strain parameters derived from feature tracking and tissue tagging (Moody et al., 2015).

Cardiopulmonary exercise testing (CPX) allows analysis of gas exchange responses at rest and during exercise and provides a non-invasive estimate of lactate threshold (LT) and measure of maximal aerobic capacity (VO_{2max}) (Balady et al., 2010). This information gives an accurate and reproducible measure of integrated cardiac, respiratory and skeletal muscle function and is frequently used to quantitatively measure performance of endurance athletes (Bentley et al., 2007). Previous studies have demonstrated a clear correlation between LV remodelling and VO_{2max} in endurance athletes (Milliken et al., 1988; Scharhag et al., 2002). In

this study we have investigated the relationship between strain-derived parameters of cardiac function and CPX-derived performance parameters that has not previously been investigated. We hypothesised that strain parameters measured at rest would be lower in athletes than in sedentary controls and lowest in athletes with the best aerobic fitness.

4.3 Methods

4.3.1 Enrolment Recruitment

35 endurance athletes were recruited from local sporting clubs. They all trained more than 6 hours a week and competed regularly at local, national or international level. Exclusion criteria were any medical illness or contraindication to CMR. 35 sedentary controls who exercised less than 3 hours a week were also recruited and prospectively matched to the athletes for age and gender. No athletes or controls had any medical condition or took any regular medication. The study was conducted in accordance with the Declaration of Helsinki and was approved by the local ethics committee (14/YH/0126). All subjects gave informed written consent.

4.3.2 Cardiac Magnetic Resonance Protocol

CMR was performed on a dedicated cardiovascular 3 Tesla Philips Achieva system equipped with a 32 channel coil and MultiTransmit® technology. Data was acquired during breath-holding at end expiration. From scout CMR images, the left ventricular long and short axes were determined.

Cine images covering the entire heart in the LV short axis plane and orthogonal long-axis planes were acquired (balanced SSFP, spatial resolution 1.2x1.2x10mm³, 30 cardiac phases TR/TE 2.6/1.3ms, flip angle 40º, field of view 300-420mm, typical temporal resolution 39ms). Then axial cine images planned to cover the right ventricle were acquired (balanced SSFP, spatial resolution 1.2x1.2x6mm³, 30 cardiac phases TR/TE 2.6/1.3ms, flip angle 40º, field of view 300-420mm).

Tissue tagging by SPAMM (spatial resolution 1.51x1.57x10mm³, tag separation 7 mm, ≥18 phases, typical TR/TE 5.8/3.5 ms, flip angle 10º, typical temporal resolution 55ms) was acquired in the three short axis slices acquired at the apex, mid-ventricle, and base. Slices were positioned using the highly reproducible "3 of 5 technique" (Messroghli et al., 2005).

Myocardial perfusion CMR was planned in the same three short axis slices using a spoiled fast gradient-echo sequence (TR/TE 1.28/ 2.8 ms, flip angle 15°, acquired spatial resolution 2.42x2.42×10 mm, field of view 300–420mm, sensitivity encoding factor 2.4, 0.65 partial Fourier acquisition and a saturation pre-pulse delay of 80ms). During the breath held acquisition 0.075 mmol/kg of gadobutrol (Gadovist®, Bayer Schering Pharma, Berlin, Germany) was administered at a rate of 4.0ml/s followed by a 20ml saline flush (Medrad Spectris Solaris power injector, Pittsburgh, Pennsylvania).

4.3.3 Image Analysis

CMR data were analysed quantitatively using commercially available software (CVI42, Circle Cardiovascular Imaging Inc. Calgary, Canada and inTag v1.0, CREATIS lab, Lyon, France). Epicardial and endocardial borders were traced on the LV and RV cine stack at end-diastole and end-systole to calculate end diastolic volume (LVEDV), end systolic volume (ESV), stroke volume (SV), ejection fraction (EF) and LV mass. Volumes were indexed to body surface area (BSA) calculated using the Mosteller equation.

For tagging analysis endocardial and epicardial contours were drawn on the short axis SPAMM sequences using a semi-automated process. Peak circumferential LV strain was measured for the three slices at apex, mid-ventricle, and base. Peak systolic and both early and late diastolic LV strain rates were measured from the mid-ventricular slice. Strain was measured in the mid-myocardial layer which has previously been reported to be the most reproducible (Swoboda et al., 2013). LV twist was calculated by subtracting the basal from apical rotation. Basal and apical radius was calculated from cine images in diastole at the same slice location as the tagged images. The equation used to determine torsion was (Young and Cowan, 2012):

$$Torsion = \frac{Peak\ Twist\ \times (Apical\ Radius + Basal\ Radius)}{2\ \times Apex\ to\ Base\ length}$$

For feature tracking analysis endocardial and epicardial contours were drawn on a long axis 4 chamber cine using a semi-automated process. Peak longitudinal strain, systolic strain rate, early and late diastolic strain rates were measured for both the

LV & RV. Late diastolic strain rates were defined as peak rate during active atrial contraction.

Contours were traced on mid-slice perfusion CMR images to define the endo- and epicardial surfaces of the left-ventricular myocardium and a region within the left-ventricular blood pool. The myocardium was segmented into four regions circumferentially (anterior, lateral, posterior and septal), each of which were split into endo- and epicardial layers of equal thickness. Rigid motion correction was applied manually for respiratory motion where required. Signal intensity-time courses were extracted from the intra-ventricular blood pool (to provide an arterial input function, AIF) and the eight myocardial regions and further analysis on these data was completed using in-house software developed in MATLAB (Mathworks, Mattick, MA, USA).

The timing of the arrival of contrast agent in the blood pool and the end of the first-pass were identified visually from the AIF for each subject. Mean pre-contrast signal intensity was subtracted from each dataset and estimates of myocardial blood flow (MBF) were derived by performing Fermi constrained deconvolution on the resulting signal enhancement-time courses (Jerosch-Herold M et al., 1998). Endo-to-epicardial perfusion ratio (EER) was calculated for each circumferential segment by dividing the MBF estimate from the endocardial layer by that from the corresponding epicardial layer.

4.3.4 Exercise Protocol

Participants were instructed to abstain from alcohol and strenuous exercise in the preceding 24 hours and caffeine for the preceding 3 hours. To non-invasively estimate the lactate threshold (LT) and determine the maximal oxygen uptake (VO_{2max}) participants undertook a ramp-incremental (RI) step-exercise (SE)(Rossiter et al., 2006) test on an electronically-braked cycle ergometer (Excalibur Sport, Lode BV, Groningen, the Netherlands). RISE test allows for determination of VO_{2max} (rather than peak VO_2) in a single test(Rossiter et al., 2006). Participants wore a nose-clip and breathed through a low-dead space, low-resistance mouthpiece which was connected to a bi-directional pitot tube flow sensor and gas sample line assembly, allowing for breath-by-breath measurement of gas volumes and

concentrations (O_2, Galvanic; CO_2 infrared), and subsequent calculation of ventilatory and pulmonary gas exchange variables (Cardio2, Medical Graphics Corporation, St Paul, MN, USA). Prior to each test the pitot tube flow sensor was calibrated over a range of flow rates using a 3 l syringe, while the gas analysers were calibrated using precision gases that spanned the inspired and expired physiological range. The RISE test was preceded by rest period (~ 2 minutes) and unloaded cycling (20W) (~ 4 minutes), with these phases continued until a steady state was attained, after which work rate increased as a linear function of time at a rate of 20-30W/min (depending upon reported training history), with the intention of bringing participants to the limit of tolerance in ~10-12 min (Buchfuhrer et al., 1983). The RI was then followed by 5 min of active recovery (20W) after which a SE was performed at 95% of the RI work rate peak, with this SE also continued to the limit of tolerance. In both RI and SE parts of the test the limit of tolerance was defined as the point at which cycling cadence fell below 50 rpm despite strong verbal encouragement.

Breath-by-breath data were edited using the VO_2 response to eliminate erroneous breaths (occurring outside the local mean 99% prediction limits), that were considered unphysiological (Lamarra et al., 1987). LT was then estimated using the V-slope method(Beaver et al., 1986), and supporting ventilatory and pulmonary gas exchange criteria (i.e. the fractional end-tidal concentrations of O_2 and CO_2, and the ventilatory equivalents for O_2 and CO_2 (Whipp et al., 1986)). VO_{2peak} was identified in both RI and SE phases as the highest 12-breath rolling average (highest mean VO_2 over ~15-20 s), with this representing an appropriate sampling duration to balance identifying VO_{2peak} in the presence of breath-by-breath noise, and including data from the transient phase of the response leading to VO_{2peak}(Rossiter et al., 2006). Within participants, the highest 12-breath rolling average from RI and SE phases were then compared using unpaired t-tests, with no difference ($p > 0.05$) between RI and SE VO_{2peak}, and thus the attainment of VO_{2max} confirmed in each test (Bowen et al., 2012).

4.3.5 Statistical Analysis

Statistical analysis was performed using IBM SPSS® Statistics 20.0 (IBM Corp., Armonk, NY). Continuous variables were expressed as means ± SD. Categorical variables were expressed as N (%). Shapiro-Wilk test was used to test normality and unpaired t tests and Mann Whitney U test used to compare athletes and controls. Pearson's coefficient was used to measure correlation between exercise and CMR parameters. Univariable analyses were performed to identify predictors of LT and VO_{2max}. Variables with a probability value <0.1 in the univariable analysis were included in a multivariable linear regression analysis. P<0.05 was considered statistically significant.

4.4 Results

4.4.1 Study Participant Demographics and Characteristics

Of 35 athletes 7 were runners, 15 cyclists and 13 triathletes. The athletes trained 11.5 ± 3.7 hours per week and had all trained >6 hours per week for 8.4 ± 6.0 years. All athletes completed both the RI and SE phases of the RISE protocol to the limit of tolerance. Mean ramp duration was 772 ± 93s reaching a peak work rate of 370 ± 64W. HR rose from 55 ± 7 at rest to 182 ± 10 at peak exercise. Mean LT was 2.60 ± 0.57 l/min, 36.5 ± 6.7ml/min/kg (normalised to body weight) or 62.1 ± 8.0% of VO_{2max}. Mean VO_{2max} was 4.2 ± 0.80l/min or 58.9 ± 8.2 ml/min/kg.

Athletes and controls were prospectively matched for age and gender (Table 4.1). BMI and resting heart rate were lower in athletes than controls (P=0.001 and P<0.001 respectively).

	Athlete	Control	P value
Age	31.3±7.6	30.6 8.5	0.72
Male, %	27 (77)	27 (77)	1.0
Height, cm	178.7±8.7	176.5±8.2	0.29
Weight, kg	71.4±9.9	77.0±14.8	0.07
BMI, kg/m^2	22.3±1.9	24.5±3.3	0.001
HR	55.0±6.5	65.1±8.7	<0.001
SBP, mmHg	118.8±8.7	114.7±10.6	0.16
DBP, mmHg	71.0±9.2	59.2±10.6	<0.001

Table 4.1   Subject characteristics BMI, body mass index; SBP, systolic blood pressure; DBP, diastolic blood pressure
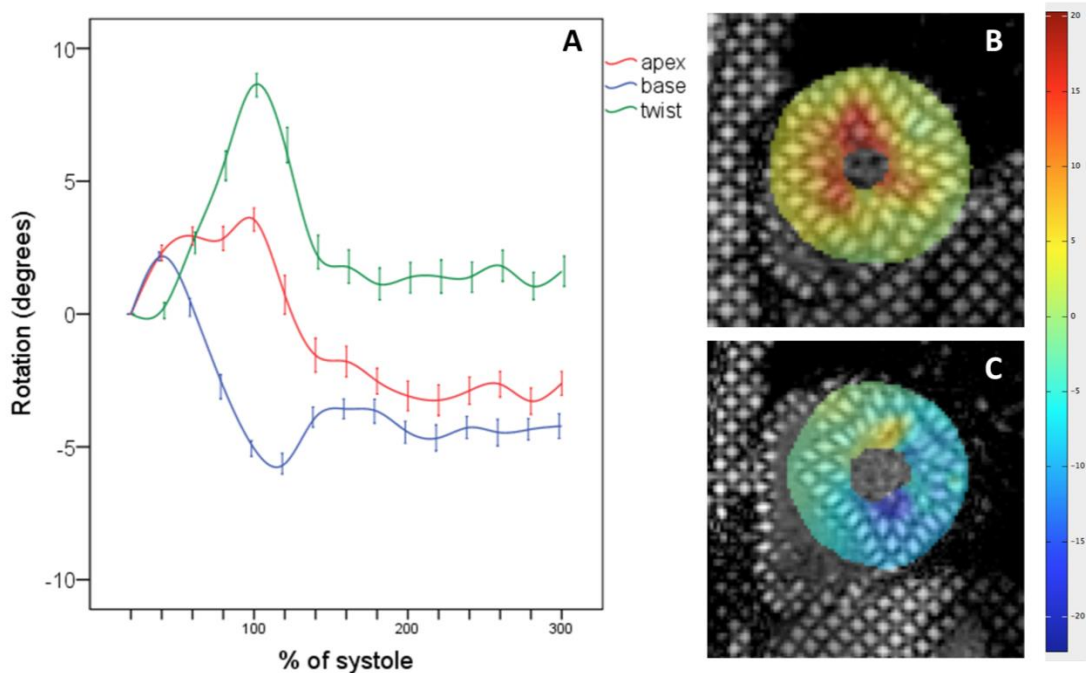
Figure 4.1 Apical rotation (red), basal (blue) rotation and twist (green) of the left ventricle of 35 endurance athletes (A). Each point represents mean rotation/twist and time in the cardiac cycle corrected to end-systole, error bars represent standard error of mean rotation/twist. Tagged images of anticlockwise apical (A) systolic rotation (yellow and red) and clockwise basal (C) rotation (green and blue).

4.4.2 CMR Findings

LV volumes for athletes and controls are shown in Table 4.2. LVEDV, LV mass and RVEDV indexed to BSA were greater in athletes than controls. LVEF was lower in athletes than controls (P=0.04) but there was no difference in RVEF (P=0.27). Strain parameters are shown in Table 4.3. LV circumferential strain at all levels, LV twist and torsion (Figure 1), LV late diastolic longitudinal strain rate (Figure 2), RV peak longitudinal strain and RV early and late diastolic longitudinal strain rate were all lower in athletes than controls.

	Athlete	Control	P value
Left ventricle			
EDV, ml	217.1±34.8	176.5±34.8	<0.001
EDV indexed to BSA, ml/m²	115.4±14.2	90.8±12.9	<0.001
ESV, ml	96.1±18.7	74.7±18.7	<0.001
EF, %	55.7±4.5	57.9±4.1	0.04
LV mass, g	127.9±24.6	100.5±23.4	<0.001
LV mass indexed to BSA, g/m²	67.8±9.9	51.5±9.1	<0.001
Right ventricle			
EDV, ml	219.7±37.2	204.8±50.1	0.16
EDV indexed to BSA, ml/m²	116.8±15.8	105.1±19.7	0.01
ESV, ml	104.2±22.7	99.5±27.5	0.44
EF, %	52.8±4.7	51.6±3.7	0.27

Table 4.2 CMR measured volumetric parameters. EDV, end diastolic volume; EF, ejection fraction; ESV, end systolic volume; LV, left ventricle

	Athlete	Control	P value
LV Circumferential Strain			
Apex, %	18.4±5.2	23.4±4.9	<0.001
Mid LV, %	19.6±3.9	21.5±2.5	0.02
Base, %	17.0±4.0	20.5±2.5	<0.001
Systolic SR, %/s	115.3±12.8	116.6±10.0	0.66
Early diastolic SR,%/s	50.8±16.4	51.0±16.0	0.95
Late diastolic SR, %/s	140.1±40.7	151.4±40.3	0.27
Torsion			
LV twist, °	9.7±3.6	13.3±3.8	<0.001
LV torsion, °	8.8±3.0	11.9±3.1	<0.001
LV twist rate, °/s	63.2±18.9	72.4±27.8	0.048
LV untwist rate, °/s	88.1±25.5	101.8±34.5	0.07
LV Longitudinal Strain			
Peak, %	17.1±2.8	17.7±2.3	0.30
Systolic SR, %/s	101.6±29.6	103.2±19.8	0.29
Early diastolic SR, %/s	90.6±32.4	102.4±31.7	0.13
Late diastolic SR, %/s	41.7±15.6	57.3±19.6	<0.001
RV Longitudinal Strain			
Peak, %	19.8±3.7	22.6±3.4	0.002
Systolic SR, %/s	137.7±49.9	138.4±37.0	0.50
Early diastolic SR, %/s	108.6±32.1	124.6±32.9	0.03
Late diastolic SR, %/s	69.2±40.2	89.5±42.4	0.02

Table 4.3 CMR measured strain parameters LV, left ventricle; SR, strain rate
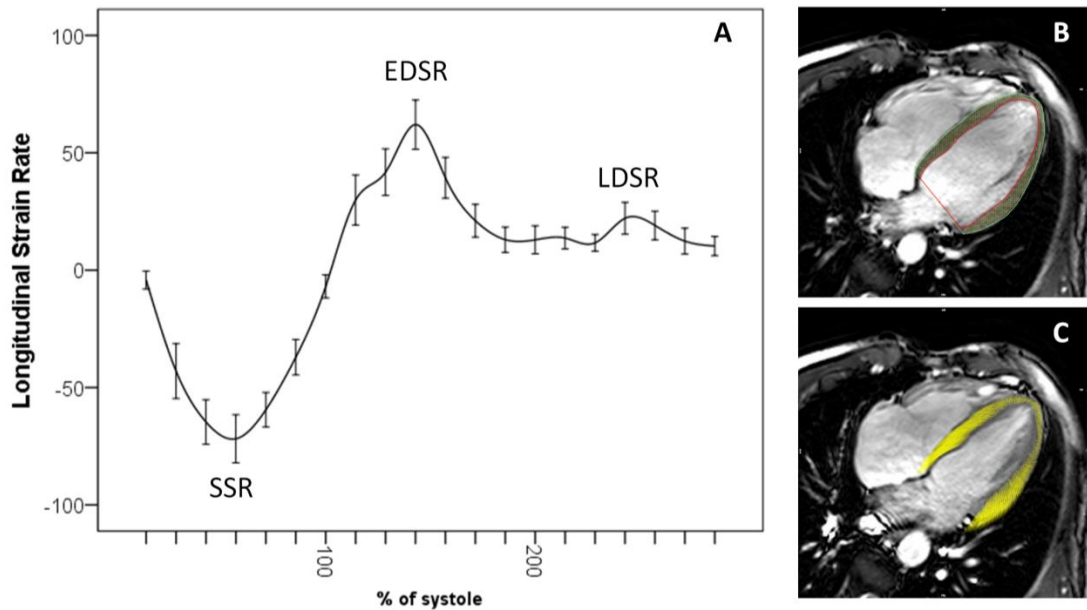
Figure 4.2 LV longitudinal strain rate of 35 endurance athletes(A). Each point represents mean longitudinal strain rate at each point in the cardiac cycle corrected to end-systole, error bars represent 95% confidence interval of mean strain. Peak systolic strain rate (SSR), early diastolic strain rate (EDSR) and late diastolic strain rate (LDSR). SSFP cine image at end diastole showing manually drawn endocardial and epicardial contours (B). Feature tracked end systolic image (C).

4.4.3 Relationship between CPX and Functional CMR Parameters

The only significant correlations with LT (as percent of VO_{2max}) were with torsion parameters. Peak twist (r=-0.45, P=0.01), peak torsion (r=-0.36, P=0.04) and twist rate (r=-0.38, P=0.03) all had a significant correlation with LT. There was no significant correlation between LT and any demographic, ventricular volume or other strain parameter.

There was a correlation between VO_{2max} and both LVMI (r=0.59, P<0.001) and LVEDVI (r=0.47, P=0.01) consistent with previously reported findings (Osborne et al., 1992; Milliken et al., 1988). There was also a trend to correlation between RVEDVI and VO_{2max} (r=0.33, P=0.05). Both age (r=-0.35 P=0.04) and sex (r=0.40, P=0.02) correlated with VO_{2max}. No LV strain parameters had a significant correlation with VO_{2max}. RV longitudinal systolic strain rate (r=-0.33, P=0.05) and RV late diastolic strain rate (r=-0.38, P=0.02) both correlated with VO_{2max}.

We identified 8 athletes in the highest quartile of LT (72.7±2.0%) and 8 in the lowest quartile of LT (51.7±2.9%). Peak twist and torsion were lower in the athletes in the highest quartile than those in the lowest quartile (8.5 ± 2.9 vs 12.9 ± 2.6° P=0.008 and 8.0 ± 3.4 vs 11.2 ± 1.8° P=0.048, respectively). There were no other significant differences between demographics, ventricular volumes or strain parameters between the groups. The difference in LV twist and torsion was secondary to decreased apical rotation in the athletes with VAT in the highest quartile (Figure 4.3) 1.0 ± 3.3 vs 6.0 ± 3.1° P<0.001. Basal rotation was not different between the groups 6.5 ± 1.4 vs 6.1 ± 2.6° P=0.75.

MBF and EER values are shown in Table 4.4. The only significant correlation was between EER in the anterior segment and absolute LT (r=0.34, P=0.047) and LT corrected for weight (r=0.39, P=0.02).
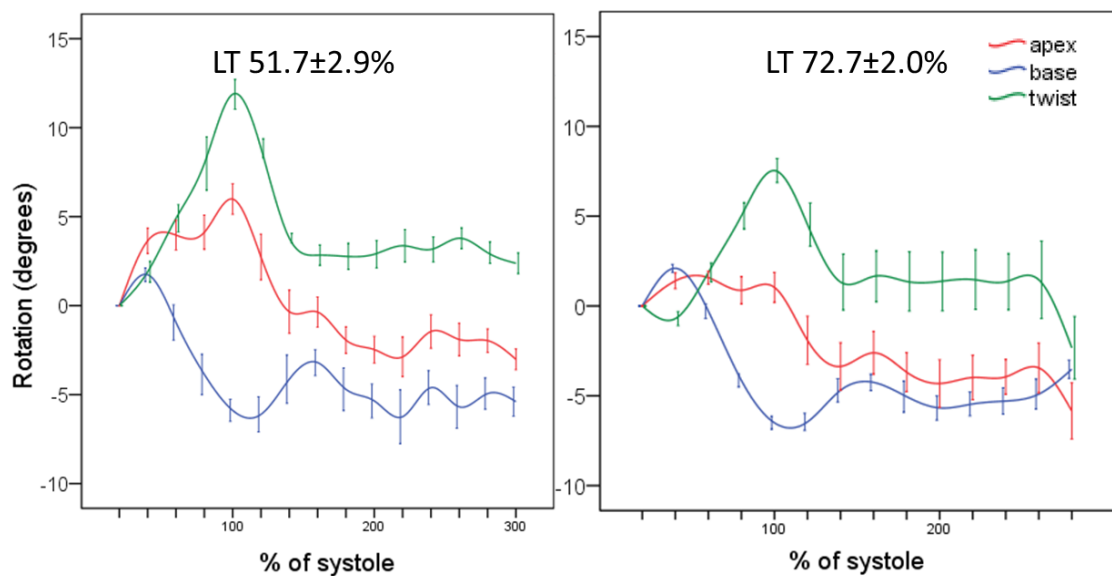
Figure 4.3 Plots showing the mean ± standard error of rotation/twist of the athletes in the lowest quartile of LT (left) and highest quartile of LT (right). Peak twist was lower in athletes in the highest quartile of LT (8.5 ± 2.9 vs 12.9 ± 2.6° P=0.008) which was secondary to a loss of apical rotation (1.0 ± 3.3 vs 6.0 ± 3.1° P<0.001).

	Anterior	Lateral	Inferior	Septum
Endocardial MBF (ml/g/min)	1.95±1.19	1.78±1.17	1.57±1.43	1.74±1.22
Epicardial MBF (ml/g/min)	1.74±1.40	1.59±1.52	1.31±1.00	1.54±0.98
EER	1.18±0.23	1.21±0.31	1.25±0.38	1.12±0.22

Table 4.4 Endocardial and epicardial myocardial blood flow (MBF) and endo-to-epicardial perfusion Ratio (EER) for athletes in 4 mid ventricular sectors

4.4.4 Regression Analysis

On univariable linear regression of the parameters shown in Table 4.5 only LV torsion and sex were associated with LT. On multivariable linear regression only LV torsion (beta=-0.37, P=0.03) had a significant association with LT.

On univariable linear regression of the parameters shown in Table 4.6 age, sex, RV longitudinal strain, RV systolic strain rate and RV diastolic strain rate were associated with VO_{2max}. On multivariable linear regression only age (beta=-0.36, P=0.01), sex (beta=0.38, P=0.04) and RV longitudinal late diastolic strain rate (beta=-0.39, P=0.02) had a significant association with VO_{2max}.

	Univariable		Multivariable	
	Beta	P value	Beta	P value
Age	-0.07	0.70		
Sex	**0.29**	**0.09**	0.29	0.08
LVEF, %	-0.43	0.81		
RVEF, %	0.10	0.56		
Apex circumferential strain, %	0.15	0.38		
Mid LV circumferential strain, %	-0.11	0.55		
Base circumferential strain, %	-0.05	0.77		
LV torsion, °	**-0.36**	**0.04**	**-0.37**	**0.03**
LV longitudinal strain, %	0.09	0.61		
LV longitudinal systolic SR, %/s	0.15	0.40		
LV longitudinal early diastolic SR, %/s	-0.23	0.19		
LV longitudinal late diastolic SR, %/s	-0.01	0.95		
RV longitudinal strain, %	-0.01	0.97		
RV longitudinal systolic SR, %/s	0.04	0.84		
RV longitudinal early diastolic SR, %/s	-0.01	0.97		
RV longitudinal late diastolic SR, %/s	-0.22	0.20		

Table 4.5 Univariable and multivariable linear regression analysis of factors with a significant association with lactate threshold. EF ejection fraction; LV, left ventricle; RV, right ventricle; SR, strain rate

	Univariable		Multivariable	
	Beta	P value	Beta	P value
Age	**-0.37**	**0.04**	**-0.36**	**0.01**
Sex	**0.40**	**0.02**	**0.38**	**0.04**
LVEF, %	-0.12	0.50		
RVEF, %	-0.52	0.77		
Apex circumferential strain, %	0.27	0.11		
Mid LV circumferential strain, %	0.18	0.92		
Base circumferential strain, %	-0.17	0.33		
LV torsion, °	-0.21	0.24		
LV longitudinal strain, %	0.17	0.32		
LV longitudinal systolic SR, %/s	0.04	0.80		
LV longitudinal early diastolic SR, %/s	-0.04	0.81		
LV longitudinal late diastolic SR, %/s	-0.14	0.41		
RV longitudinal strain, %	**0.30**	**0.08**	-0.05	0.78
RV longitudinal systolic SR, %/s	**-0.33**	**0.05**	-0.25	0.09
RV longitudinal early diastolic SR, %/s	-0.01	0.96		
RV longitudinal late diastolic SR, %/s	**-0.38**	**0.02**	**-0.39**	**0.02**

Table 4.6 Univariable and multivariable linear regression analysis of factors with a significant association with VO2max. EF ejection fraction; LV, left ventricle; RV, right ventricle; SR, strain rate

4.5 Discussion

We have carried out comprehensive cardiac functional assessment of 35 endurance athletes from a broad spectrum of sport, age and athletic ability. This diverse, but well characterised group has allowed us to investigate specifically the ventricular strain parameters that have a relationship with quantitative measures of athletic performance, namely LT and VO_{2max} (Bassett and Howley, 2000).

The most striking finding was the inverse linear correlation between both LV twist and torsion, and LT. On multivariable linear regression no other factors significantly influenced LT. To our knowledge this is the first time a significant association between a cardiac structural or functional parameter and LT has been reported. Furthermore we have found that in athletes with the highest LT the decrease in torsion is secondary to decreased apical rotation.

We have reported with high statistical significance that LV torsion was lower in endurance athletes than sedentary controls. Previous CMR tagging studies have been small and insufficiently powered and therefore unable to report a difference in baseline torsion parameters between endurance athletes and sedentary controls (Scott et al., 2010; Esch et al., 2010). Scott et al. reported in 9 highly trained endurance athletes that LV ejection fraction, untwist rate, apical rotation rate and circumferential strain were all depressed 30 minutes after high intensity interval training (Scott et al., 2010). Athletes with the highest LT undertake high intensity training (Bentley et al., 2007) and it is therefore likely that our finding of decreased torsion in these athletes is due to the cumulative effect of many years of high intensity interval training.

Several echocardiography studies using techniques including tissue Doppler imaging and speckle tracking have been used to investigate left ventricular torsion in athletes. Previous echocardiographic studies have reported similar findings to ours of decreased apical rotation and LV torsion in athletes with high levels of aerobic fitness (Stohr et al., 2012) whereas others have reported that high intensity exercise either had no effect (Stewart et al., 2015), or even caused an increase (Weiner et al., 2010) in LV torsion. The inconsistent results that have been reported may in part reflect different sport and training techniques, research

methodology used and also the difficulty in positioning the apical and basal slices in echocardiography studies, which is based upon anatomical landmarks with a degree of subjectivity. In CMR on the other hand, positioning of the slices is carried out objectively based upon the length of the ventricle (Messroghli et al., 2005).

There are several possible mechanisms that explain the association between LT and LV torsion. In diffuse myocardial diseases such as aortic stenosis (Stuber et al., 1999) and type 1 diabetes mellitus (Chung et al., 2006) increased LV torsion is attributed to subendocardial microvascular hypoperfusion and contractile dysfunction. It is hypothesized that there is a compensatory increase in subepicardial fibre contraction giving rise to increased LV torsion yet unchanged overall circumferential strain. It is possible that the converse could be true in athletes with high LT. It is recognised that interval training leads to increased vascularity (Pereira et al., 2013) and improved substrate utilisation (Hafstad et al., 2011) within the myocardium. It is possible that these changes may improve myocyte contractile function in the subendocardium to such an extent that subepicardial contraction is not needed at rest and there is a subsequent reduction in LV torsion.

We have demonstrated a correlation between LT and EER in the anterior segment, which is in keeping with this hypothesis. Although the correlation is relatively weak and only seen in one segment, it does suggest that athletes with the highest LT who undergo regular high intensity training may have increased subendocardial blood flow and myocardial capillary vascularity which may in part explain the decrease in torsion parameters that we have reported. Measuring EER is technically challenging because the segments assessed are relatively small and therefore vulnerable to dark rim and respiratory artefact. This may explain why the relationship was not seen in all segments.

It has been reported that spherical remodelling of the LV, particularly in disease states, leads to impairment of LV twist (van Dalen et al., 2010). Although we did not find a significant association between LT and LV remodelling an alternative hypothesis is that many years of high intensity training leads to changes in fibre orientation and therefore decreased apical rotation and LV torsion.

We have also reported lower global LV late diastolic strain rate, RV early and late diastolic longitudinal strain rates in athletes versus controls. On multivariable linear regression only increasing RV late diastolic strain rate, female gender and older age were significantly associated with lower VO_{2max}. To our knowledge this is the first time that CMR strain techniques have been used to compare longitudinal functional changes in athletes and controls. Conflicting findings have been reported when echocardiographic assessment of diastolic function has been used with some studies reporting augmented relaxation of both ventricles in endurance athletes (Caselli et al., 2015; Baggish et al., 2008) and others reporting no difference from controls (Pluim et al., 2000). Our finding of reduced longitudinal late diastolic strain rates of both ventricles of athletes and a negative correlation between longitudinal late diastolic strain rate and VO_{2max} can be attributed to reduced active atrial contraction late in diastole. In athletes the atrial contribution to ventricular filling is not required at rest but of course can be utilised when required during exercise.

The observations from this study, particularly of the relationship between LT and LV torsion, have potential uses both in sports science and in clinical medicine. Some endurance athletes display a cardiac phenotype of dilated left ventricle, low normal ejection fraction and decreased LV torsion. This can be difficult to differentiate clinically from early dilated cardiomyopathy (Abergel et al., 2004). We have demonstrated that only athletes with high LT had depressed LV torsion. Therefore it may be possible to differentiate athletic remodelling from early cardiomyopathy by carrying out CPX. If the subject has a normal LT then it should not be assumed that their cardiac changes are due to athletic remodelling. LV torsion also has the potential to be used as a quick and non-invasive assessment of cardiac function in endurance athletes as a quantitative measure of the effect of training.

4.6 Limitations

Our study was carried out on a cross sectional cohort and it is important in the future to demonstrate that these findings can be replicated in a longitudinal study. The cohort in the study also has a wide range of age and athletic ability although

this was deliberate to allow study of athletes with a range of CPX results. All of the cardiac changes reported are during rest. We have used feature tracking rather than SPAMM for the analysis of longitudinal strain. However, tissue tagging is hampered by a lower temporal resolution than cine imaging and tag fading during diastole. As we specifically wanted to examine longitudinal strain rates in diastole we therefore chose to use feature tracking for this while using SPAMM tagging for assessment of circumferential strain parameters.

4.7 Conclusions

This cohort of endurance athletes had lower LV circumferential strain, LV torsion and biventricular diastolic strain rates than sedentary controls. There was a linear association between LT and LV torsion, which is secondary to decreased apical rotation in athletes with high LT. This association could be utilised to differentiate athletic remodelling from early dilated cardiomyopathy.

5. Study 4- Quantification of extracellular fibrosis in patients with type 2 diabetes at high risk of developing heart failure

5.1 Abstract

Background

Type 2 diabetes is an independent risk factor for the development of heart failure. Patients with elevated urinary albumin creatinine ratio (ACR), high sensitivity cardiac troponin T (hs-cTnT) and amino-terminal pro-brain natriuretic peptide (NT-proBNP) appear to be at the highest risk of heart failure although mechanisms by which this occurs are not clear. We hypothesised that increased risk of heart failure would be mediated by both diffuse fibrosis and silent MI.

Methods

We carried out comprehensive cardivascular magnetic resonance (CMR), assessment in 100 asymptomatic patients with type 2 diabetes and 30 controls. 50 patients had persistent microalbuminuria but were yet to start an ACE inhibitor and 50 had never had microalbminuira. The CMR protocol included T1 mapping using Modified Look-Locker Inversion (MOLLI) to assess for diffuse fibrosis and late gadolinium enhancement imaging (LGE) to assess for focal fibrosis or prior myocardial infarction (MI).

Results

Extracellular volume (ECV), a CMR marker of diffuse fibrosis, was higher in ACR +ve than ACR -ve patients 27.2±4.1 vs 25.1±2.9% P=0.004. ECV was also higher in hs-cTnT +ve than hs-cTnT -ve patients 30.3±4.8 vs 25.6±3.2%, P<0.0001   and   NT-proBNP +ve than NT-proBNP -ve patients 29.3±4.5 vs 25.7±3.4%, P=0.002. The rate of silent MI was higher than expected in this low risk asymptomatic cohort (17%) but there were no differences in the rate according to biomarker (ACR, hs-cTnT or NT-proBNP) status. Patients with 2 or 3 +ve biomarkers had the highest ECV which

was significantly higher than those with 1 or 0 +ve risk factors 30.7±4.2 vs 25.5±3.1%, P<0.0001.

Conclusions

The increased risk of heart failure in patients with persistent microalbuminuria, +ve hs-cTnT and NT-proBNP appears to be mediated by increased cardiac ECV and diffuse fibrosis. The rate of silent MI was high but not related to biomarker status.

5.2 Introduction

Type 2 diabetes mellitus is well established as an independent risk factor for the development of heart failure (Kannel and McGee, 1979). The risk of heart failure is approximately doubled by the presence of diabetes and appears to be independent of conventional risk factors including age, gender, existing coronary disease and hypertension (Gottdiener et al., 2000). Once patients with diabetes establish heart failure they have higher mortality than normoglycaemic heart failure patients (MacDonald et al., 2008; Cubbon et al., 2013). Epidemiological evidence suggests that poor control of blood glucose in type 2 diabetes is associated with increased rates of heart failure (Iribarren et al., 2001). However data from randomised controlled trials demonstrate that intensive control of glucose does not reduce the risk of hospitalisation for heart failure (Castagno et al., 2011). To complicate matters, several pieces of evidence suggest that type of hypoglycaemic agents used can modulate the risk of heart failure in patients with diabetes (Dormandy et al., 2005; Zinman et al., 2015).

Patients with type 2 diabetes and nephropathy appear to be at the highest risk of heart failure and treatment directed at modulating the renin-angiotensin-aldosterone system decreases rate of hospitalisation with cardiac decompensation. In both the LIFE and RENAAL studies, patients with type 2 diabetes and nephropathy were randomised to treatment with losartan versus atenolol (LIFE) or Losartan versus placebo (RENAAL) (de Zeeuw et al., 2004). In both studies, the albumin creatinine ratio (ACR) at baseline was found to be associated with an increased risk of first heart failure admission (hazard ratio 1.3 in LIFE and 1.4 in RENAAL over 4-5 years follow up) (Carr et al., 2005). In both studies treatment with losartan was associated with decreased rates of hospitalisation for heart failure (Carr et al., 2005). Given the poor clinical outcome of patients with diabetes and heart failure, studies attempted to identify a reliable biomarker for heart failure risk in this population. Elevated high sensitivity cardiac troponin T (hs-cTnT) in patients without overt cardiovascular disease has shown an association with increased risk of heart failure (hazard ratio 6.37 [confidence interval, 4.27-9.51]) over 14 years follow up) (Selvin et al., 2014). Elevated B-type natriuretic peptide

(BNP) has been associated with increased risk of both myocardial ischaemia detected by exercise tolerance test (Rana et al., 2006) and cardiovascular events (Huelsmann et al., 2008). However, these tests fail to reliably detect all patients with early stages heart failure and more robust techniques are needed for the timely identification of those at risk.

CMR allows for further investigation of the relationship between diabetes and heart failure *in vivo*. CMR studies have demonstrated that diabetes is associated with increased LV mass (Heckbert et al., 2006) and concentric LV remodelling (Velagaleti et al., 2010) independently of other factors such as age, blood pressure, tobacco use and alcohol use.

Furthermore, CMR is able to measure and quantify the presence of focal and diffuse fibrosis in patients with diabetes. With LGE CMR focally scarred myocardium can be detected and the location and transmural distribution of scar provide an indication of the aetiology of heart failure. The scar most commonly detected in diabetes is due to previous myocardial infarction (MI), either recognised or silent (Schelbert et al., 2012), and is associated with increased mortality (Kwong et al., 2006). CMR is also able to measure diffuse fibrosis using T1 and ECV mapping based techniques. Type 2 diabetes is associated with increased ECV when measured by these techniques (Jellis et al., 2011) and those with the highest ECV have highest cardiovascular mortality and increased heart failure admissions (Wong et al., 2013).

We hypothesised that CMR offers an accurate tool to characterise cardiac change in asymptomatic patients with type 2 diabetes with the ability to stratify those at high and low risk of heart failure. We aimed to establish whether the high risk of heart failure in certain patients was mediated by diffuse fibrosis or silent MI.

5.3 Methods

5.3.1 Enrolment Criteria

The study was approved by the local ethical committee (13/YH/0098) and individuals were enrolled onto the study after informed consent. A total of 100 patients with type 2 diabetes were recruited from 30 primary care health centres

in the local area. 50 consecutive ACR +ve patients were recruited after their annual diabetes check before commencement on an angiotensin converting enzyme (ACE) inhibitor in line with national guidelines (Sibal and Home, 2009). All ACR +ve patients had laboratory albumin: creatinine ratio repeated within 4 months to confirm persistent microalbuminuria. Thresholds to diagnose microalbuminuria were two or more measurements >2.5mg/mol in males and >3.5mg/mol in females (Sibal and Home, 2009). In addition, 50 patients with type 2 diabetes were recruited who had never had ACR above the thresholds (ACR -ve). This group was prospectively matched for age, gender and clinic blood pressure to ACR +ve patients.   Exclusion criteria for ACR +ve and ACR -ve were known cardiac disease, kidney disease (eGFR <30), uncontrolled hypertension, treatment with insulin or ACE inhibitor/angiotensin receptor blocker (ARB). Patients taking an ACEi or ARB were excluded because observational data has suggested that it may influence ECV in patients with diabetes (Wong et al., 2013). Finally, 30 age and gender matched controls were recruited.

5.3.3 CMR protocol

All patients and controls underwent CMR using an identical protocol on a dedicated cardiovascular 3 Tesla Philips Achieva TX system equipped with a 32 channel coil and MultiTransmit® technology (Philips, Best, The Netherlands). Data were acquired during breath-holding at end expiration. From scout CMR images, the left ventricular long and short axes are determined. Then, precontrast T1 maps were acquired at the apex, mid-ventricle, and base positioned with the highly reproducible "3 of 5 technique" (Messroghli et al., 2005). T1 mapping used a breath-held Modified Look-Locker Inversion recovery (MOLLI) acquisition (ECG triggered 5(3s)3 balanced turbo gradient recalled echo (GRE) acquisition, spatial resolution 1.98x1.98x10mm³ (reconstructed to 1.25*1.25mm), single-shot, SENSE factor 2, prepulse delay 350ms, trigger delay set for end-diastole (adaptive), flip angle 35°, acquisition duration per image 170-185ms (dependent on field of view (FOV)).

Tissue tagging by spatial modulation of magnetization (SPAMM) imaging (spatial resolution 1.51×1.57×10mm³, tag separation 7 mm, ≥18 phases, typical TR/TE

5.8/3.5 ms, flip angle 10°) was then performed in the same three short axis slices as T1 maps.

Next, myocardial perfusion CMR was planned in the same three short axis slices using a spoiled turbo gradient-echo sequence (TR/TE 1.28/ 2.8 ms, flip angle 15°, acquired spatial resolution 2.42x2.42×10 mm, FOV 300–420, variable matrix between 124x124 – 172x172 (dependent on FOV), sensitivity encoding factor 2.4, 0.65 partial Fourier acquisition and a saturation pre-pulse delay of 80ms). Intravenous adenosine was administered at 140mcg/kg/min for 3 minutes under continuous ECG monitoring. Adequate haemodynamic response was assessed by either a heart rate increase by ≥10% or symptoms attributed to adenosine administration. Imaging was undertaken during the last minute of adenosine infusion with a weak intravenous bolus of 0.0075mmol/kg followed by a strong bolus of 0.075 mmol/kg of gadobutrol (Gadovist®, Bayer Schering Pharma, Berlin, Germany). Both were administered at a rate of 4.0ml/s followed by a 20ml saline flush (Medrad Spectris Solaris power injector, Pittsburgh, Pennsylvania).

Cine images covering the entire heart in the LV short axis plane were acquired (balanced SSFP, spatial resolution 1.2x1.2x10mm³, 50 cardiac phases TR/TE 2.6/1.3ms, flip angle 40°, field of view 300-420mm) and in orthogonal long-axis planes. Cine images planned to cover the entire left atrial short axis plane in end systole were acquired (balanced SSFP, spatial resolution 1.2x1.2x5mm³, 50 cardiac phases TR/TE 2.6/1.3ms, flip angle 40°, field of view 300-420mm) and in orthogonal long-axis planes.

Rest perfusion imaging was acquired a minimum of 15 minutes after stress perfusion with a further injections of 0.0075mmol/kg and 0.075mmol/kg of gadobutrol in an identical geometry to the stress images. Rest images were acquired with the same FOV and acquisition duration as the stress scan.

LGE was then carried out more than 6 minutes after rest perfusion imaging using inversion recovery-prepared T1-weighted echo. The optimal inversion time to null signal from normal myocardium was determined using a Look-Locker approach. Typical parameters were TR/TE 3.5/2.0 ms, flip angle 25°, acquired spatial resolution 1.54x1.76x10mm³ and performed in 10-12 short axis slices with further slices acquired in the vertical and horizontal long axis orientations, or phase-

swapped, if indicated based on LGE imaging obtained, wall-motion or perfusion defects. Post contrast T1 mapping was carried out exactly 15 minutes following last contrast injection (as above).
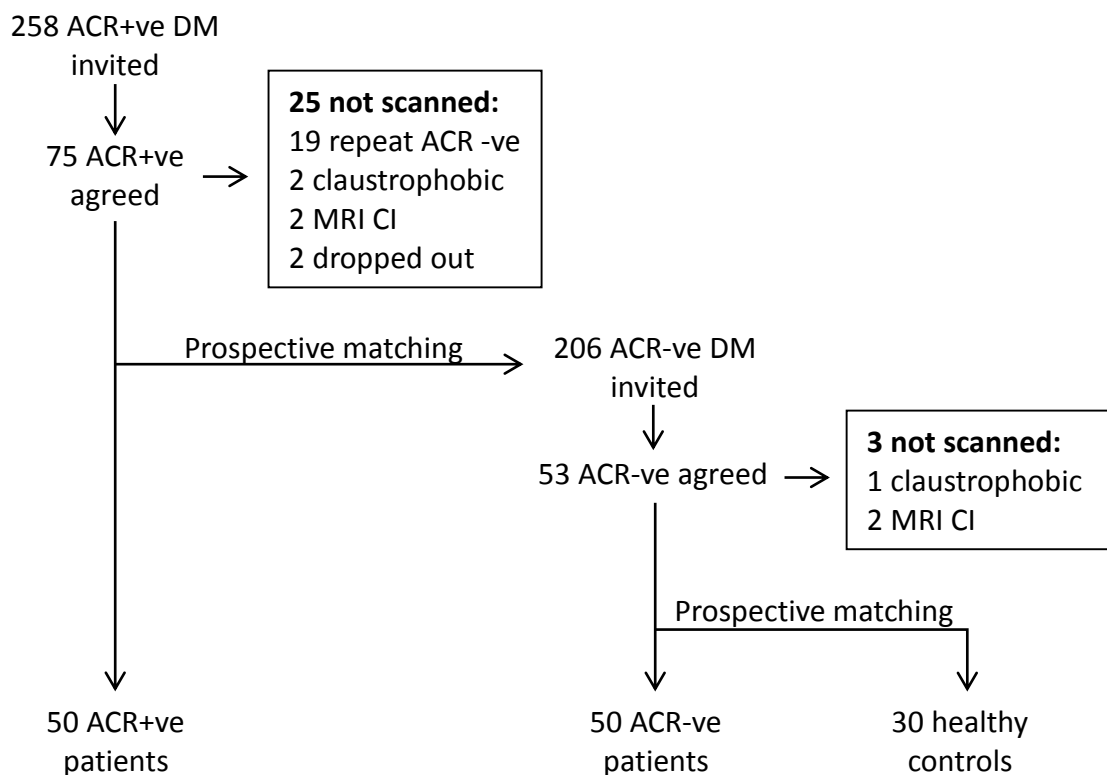
Figure 5.1 Recruitment flowchart.

5.3.4 CMR interpretation

CMR data was assessed quantitatively using commercially available software (CVI42, Circle Cardiovascular Imaging Inc. Calgary, Canada). Epicardial and endocardial borders were traced offline on the LV cine stack at end-diastole and end-systole to calculate end-diastolic (ED), end- systolic (ES) LV volumes, stroke volume (SV), ejection fraction (EF) and LV mass. Left atrial (LA) volume was calculated by tracing the LA endocardial border at end-systole when the left atrium was largest.

Pre and post contrast myocardial T1 values with a 3-parameter exponential fit with Look-Locker correction were measured from the mid ventricular short axis slice in the septum. ECV was calculated from native and post contrast T1 times of

myocardium and blood pool and haematocrit as previously reported (Flett et al., 2010). Mass of LGE was quantified using the Otsu automated threshold method and divided by LV mass calculated from short axis cines to give a percentage of LV with LGE.

5.3.5 Echocardiogram protocol and analysis

All patients underwent echocardiography (vivid e9, GE Medical Systems, Milwaukee, WI) focused on Doppler measurements of mitral inflow and tissue Doppler imaging (TDI) of the mitral annulus. E/A ratio, E', A' and S' are measured on the machine using inbuilt software. Diastolic dysfunction was graded 0-3 by a according to the international guidelines (Nagueh et al., 2009) by an accredited echocardiographer blinded to clinical details.

5.3.6 Ambulatory blood pressure

All patients underwent 24 hour blood pressure monitoring using a Welch-Allyn 6100 ambulatory blood pressure monitor (Welch-Allyn, NY, USA) that has been validated for clinical use by the British Hypertension Society. The cuff was set to inflate every 30 minutes during the day and every 60 minutes during the night. Mean 24 hour systolic and diastolic BP were recorded.

5.3.7 Biomarker assessment

20mL of blood was drawn from each subject at the time of CMR. Full blood count, urea & electrolytes and HbA1c are measured at that time. Serum was stored at -70C and tested in one batch for hs-cTnT typical CV 4.4% at 13.7ng/L and 3.6% at 95.3 ng/L, amino-terminal pro-brain natriuretic peptide (NT-proBNP) typical CV 2.9% at 91 ng/L and 2.1% at 415 ng/L (Cobas 8000, Roche Diagnostics, Burgess Hill, West Sussex) and aldosterone ('in-house' radioimmunoassay) typical between batch CV <10% at 282, 402 and 1833 pmol/L

5.3.8 Statistical analysis

Statistical analysis was performed using IBM SPSS® Statistics 20.0 (IBM Corp., Armonk, NY). Continuous variables were expressed as means ± SD. Categorical variables were expressed as N (%) and compared using Fisher exact test. Shapiro-

Wilk test was used to test normality and depending on the result analysis of variance (ANOVA) & and Kruskal Wallis test were used to compare means of ACR +ve, ACR -ve and controls. Unpaired t test and Mann Whitney U test were used to calculate significance when there were 2 variables. Correlations were calculated using Spearmans correlation coefficient. $P<0.05$ was considered statistically significant.

A power calculation based on previous studies of ECV in diabetes estimated that 50 subjects would be needed in the ACR +ve and ACR -ve groups (power 0.9 and type 1 error 0.05) (Jellis et al., 2011). We estimated that the difference in ECV in those with and without microalbuminuria would be similar to those with and without diastolic impairment in the previous study.

5.4 Results

A total of 464 patients with diabetes were approached of whom 128 patients agreed to participate. 50 ACR +ve and 50 ACR -ve completed the full protocol (Figure 5.1). 30 age and sex matched controls (N=30) were also recruited. 6/30 controls chose not to receive adenosine stress after learning of possible symptoms. Patient and control characteristics and regular medications are shown in Table 5.1. There was no difference between ACR +ve and ACR -ve patients in age, gender, BMI, diabetes duration, HbA1c or 24 hour blood pressure.

Native T1 and ECV were higher in patients with diabetes than in controls 1242.2±53.9 vs 1209.7±47.4ms, P=0.004 and 26.1±3.4 vs 23.3±3.0% P=0.0002. Native T1 and ECV were also higher in ACR +ve than ACR -ve patients 1252.6±66.0 vs 1231.72±35.8ms, P=0.05 and 27.2±4.1 vs 25.1±2.9%, P=0.004 (Figure 5.2).

A total of 17/100 patients with diabetes had silent MI compared with 0/30 controls, P=0.01. There was no difference in the rate of silent MI between ACR +ve and ACR-ve patients (9/50 vs 8/50, respectively P=0.79). 2/50 ACR +ve and 2/50 ACR -ve patients had significant inducible ischaemia on adenosine stress perfusion imaging. The location and mass of infarction is shown in Table 5.2. Figure 5.3 shows an example of a patient with 2 distinct silent subendocardial myocardial infarctions.

There were no significant differences in LV EDV, LV mass, EF or left atrial volume between ACR +ve, ACR -ve or control (Table 5.2). LV mass/EDV was higher in patients with diabetes than in control 0.61±0.11 vs 0.66±0.13 g/ml P=0.008. Although a difference was detected in LV mass/EDV comparing ACR +ve with ACR -ve, this failed to reach statistical significance (0.65±0.14 vs 0.68±0.12 g/ml, P=0.07 (Figure 5.4).
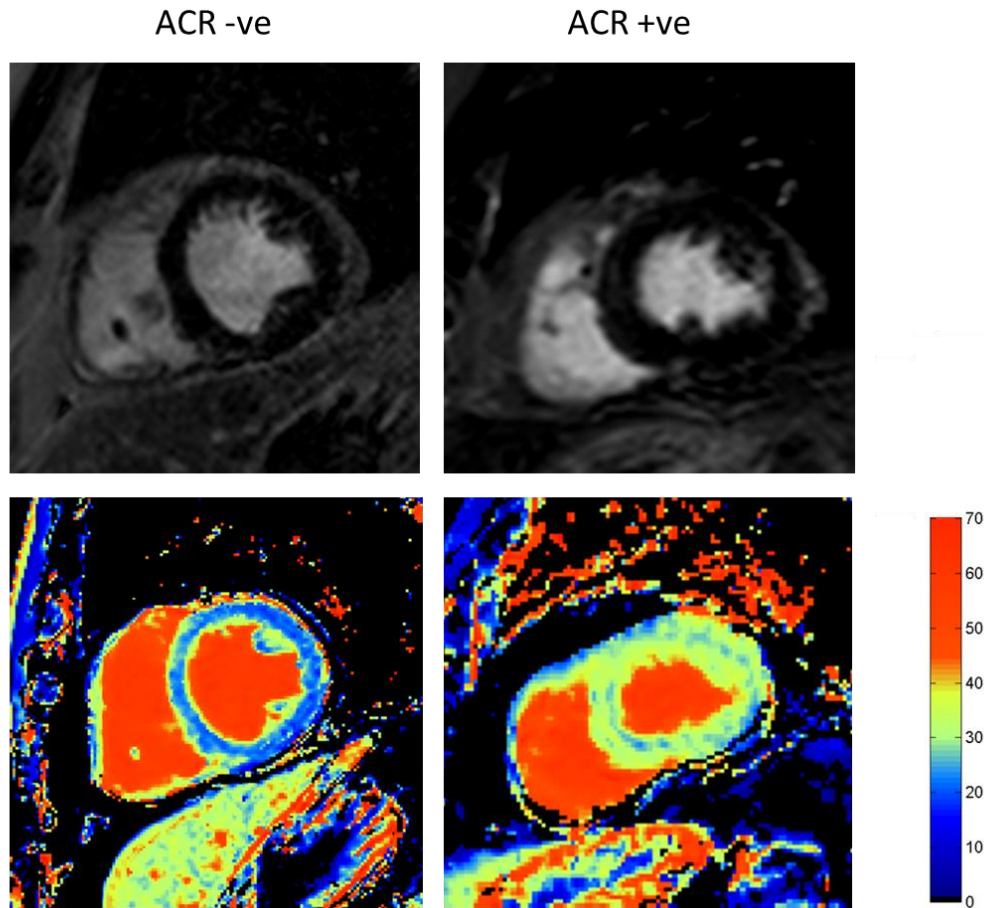
Figure 5.2 Late gadolinium enhancement (LGE) and extracellular volume (ECV) maps of an ACR -ve patient (left) and ACR +ve patient (right). LGE imaging showed no focal fibrosis in either patient but ECV mapping demonstrated the ECV to be significantly higher in the ACR +ve patient.

Circumferential strain was lower in patients with diabetes compared to control at apex, mid LV and base (-0.22, -0.22 & -0.20 vs -0.19, -0.18 & -0.18; P=0.001, P<0.0001 & P=0.001 respectively). Circumferential strain was also lower at the mid LV level in ACR +ve than ACR-ve patients-0.17±0.03 vs -0.19±0.05, P=0.01. There

was no difference in strain rates, LV twist or LV torsion between patients with diabetes or control (Table 5.1).

There was no difference in any echocardiography measured Doppler parameter between ACR +ve and ACR -ve patients (Table 5.3). There were no significant differences in hs-cTnT, NT-proBNP and serum aldosterone between ACR +ve and ACR -ve.

	Control	ACR -ve	ACR +ve	P value for trend	P value for ACR -ve vs +ve
N	30	50	50		
Age	59.1±11.5	61.1±9.1	60.2±12.7	0.76	0.69
Male gender, n (%)	21 (70)	42 (84)	40 (80)	0.32	0.60
Body mass index , kg/m^2	26.6±3.2	28.6±4.0	29.1±4.6	0.04	0.61
Duration of diabetes, years	-	4.6 ± 4.4	5.3±4.4	-	0.40*
HbA1c, mmol/mol	36.2±3.8	60.2±13.7	65.9±23.9	<0.0001	0.47
Systolic BP, mmHg	130±13	130±13†	133±17†	0.66	0.46
Diastolic BP, mmHg	70±11	71±8†	74±10†	0.20	0.12
Total cholesterol	-	4.4±1.2	4.4±1.1	-	0.94
Smoking	0	6	9		0.40
Metformin	0	49	38	<0.0001	0.002
Sulphonylurea	0	12	21	<0.0001	0.09
Other OH	0	3	1	0.28	0.62
Insulin	0	0	0	1.0	1.0
ACE inhibitor	0	0	0	1.0	1.0
Beta blocker	0	1	3	0.28	0.62
Calcium channel blocker	1	6	4	0.40	0.74
Diuretic	0	2	3	0.40	1.0
Statin	2	36	33	<0.0001	0.67
Aspirin	3	4	14	0.01	0.02

Table 5.1 Subject characteristics. *ACR -ve vs ACR +ve only. †24 hour BP; OH, oral hypoglycaemic agent

	Control	ACR -ve	ACR +ve	P value for trend	P value for ACR -ve vs +ve
LV EDV, ml	162.2±41.4	149.2±32.4	147.2±36.3	0.16	0.40
LV EDV index, ml/m^2	83.5±18.7	74.1±13.9	73.1±14.5	0.03	0.34
Ejection fraction, %	60.5±6.6	61.2±5.1	60.6±6.9	0.59	0.93
LV mass, g	95.5±22.6	93.9±17.6	98.5±23.3	0.65	0.35
LV mass index, g/m^2	49.1±9.3	46.8±7.7	48.9±9.4	0.48	0.30
Mass/EDV, g/ml	0.61± 0.11	0.65±0.14	0.68±0.12	0.02	0.07
LAV, ml	91.6±26.6	87.5±17.0	89.8±22.5	0.92	0.99
LAV index, ml/m^2	46.9±12.3	43.7±8.2	44.9±9	0.69	0.78
Native T1, ms	1209.7±47.4	1231.72±35.8	1252.6±66.0	0.002	0.05
Extracellular volume, %	23.3±3.0	25.1±2.9	27.2±4.1	<0.0001	0.004
Myocardial Infarction, n (%)	0 (0)	8 (16)	9 (18)	0.01*	0.79
Mass of Infarction, g	-	3.1±2.1	8.7±11.7	-	0.50†
Mass of infarction, % of LV	-	2.9±1.8	8.5±11.2	-	0.50†
Apex Ecc	-0.22±0.05	-0.19±0.05	-0.18±0.05	0.001α	0.12
Mid LV Ecc	-0.22±0.02	-0.19±0.05	-0.17±0.03	<0.0001	0.01
Base Ecc	-0.20±0.03	-0.18±0.04	-0.17±0.03	0.001β	0.14
Mid LV systolic SR	-1.11±0.12	-1.06±0.16	-1.02±0.20	0.10	0.27
Mid LV early diastolic SR	0.53±0.15	0.45±0.20	0.44±0.18	0.02γ	1.0
Mid LV late diastolic SR	1.37±0.26	1.13±0.30	1.06±0.32	<0.0001δ	0.29
Peak LV twist	14.6±4.2	15.0±3.0	15.4±4.3	0.67	0.57
Peak LV torsion	13.4±3.1	14.5±3.6	14.4±3.7	0.45	0.92

*Table 5.2 CMR findings. BSA, body surface area; Ecc, circumferential strain EDV, end diastolic volume; ESV, end systolic volume; LAV, left atrium volume; LV, left ventricle; SR, strain rate *DM vs control. †One ACR +ve patient had discrete lateral and antero-apical infarction that corresponded to two coronary severe stenoses on subsequent coronary angiography. α DM vs control P=0.001. β DM vs control P=0.001. γ DM vs control P=0.01. δ DM vs control <0.0001.*
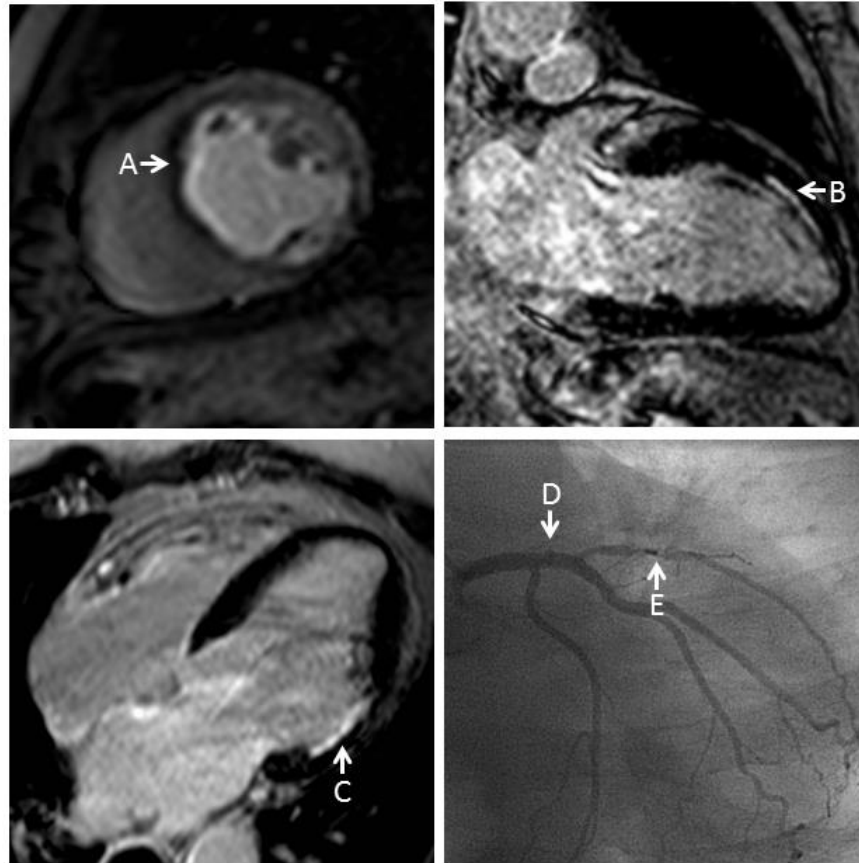
Figure 5.3 Adenosine stress perfusion imaging showing severe anteroseptal inducible ischaemia (A). Late gadolinium enhancement images showing 2 distinct silent myocardial infarctions in one ACR +ve patient. Antero-apical (B) and lateral (C) subendocardial infarctions caused by a chronic total occlusion of the left anterior descending artery (D) and severe obtuse marginal disease (E)

5.4.1 High Sensitivity cardiac Troponin T

Eleven of all 100 patients with diabetes had hs-cTnT ≥14ng/L. CMR findings of these patients are shown in Table 5.4. Both native T1 and ECV were higher in patients with hs-cTnT ≥14ng/L than those with normal hs-cTnT levels (1293.3±80.2 vs 1235.8±46.5ms, P=0.0001 and 30.3±4.8 vs 25.6±3.2%, P<0.0001 respectively). Hs-cTnT level had a modest correlation with CMR tagging derived late diastolic strain rate r=-0.25 P=0.02. Hs-cTnT also had a modest correlation with E wave by spectral mitral Doppler -0.211, P=0.04, medial and lateral E' by TDI r=-0.32 P=0.001 and r=-0.22, P=0.03 respectively. There was also a significant correlation between Hs-cTnT and NT-proBNP r=0.30, P=0.003.

5.4.2 NT-ProBNP

There were 11 patients with NT-proBNP ≥125ng/L. CMR findings of these patients are shown in Table 5.4. Patients with NT-proBNP ≥125ng/L had increased LA volume indexed to BSA compared with patients with normal NT-proBNP (54.3±16.0 vs 43.1±7.6 ml/m^2, P=0.004), as well as higher native T1 1285.6±79.6 vs 1236.8±47.8ms, P=0.07 and ECV 29.3±4.5 vs 25.7±3.4%, P=0.002. S' average by TDI was lower in those with NT-proBNP ≥125ng/L -3.2 vs-4.3 cm/s, P=0.02.
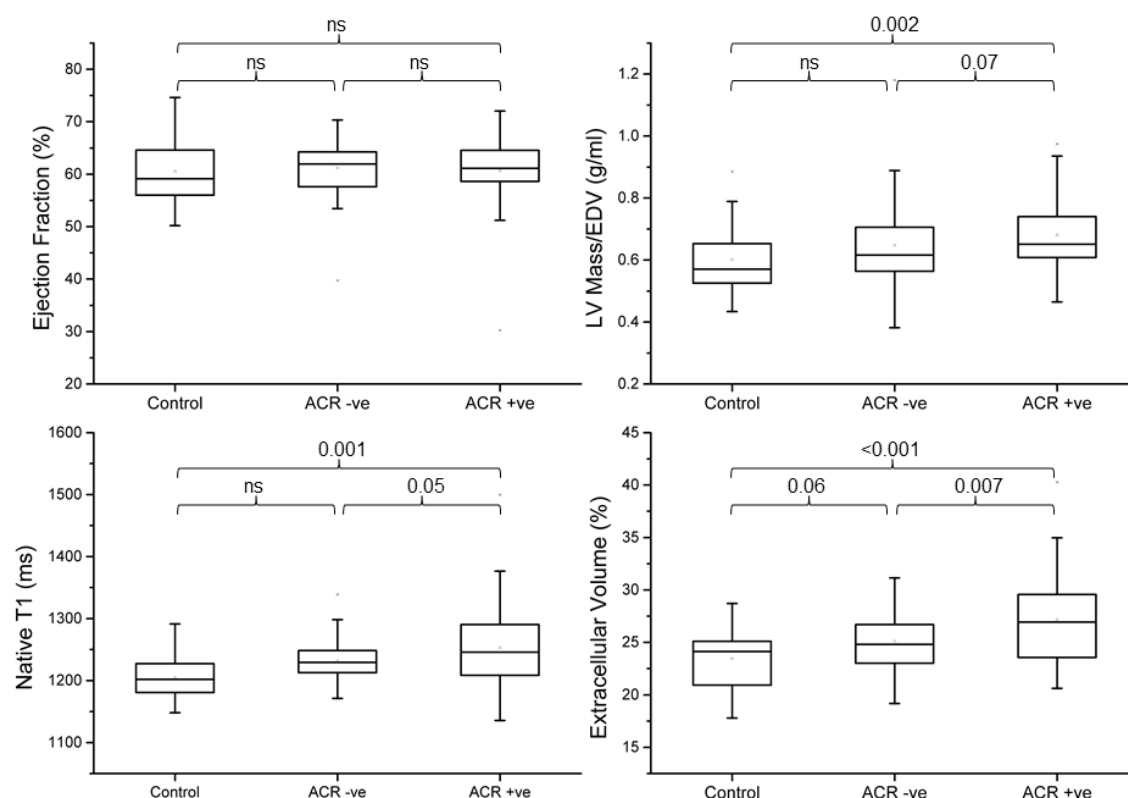
Figure 5.4 Box and whisker plots showing ejection fraction, LV mass/EDV, native T1 and extracellular volume according to ACR status. Brackets above show the P value between groups.

5.4.3 Correlates of ECV

Of the patient characteristics listed in Table 5.4 only HbA1c (r=0.28, P=0.004) and female gender (r=0.38, P<0.0001) were associated with higher ECV. None of the medications listed in Table 5.1 were associated with increased ECV. LV mass, EDV and ESV all had a significant correlation with ECV (r=-0.24, P=0.02; r=-0.30, P=0.002 and r=-0.36, P<0.001 respectively). There were no significant correlations between

any of the strain parameters measured by CMR shown in Table 5.2 or by echocardiography shown in Table 5.3 and ECV.

5.4.4 Correlates of Native T1

Of the patient characteristics listed in Table 5.4 only female gender (r=0.22, P=0.03) was associated with higher native T1 (r=0.38, P<0.0001). No medication was associated with increased native T1. EDV and ESV had a significant correlation with native T1 (r=-0.24, P=0.02 and r=-0.29, P=0.003). Of the strain parameters measured by CMR shown in Table 5.2 only peak systolic strain rate had a significant correlation with native T1 (r=0.25, P=0.01). None of the strain parameters measured by echocardiography shown in Table 5.3 had a correlation with native T1.

	ACR -ve	ACR +ve	P value
E/A ratio	0.87±0.27	0.85±0.34	0.28
E/E' medial	8.6±2.6	8.6±2.2	0.89
E/E' lateral	6.1±2.4	6.4±2.2	0.32
E/E' average	7.0±2.3	7.2±2.0	0.40
Diastolic dysfunction grade	0.84±0.58	0.98±0.47	0.12
0	12	5	
1	35	42	
2	2	2	
3	1	1	
S' medial, cm/s	9.1±2.4	9.3±2.3	0.87
S' lateral, cm/s	10.2±2.5	9.5±2.1	0.11
S' average, cm/s	9.7±2.0	9.4±1.8	0.42
hs-cTnT, ng/L	6.4±4.3	8.4±5.8	0.09
NT-proBNP, ng/L	54.0±81.9	67.0±129.7	0.34
Serum Aldosterone, pmol/L	299.0±194.6	322.55±182.5	0.32

Table 5.3 Echocardiography & biomarker results

5.4.5 Combinations of ACR, hs-cTnT and NT proBNP

Eleven patients had elevated levels of 2 or 3 of the bioamrkers for developing heart failure (ACR, hs-cTnT or NT-proBNP, Figure 5). In those with 2 or 3 positive biomarkers native T1 and ECV were higher than in those with only one positive biomarker (1293.4±76.7 vs 1240.7±54.6ms, P=0.005 and 30.7±4.2 vs 26.2±3.5%, P=0.0001 respectively) or none (1293.4±76.7   vs 1229.9±36.6ms, P=0.001 and 30.7±4.2 vs 24.9±2.7%, P<0.0001).
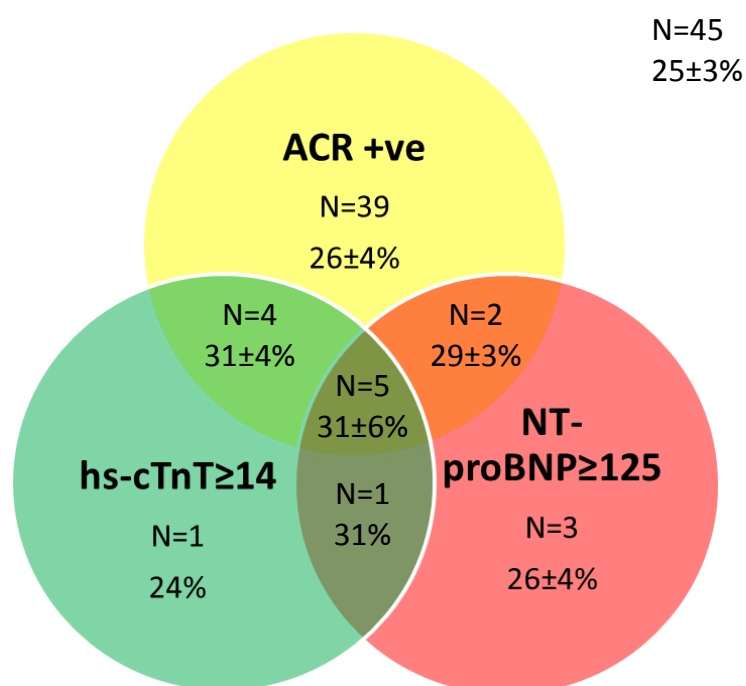
Figure 5.5 Venn diagram showing overlap between positive ACR, hs-cTnT≥14ng/ml and NT-proBNP≥125ng/ml and their relationship with ECV.

	hs-cTnT≥14	hs-cTnT<14	P value	NT-proBNP≥125	NT-proBNP<125	P value
N	11	89		11	89	
ACR +ve, N (%)	9 (82)	41 (46)	0.05	7 (64)	41 (46)	0.53
hs-cTnT, ng/L	19.5±4.0	5.9±2.7	-	12.7±6.8	6.7±4.5	0.01
NT-proBNP, ng/L	201.8±227.1	43.0±67.0	0.01	279.5±218.1	33.4±31.8	-
24 hour SBP, mmHg	125±10	132±15	0.18	125±11	132±15	0.14
24 hour DBP, mmHg	64±10	74±9	0.001	63±9	74±8	<0.001
LV EDV, ml	141.0±38.5	149.1±33.8	0.46	143.7±39.9	148.7±33.7	0.65
LV EDV index, ml/m^2	69.7±16.4	74.1±13.9	0.33	72.7±16.2	73.8±14.0	0.81
Ejection fraction, %	60.6±10.7	61.0±5.3	0.84	60.5±10.6	61.0±5.3	0.80
LV mass, g	97.2±13.8	96.0±21.4	0.86	90.7±14.9	96.8±21.2	0.36
LV mass index, g/m^2	48.7±9.2	47.8±8.6	0.74	46.0±5.3	48.1±9.0	0.46
Mass/End diastolic volume, g/ml	0.72±0.14	0.66±0.13	0.15	0.66±0.13	0.67±0.13	0.82
Left atrial volume, ml	103.0±31.4	86.8±17.4	0.12	106.1±31.7	86.4±17.0	0.07
Left atrial volume index, ml/m^2	51.3±15.0	43.4±8.3	0.12	54.3±16.0	43.1±7.6	0.004
Native T1, ms	1293.3±80.2	1235.8±46.5	0.0001	1285.6±79.6	1236.8±47.8	0.07
Extracellular volume, %	30.3±4.8	25.6±3.2	<0.0001	29.3±4.5	25.7±3.4	0.002
Myocardial Infarction , n (%)	2 (18)	15 (17)	1.0	3 (27)	14 (16)	0.39
Mass of Infarction, g	19.8±23.8	4.3±4.3	0.53	13.3±20.2	4.6±4.3	0.53
Mass of infarction, % of LV	19.9±22.0	4.0±4.0	0.49	13.4±19.2	4.2±4.0	0.49

Table 5.4 CMR and biomarker findings of 100 patients with type 2 diabetes according to whether they had elevated hs-cTnT or NT-proBNP.

ACR, albumin creatinine ratio; DBP, diastolic blood pressure; SBP, systolic blood pressure; EDV, end diastolic volume

5.5 Discussion

Data from our prospectively recruited cohort of low risk asymptomatic patients with diabetes demonstrates that patients who are at a higher risk of heart failure have higher ECV and extracellular matrix (ECM) expansion. ACR, hs-cTnT and NT-proBNP are all known surrogates of heart failure risk and all correlated with an increased ECV. There was also a high rate of silent MI in this low risk asymptomatic cohort however there was no correlation between silent MI and ACR, hs-cTnT or NT-proBNP status.

There is now considerable data demonstrating that diabetes is associated with increased ECV and diffuse cardiac fibrosis (Jellis et al., 2011; Ng et al., 2012; van Heerebeek et al., 2008) and that elevated ECV is associated with increased heart failure and mortality (Wong et al., 2013). Several biomarkers including urine ACR (Carr et al., 2005), hs-cTnT (Selvin et al., 2014) and NT-proBNP (Rana et al., 2006) have also been linked with increased heart failure risk in diabetes although the mechanisms underlying this risk are not clear. We have shown that elevated levels in each of these biomarkers are associated with increased ECV suggesting ECM expansion as a mechanism for heart failure in this population.

Microalbuminuria is typically the earliest clinical manifestations of diabetic kidney disease as well as a marker of vascular pathology. The mechanisms that lead from hyperglycaemia to renal dysfunction are complex and are thought to involve altered pathways of cellular glucose metabolism, increased fatty acid oxidation, increased reactive oxygen species secondary to mitochondrial dysfunction and ultimately production of advanced glycation end products within vulnerable cells of the kidney (Brownlee, 2005; Wendt et al., 2003). These pathways lead to the microscopic changes within the kidney including glomerular basement thickening, mesangial cell enlargement and increased extracellular matrix secretion which all may be detected in patients with microalbuminuria (Tervaert et al., 2010) .

The cellular processes that lead from hyperglycaemia to cardiac fibrosis and dysfunction are similar to those in the kidney and involve altered substrate metabolism, impaired calcium handling, increased reactive oxygen species and microvascular advanced glycation end product deposition (Boudina and Abel, 2007;

Seferovic and Paulus, 2015). These pathways lead to increased cardiac interstitial fibrosis (van Heerebeek et al., 2008) that can ultimately be detected by CMR T1 mapping. It is therefore likely that similar cellular mechanisms lead to both cardiac and renal fibrosis and dysfunction in type 2 diabetes. This may explain the relationship between microalbuminuria and cardiac extracellular matrix expansion that we have reported.

It is also likely that renal dysfunction in patients with microalbuminuria leads to cardiac fibrosis. In diabetes there is increased expression of angiotensin II in the leading to volume expansion via salt and water reabsorption in the kidney (Price et al., 1999). This increases cardiac afterload and may explain the concentric remodelling with increased LV mass/EDV we have reported in patients with microalbuminuria. We had also anticipated that serum aldosterone level would be elevated in ACR +ve patients, which was not the case. Rao *et al* have previously reported a correlation between urinary aldosterone excretion and ECV which fits with the hypothesis that angiotensin II expression is important in cardiac fibrosis. Despite deliberate exclusion of ACE inhibitors and low use beta blockers that both influence aldosterone levels we did not find an association between ECV and serum aldosterone level in our cohort. It is possible that factors such as fluid status and posture prior to blood testing have had a deleterious effect on the measured aldosterone levels.

We have also reported the novel finding of an association between cardiac biomarkers and cardiac extracellular matrix expansion in diabetes. This finding is in keeping with other disease states that involve expansion of the extracellular matrix including cardiac amyloidosis (Barison et al., 2015) and HCM (Kawasaki et al., 2013) where diffuse cardiac fibrosis detected by CMR has been shown to correspond with both BNP and cardiac troponin.

Our finding that rates of silent MI did not vary according to ACR status was surprising. ACR reflects a microvascular complication of diabetes which is recognised to be directly related to glycaemic control (Stratton et al., 2000). Elevated ACR however, is also a marker of vascular injury. The relationship between risk of MI and glycaemic control is complex. For example, only after 10 years post study follow up of improved glycaemic control in UKPDS was a decrease

in rates of MI apparent (Holman et al., 2008). Our finding that ACR status did not influence the chance of silent MI likely reflects this complex relationship.

Diastolic dysfunction detected by echocardiography was a very common finding in our study in 83/100 patients which is in keeping with previously reported rates (Poirier et al., 2001). Previous studies have demonstrated that diastolic dysfunction in type 2 diabetes is strongly influenced by age, hypertension and coronary disease and have given conflicting results about whether it leads to heart failure and increased mortality (From et al., 2010; Poulsen et al., 2013) . We have reported no difference in any measure of diastolic dysfunction between ACR +ve and ACR -ve and furthermore that there was no correlation between any echocardiographic measure of diastolic dysfunction and ECV. Our finding add further weight to the argument that diastolic dysfunction is influenced by too many factors to be a useful screening tool for subclinical cardiac dysfunction secondary to diffuse fibrosis in type 2 diabetes.

However mid LV circumferential strain measured by CMR tagging was lower in ACR +ve than ACR -ve patients, although there was no significant correlation with ECV. Previous studies have suggested that impairment of this parameter is associated with increased risk of heart failure on follow up (Choi et al., 2013). This was the only functional parameter that was different between ACR +ve and ACR -ve and further studies are required to establish whether it may have prognostic value in type 2 diabetes.

It has been postulated that future clinical trials should be directed at patients with diabetes and increased ECV to try and prevent the onset of heart failure. ACR, hs-cTnT, NT-proBNP, or even a combination of all three, have the potential to be relatively simple and cost effective screening tools to detect patients with diabetes most likely to have elevated ECV. Recruiting those most likely to have elevated ECV to clinical trials could increase the event rate and decrease sample size.

5.6 Limitations

In this study we have explored the relationships between ECV and three biomarkers associated with increased risk of heart failure in diabetes. Our study was not powered to compare clinical outcomes or risk of heart failure. We have

not carried out invasive coronary angiography because it would not be ethically appropriate to put asymptomatic low risk patients through an invasive procedure. However we have carried out high resolution stress perfusion imaging to exclude significant silent ischaemia and the prevalence of which was the same between groups. For the same reasons we did not carry out myocardial biopsy to confirm increased ECM histologically. However ECV measured by CMR has been validated against histology in other disease processes (Iles et al., 2008) and there is now considerable evidence suggesting that the increased ECV in diabetes represents ECM expansion and diffuse cardiac fibrosis (Jellis et al., 2011; Ng et al., 2012; Rao et al., 2013).

5.7 Conclusions

Patients with type 2 diabetes and persistent microalbuminuria, positive hs-cTnT or NT-proBNP have cardiac extracellular matrix expansion detected by CMR, suggesting that the increased risk of heart failure in these patients is mediated by diffuse cardiac fibrosis. There was a high rate of silent MI in this low risk cohort that was not related to biomarker status.

6. Study 5– Identification of patients with type 2 diabetes with evidence of silent myocardial infarction

6.1 Abstract

Aims

Silent myocardial infarction (SMI) is a prevalent finding in patients with type 2 diabetes and is associated with significant mortality and morbidity. Late gadolinium enhancement (LGE) by cardiovascular magnetic resonance (CMR) is the best validated technique for detection of SMI but is time consuming, costly and requires administration of intravenous contrast. We therefore planned to develop a population screening tool to identify those at highest risk of SMI.

Methods

100 asymptomatic patients with type 2 diabetes underwent ECG, 24 hour blood pressure, echocardiography, biomarker assessment and CMR at 3.0T including assessment of ejection fraction (EF) and LGE. Global longitudinal strain (GLS) measured from basic 2 and 4 chamber cines was measured using feature tracking. Risk factors, imaging and biomarker findings were compared in those with and without SMI.

Results

17/100 patients had SMI. Risk factors for SMI included older age but not fasting cholesterol, 24hrBP, smoking or hsCRP. Q waves on ECG, Doppler echocardiography EA ratio ≤ 0.79, GLS ≥ -18.4% and NT-proBNP > 29ng/L were all associated with SMI. We tested a simple risk score derived from these 4 factors and age. The combined score had an AUC of 0.836 (0.749-0.902), P<0.0001. A score of ≥3/5 had 88% sensitivity and 70% specificity for SMI.

Conclusions

We have developed a simple screening test, using measures that can be derived in a cardiology outpatient clinic, for the detection of SMI in type 2 diabetes. Identifying those most likely to have SMI would allow appropriate investigation and initiation of treatment.

6.2 Introduction

Cardiovascular disease, primarily stroke and myocardial infarction, account for the vast majority of mortality associated with type 2 diabetes (Morrish et al., 2001). Silent myocardial infarction (SMI) is a relatively common finding in patients with type 2 diabetes (Kwong et al., 2006; Schelbert et al., 2012) although the exact prevalence in contemporary asymptomatic populations is unknown (Davis et al., 2013).

Currently the most extensively validated method to assess for the presence and extent of silent MI is the LGE technique measured by CMR. Using this technique it is possible to establish the location and distribution of scar tissue. The prevalence of SMI according to the presence of LGE in symptomatic patients with type 2 diabetes is reported to be between 21-28% (Kwong et al., 2006; Schelbert et al., 2012). In these cohorts the presence of SMI was strongly associated with an increase in MACE and mortality.

There has been a decrease in the rate of acute MI in type 2 diabetes in the past two decades (Gregg et al., 2014). This may reflect improvements in glycaemic control and modification of other concomitant risk factors such as smoking, dyslipidaemia and blood pressure. It is unknown whether these same risk factors influence the likelihood of SMI. Comparatively the detection of LGE by CMR is time consuming, costly and requires administration of intravenous contrast making it a less than ideal population screening tool.

Several imaging and biomarker tests have been shown to be able to detect the presence and determine the extent of MI measured by LGE including Q waves on 12 lead electrocardiogram (ECG) (Moon et al., 2004a), ejection fraction (Ingkanisorn et al., 2004), strain parameters (Biere et al., 2014), hs-cTnT (Nguyen et al., 2015) and NT-proBNP (Garcia-Alvarez et al., 2009). However, the sensitivity and specificity of these tests to detect SMI in type 2 diabetes is at present unknown.

We hypothesised that a risk score derived from routinely acquired clinical measurements could accurately predict the presence of SMI.

6.3 Methods

6.3.1 Enrolment Criteria

100 asymptomatic patients with type 2 diabetes were recruited from 30 primary care health centres in the local area. Exclusion criteria were known cardiac disease, kidney disease (eGFR <30), uncontrolled hypertension, treatment with insulin or ACE inhibitor/angiotensin receptor blocker.

6.3.2 CMR protocol

All patients underwent an identical CMR study on a dedicated cardiovascular 3 Tesla Philips Achieva TX system (Philips, Best, The Netherlands) equipped with a 32 channel coil and MultiTransmit® technology. Data were acquired during breath-holding at end expiration.

From scout CMR images, the left ventricular long and short axes were determined. Cine images covering the entire heart in the LV short axis plane and orthogonal long-axis planes were then acquired (balanced SSFP, spatial resolution 1.2x1.2x10mm³, 50 cardiac phases TR/TE 2.6/1.3ms, flip angle 40°, field of view 300-420mm). Cines planned to cover the entire left atrium (LA) short axis plane in end systole were also acquired (as LV stack but slice gap 5mm).

LGE imaging was carried out more than 6 minutes after contrast injection using inversion recovery-prepared T1-weighted echo. The optimal inversion time to null signal from normal myocardium was determined using a Look-Locker approach. Typical parameters are TR/TE 3.5/2.0 ms, flip angle 25°, acquired spatial resolution 1.54x1.76x10mm³ and performed in 10-12 short axis slices with further slices acquired in the vertical and horizontal long axis orientations, phase-swapped or imaged in systole, if indicated based on LGE imaging obtained or wall-motion abnormality.

6.3.3 CMR interpretation

CMR data were assessed quantitatively using commercially available software (CVI42, Circle Cardiovascular Imaging Inc. Calgary, Canada). LV mass, ejection fraction (EF) and LA volume were measured from short axis cine images.

For feature tracking analysis endocardial and epicardial LV contours were drawn on long axis 4 chamber and 2 chamber cines using a semi-automated process. Peak global longitudinal strain, systolic strain rate, early and late diastolic strain rates were measured. Late diastolic strain rates were defined as peak rate during active atrial contraction.

The presence of SMI was identified by 2 physicians experienced in CMR interpretation based upon typical subendocardial distribution of LGE present. The mass of LGE was quantified by the Otsu method (Vermes et al., 2013).

6.3.4 Echocardiography & Electrocardiography

All patients underwent echocardiography (Vivid e9, GE Medical Systems, Milwaukee, WI, USA) focused on Doppler measurements of mitral inflow and tissue Doppler imaging (TDI) of the lateral and medial mitral annulus. E/A ratio, E', A' and S' are measured on the machine using inbuilt software. Diastolic dysfunction was graded 0-3 by an accredited echocardiographer blinded to clinical details according to international guidelines (Nagueh et al., 2009). 12 lead electrocardiography (MAC500, GE Medical Systems, Milwaukee, WI, USA) was analysed by 2 physicians blinded to clinical details for the presence of Q waves according to international guidelines (Thygesen et al., 2012).

6.3.5 Ambulatory blood pressure

All patients underwent 24 hour ambulatory blood monitor that has been validated for clinical use by the British Hypertension Society (6100, Welch-Allyn, NY, USA). The cuff was set to inflate every 30 minutes during the day and every 60 minutes during the night. Mean 24 hour systolic and diastolic BP were recorded.

6.3.6 Blood tests

Blood was drawn from each subject at the time of CMR and tested for HbA1c. Serum was stored at -70C and tested in one batch for hs-cTnT typical CV 4.4% at 13.7ng/L and 3.6% at 95.3 ng/L, NT-proBNP typical CV 2.9% at 91 ng/L and 2.1% at 415 ng/L (Cobas 8000, Roche Diagnostics, Burgess Hill, West Sussex) and HS-CRP

(Advia, Siemens Healthcare Diagnostics, Marburg, Germany). Fasting cholesterol and previous HbA1c were recorded from review of electronic records.
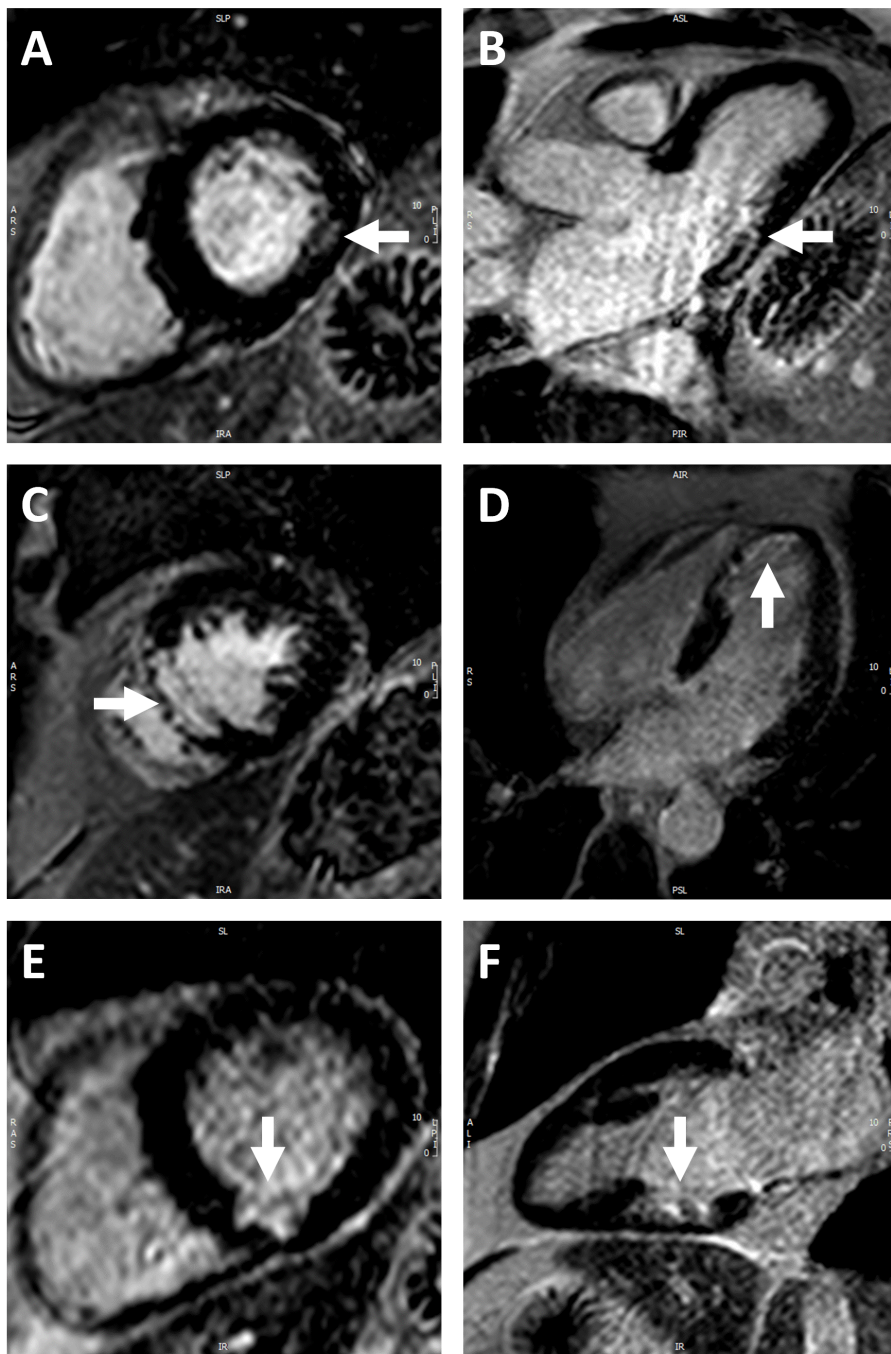
Figure 6.1 Examples of SMI detected by LGE. Horizontal panels are from the same patient and white arrows denote the area of MI. A and B show basal and mid inferolateral subendocardial MI. C and D show apical and mid septal near transmural infarction. E and F show basal inferior subendocardial infarction.

6.3.7 Statistical analysis

Statistical analysis was performed using IBM SPSS® Statistics 20.0 (IBM Corp., Armonk, NY). Continuous variables were expressed as means ± SD and compared using Mann Whitney U test. Categorical variables were expressed as N (%) and compared using Fisher exact test. Spearman rank correlation was used to test for correlation.

Receiver operating characteristic (ROC) analysis was used to determine the diagnostic accuracy of parameters that had been significantly different in those with SMI. The diagnostic accuracy is expressed as area under the curve (AUC) and 95% confidence interval. Optimal sensitivity and specificity were calculated using Youden index. Nested models were used to assess the additive value variables associated with SMI. AUCs were compared by using validated methods described by DeLong et al (DeLong et al., 1988).

Using the cut offs derived from the Youden analysis of the ROC curves each variable was given a binary classification. These five categorical variable were summed to calculate a SMI risk score (range 0-5). $P < 0.05$ was considered statistically significant.
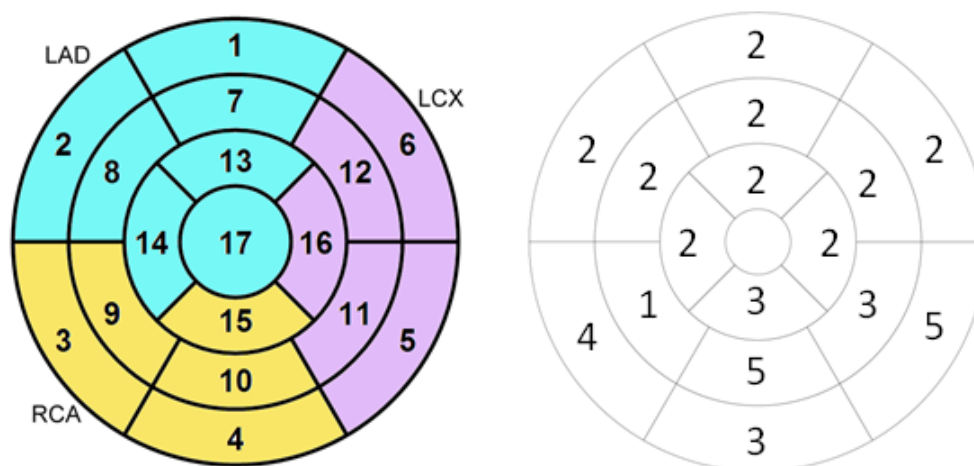
Figure 6.2 American Heart Association bullseye model (right) demonstrating 6 basal, 6 mid ventricular and 4 apical segments and their typical coronary arterial supply (LAD, left anterior descending; LCX, left circumflex; and RCA, right coronary artery). The right bullseye plot shows the location of infarcted segments from the 17 patients with SMI.

	SMI	No SMI	P value
N	17	83	
Age	65.4±9.2	59.8±11.0	**0.05**
Male gender, n (%)	16 (94)	66 (80)	0.30
Body mass index , kg/m^2	27.8±3.1	28.9±4.6	0.32
Duration of diabetes, years	4.1±4.1	5.2±4.4	0.24
HbA1c, mmol/mol	57.1±12.5	64.3±20.6	0.23
Median HbA1c, mmmol/mol	63.3±10.9	64.8±18.2	0.77
24 hr systolic BP, mmHg	135.3±15.9	130.8±14.7	0.24
24 hr diastolic BP, mmHg	72.5±10.1	72.7±8.9	0.89
Total cholesterol	4.3±1.2	4.4±1.1	0.69
Smoking, n (%)	4 (24)	11 (13)	0.28
Metformin	13	74	0.227
Sulphonylurea	5	28	1.0
Other oral hypoglycaemic	0	4	1.0
Insulin	0	0	-
ACE inhibitor	0	0	-
Beta blocker	2	2	0.133
Calcium channel blocker	4	6	0.064
Diuretic	1	4	1.0
Statin	14	56	0.262
Aspirin	2	16	0.73

Table 6.1 Patient characteristics according to the presence or absence of SMI ACE, angiotensin-converting enzyme; BP, blood pressure

6.4 Results

Seventeen of the 100 patients had evidence of SMI on LGE CMR. Figure 6.1 shows examples from 3 patients. Patient characteristics are shown in Table 6.1 according to SMI status. There was a significant range in the extent of SMI from 0.4g to 36.6g. Mean mass of infarction was 6.1±8.8g or as a percentage of the LV 5.8±8.5%. Mean

transmurality of infarction was 60.3±28.0%. Figure 6.2 shows a bullseye plot of the areas affected by SMI demonstrating that SMI could occur in any segment.

There was a trend to patients with SMI being older (65.4±9.2 vs 59.8±11.0, P=0.05) but there was no difference in any other patient characteristic or use of medication. There was no significant difference in any cardiac risk factors including 24 hour BP, fasting cholesterol or smoking (P=0.24, 0.69 and 0.28 respectively).

The mean number of previous HbA1c measurements included in the analysis was 9.7±5.7 per patient over 4.3±2.7 years. There was no significant difference between mean, median or maximum HbA1c between those with and without SMI (P=0.69, 0.77 and 0.28 respectively).

6.4.1 Electrocardiography

Pathological Q waves on ECG were only present in 4/17 with SMI and 6/83 without SMI (sensitivity 24%, specificity 93%). Other ECG abnormalities were present in 19/100 patients and included left axis deviation 5, right bundle branch block 5, left ventricular hypertrophy by voltage criteria 4, left anterior hemiblock 3, T wave abnormalities 3 and trifascicular block 1.

6.4.2 Echocardiography

Results of echocardiography are shown in Table 6.2. The only significant difference between those with and without SMI was a lower E/A ratio (0.75±0.30 vs 0.89±0.30, P=0.03) in patients with SMI. Grade of diastolic dysfunction was not significantly different between those with and without SMI (grade 0, 6 vs 19%; grade 1, 88 vs 75%; grade 2, 0 vs 5%; and grade 3, 6 vs 1% P=0.24).

6.4.3 Cardiovascular Magnetic Resonance

CMR results are shown in Table 6.2. LV mass index to BSA was higher in those with SMI than those without (51.4±6.5 vs 47.2±8.7 g/m^2, P=0.01). There was no other difference in volumetric parameters. Of the longitudinal strain parameters measured by feature tracking, global longitudinal strain (GLS-FT) -15.2±3.7 vs -17.7±3.1%, P=0.004, peak systolic strain rate (SSR-FT) -93.8±31.8 vs -111.2±42%, P= 0.04 and early diastolic strain rate (EDSR-FT) 64.1±16.6 vs 84.0±33.1%, P=0.02

were all significantly lower in those with SMI. There was no difference in late diastolic strain rate (LDSR-FT) P=0.89.

Of the patient characteristics shown in Table 6.1 none had a significant association with mass of SMI. Of the investigation findings shown in Table 6.2 the mass of SMI only had significant correlations with EF (R=-0.81, P<0.0001), E/E' (R=-0.58, P0.02) and hs-cTnT (R=0.58, P=0.02).

	SMI	No SMI	P value
CMR			
LV EDV, ml	140.5±39.1	150.0±32.8	0.30
LV EDV index, ml/m²	70.4±17.1	74.5±13.4	0.27
Ejection fraction, %	58.0±9.7	61.7±4.9	0.30
LV mass, g	102.5±16.3	95.0±21.0	0.34
LV mass index, g/m²	51.4±6.5	47.2±8.7	**0.01**
LA volumes, ml	89.0±31.6	88.5±16.8	0.93
LA volume index, ml/m²	44.9±15.9	44.2±7.7	0.87
Feature Tracking			
GLS-FT	-15.2±3.7	-17.7±3.1	**0.004**
SSR-FT	-93.8±31.8	-111.2±42	**0.04**
EDSR-FT	64.1±16.6	84.0±33.1	**0.02**
LDSR-FT	87.4±39.9	91.4±41.2	0.89
Echocardiography			
E/A ratio	0.75±0.30	0.89±0.30	**0.03**
E/E' average	7.4±2.4	7.1±2.1	0.96
S' average, cm/s	9.8±2.2	9.5±1.8	0.72
Electrocardiography			
Q waves (%)	4 (20)	6(7)	0.06
Biomarker findings			
Hs-cTnT, ng/L	7.5±4.1	7.4±5.4	0.42
NT-proBNP, ng/L	105.8±132.2	51.9±100.8	**0.003**
HS-CRP, mg/L	3.5±3.5	3.7±5.9	0.57

Table 6.2 Investigations according to SMI status. EDSR, early diastolic strain rate; EDV, end diastolic volume; FT, feature tracking; GLS, global longitudinal strain; LA, left atrium; LDSR, late diastolic strain rate; LV, left ventricle; SSR, systolic strain rate
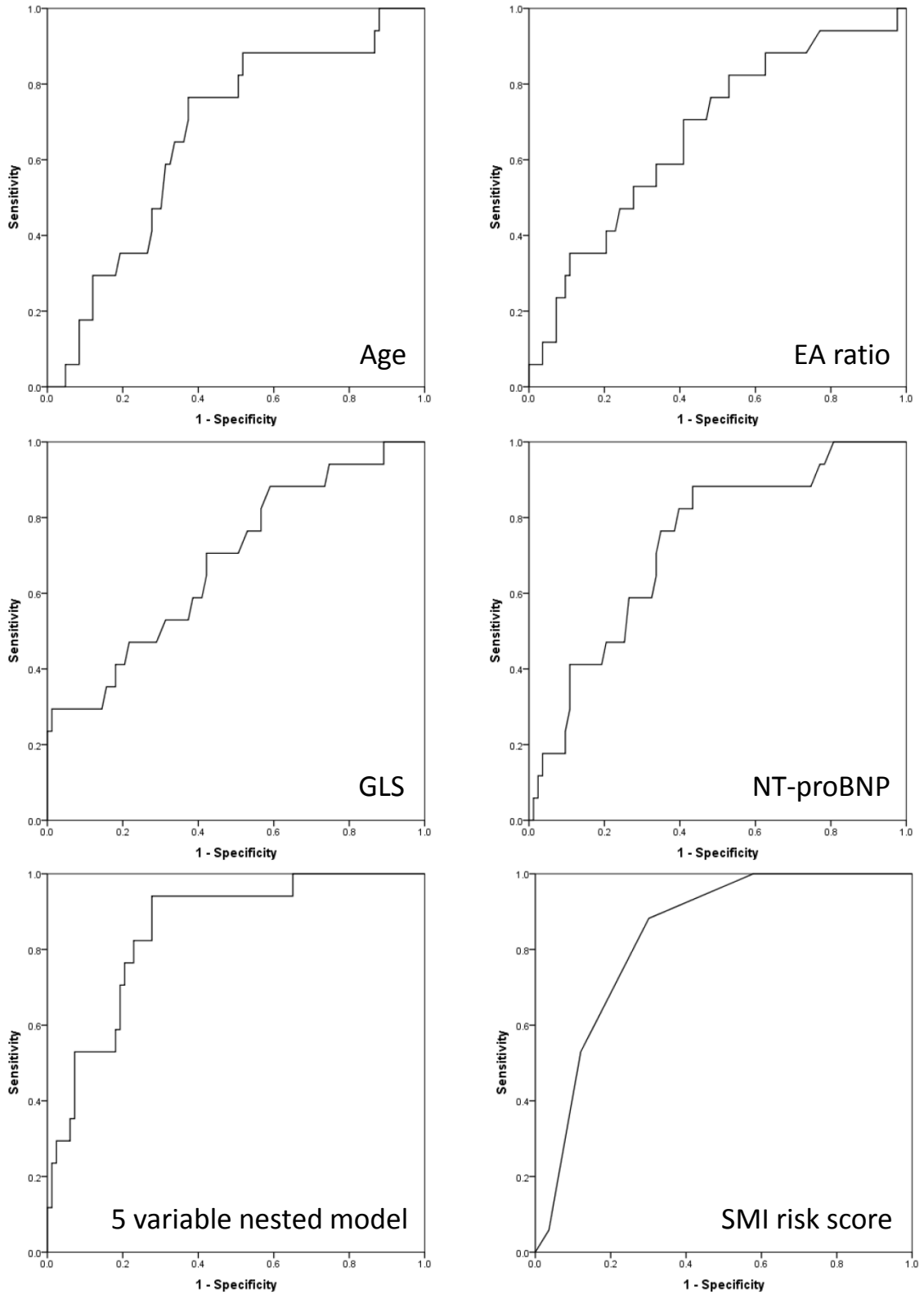
Figure 6.3 Receiver operator characteristic curves for age, E/A ratio, NT-proBNP global longitudinal strain (GLS) measured by feature tracking, the 5 variable nested model of age, Q waves, EA ratio , GLS and NT-proBNP (AUC= 0.85, P<0.0001) and the SMI risk score using the same 5 variables (AUC=0.84, P<0.0001).

	AUC	P value	Optimum cut-off	Sensitivity at cut-off	Specificity at cut-off
Age	0.668 (0.522-0.803)	0.02	>62	76%	63%
E/A ratio	0.673 (0.71-0.763)	0.005	≤0.72	71%	59%
GLS-FT	0.684 (0.540-0.828)	0.01	≥-18.4%	88%	41%
NT-proBNP	0.730 (0.604-0.855)	<0.001	>29ng/L	88%	57%
5 variable nested model	0.851 (0.766-0.914)	<0.0001	-	94%	72%

Table 6.3 Area under the curve (AUC) of continuous parameters for detecting silent MI for each of the 5 factors used in the SMI risk score and the 5 variable nested model. Optimum cut-off, sensitivity and specificity derived from Youden index are also shown.

6.4.4 Biomarkers

NT-proBNP was significantly higher in those with SMI (105.8±132.2 vs 51.9±100.8ng/L, P=0.003). There was no difference in HS-CRP or hs-cTnT (P=0.57 and 0.42 respectively).

6.4.5 ROC analysis

The area under the curve (AUC) for age, Q waves, E/A ratio, GLS-FT, and NT-proBNP are shown in Table 6.3 and Figure 6.3. The AUC for the nested model of all 5 variables was 0.851 (0.766-0.914), P<0.0001 and the maximum possible sensitivity was 94% and specificity 72%. The nested model had higher diagnostic accuracy than Q waves, GLS, age and E/A ratio alone (P<0.0001, 0.02, 0.02 and 0.006 respectively). The improvement over NT-proBNP did not reach statistical significant (P=0.06).

6.4.6 Development of a screening tool

The number of patients with SMI according to their SMI risk score is shown in Figure 6.4. The combined score had an AUC of 0.836 (0.749-0.902), P<0.0001 and better diagnostic accuracy than Q waves, age and EA ratio (P<0.001, 0.01 and 0.02 respectively). The improvement in diagnostic accuracy against GLS-FT and NT-proBNP did not reach significance (P=0.05 and 0.09 respectively). The sensitives and specificities for each possible SMI risk score are shown in Table 6.4.

SMI risk score	Sensitivity	95% CI	Specificity	95% CI
0	100.0	-	0.0	-
1	100.0	-	0.0	-
2	100.0	80.5 - 100.0	42.17	31.4 - 53.5
3	88.2	63.6 - 98.5	69.9	58.8 - 79.5
4	52.9	27.8 - 77.0	88.0	79.0 - 94.1
5	5.9	0.1 - 28.7	96.39	89.8 - 99.2

Table 6.4 SMI risk score calculated from age > 62, presence of Q waves on ECG, GLS ≥ -18.4%, EA ratio ≤ 0.79 and NT-proBNP >29ng/L. The sensitivity and specificity to detect SMI for each possible score is shown.

6.5 Discussion

The prevalence of SMI (17%) detected by LGE imaging in this low risk asymptomatic cohort was higher than expected. We have found increasing age to be the only conventional risk factor associated with SMI. We have identified several markers of SMI that can be detected by ECG, echocardiography or blood test and have shown that these markers can be added to develop a simple screening tool with good diagnostic accuracy.

We have demonstrated that a simple risk score can predict the presence of SMI in patients with type 2 DM as shown by LGE on CMR. The risk score is composed of

age, Q waves on ECG, EA ratio ≤ 0.79, GLS ≥ -18.4% and NT-proBNP > 29ng/L. These are all parameters that are often measured in a cardiology clinic or could easily be measured in community based screening. In the model we derived GLS from feature tracking of CMR cines. However if such a model was to be validated and used in larger populations GLS could be measured from standard echocardiography which has been demonstrated to show good agreement with GLS measured from CMR (Obokata et al., 2015).
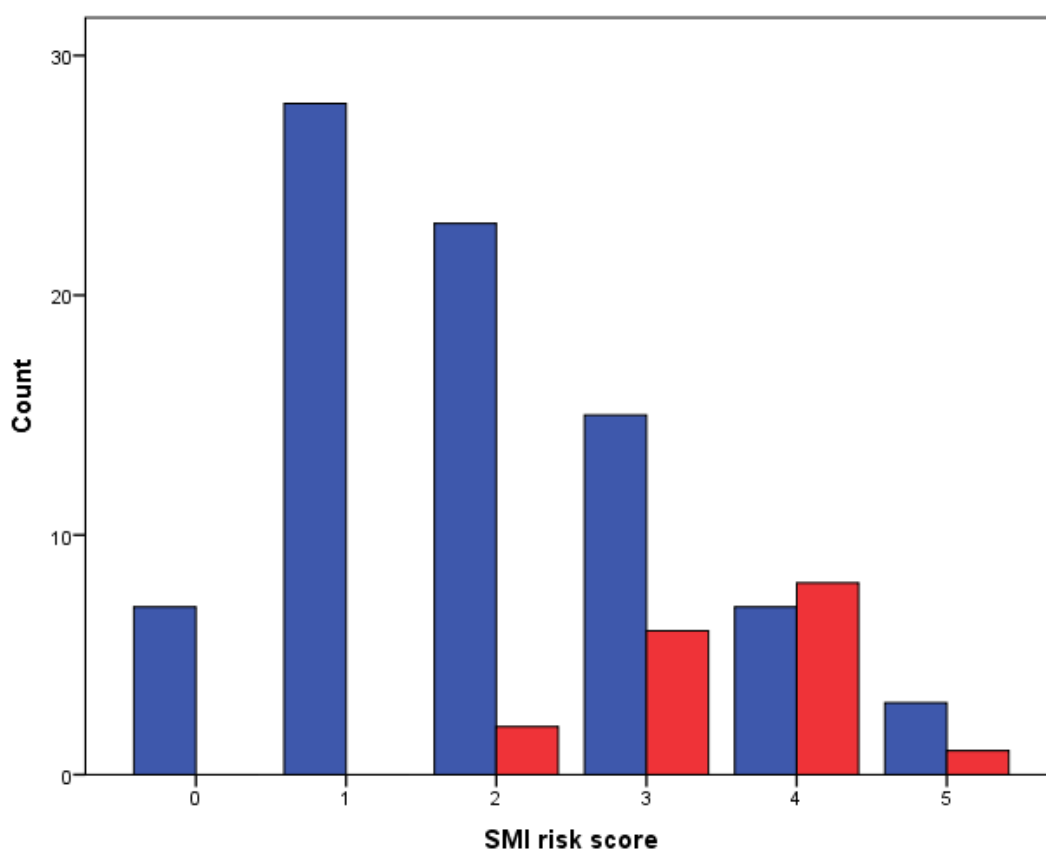
Figure 6.4 Number of patients with SMI (red) and without SMI (blue) according to their SMI risk score.

The decision about where to make the cut off to recommend further investigation depends on whether sensitivity or specificity is the main clinical priorities (Table 6.4). If the cut off was set at a score ≥2 (100% sensitivity and 42% specificity) it would ensure that the vast majority of SMI was detected with only 2.5 patients needing CMR to identify one patient with SMI. Alternatively if the cut off was

higher with a score ≥3 (88% sensitivity and 70% specificity) roughly 1 in 9 patients with SMI would be missed but only 1.5 patients would need to be screened to detect one patient with SMI.

All of the measured components within the score that is impaired GLS (Holland et al., 2015), elevated NT-proBNP (Huelsmann et al., 2008), EA ratio (From et al., 2010) and Q waves on ECG (Davis et al., 2013) have been associated with adverse outcomes in patients with type 2 diabetes without prior history of MI. It is likely that a proportion of the mortality reported in these patients is due to SMI. It has also been shown that larger infarcts have greater impairment of GLS (Biere et al., 2014), higher NT-proBNP (Garcia-Alvarez et al., 2009), altered mitral inflow (Nijland et al., 1997) and are more likely to develop Q waves (Moon et al., 2004a). Therefore all of the measured parameters have biological validity and prognostic significant that supports their inclusion in a risk score.

The imaging parameters associated with mass of SMI were different from those included in the SMI risk score and included EF, E/E' and hs-cTnT. These parameters are all recognised to correlate with extent of infarction and prognosis after symptomatic MI (Ingkanisorn et al., 2004; Nguyen et al., 2015; Naqvi et al., 2006). However, we have demonstrated that they were insensitive for the detection of SMI in type 2 diabetes and of limited value in this setting.

It was an unexpected finding that conventional risk factors including fasting cholesterol, 24 hour BP, smoking and even previous glycaemic control had no influence on the likelihood of SMI in our cohort. It is unclear whether the pathological processes that lead to SMI are identical to acute MI. The lack of association with conventional risk factors suggests that further research is needed to identify alternative risk factors specifically for SMI.

To our knowledge this is the first time that the rate of SMI assessed by LGE CMR has been assessed in a truly asymptomatic diabetic cohort. Previous studies have demonstrated that in patients with diabetes silent MI detected on CMR is associated with increased mortality and adverse cardiovascular events (Kwong et al., 2006; Schelbert et al., 2012). Kwong *et al* reported an incidence of silent MI of 28% in symptomatic patients with diabetes undergoing clinical CMR (Kwong et al., 2006). Schelbert *et al* reported a prevalence of 21% of silent MI of diabetic patients

enrolled in the ICELAND MI study who underwent CMR between 2004 and 2007 (Schelbert et al., 2012). However patients in both studies were not necessarily asymptomatic and in ICELAND MI and in fact 28% of those with silent MI had prior coronary revascularisation. The rate of infarction was the same between our study and the work of Schelbert *et al* despite patients in our study being younger, lower risk and asymptomatic.

SMI in type 2 diabetes is associated with significant mortality and morbidity (Kwong et al., 2006; Schelbert et al., 2012). However, it remains to be established if this prognosis can be altered by pharmacological or invasive intervention. Before recommending that a screening test can be used clinically it is of fundamental importance that an intervention exists that can alter the prognosis (Wilson and Jungner, 1968). This remains to be established in SMI in type 2 diabetes and should be the focus of future work. The SMI screening components that we have identified may help in future clinical studies by identifying those most likely to have SMI who could be targeted with a lifestyle, pharmacological or interventional procedure.

6.6 Limitations

The subjects we recruited were specifically low risk, for example those on insulin or ACE inhibitors were excluded. The SMI risk model would need to be validated in larger more varied populations to broaden its clinical use. We have not performed coronary angiography to confirm that SMI was caused by coronary disease. However in an asymptomatic cohort an invasive procedure would not be appropriate. The cut off points that we have used are based on Youden index which assigns equal importance to sensitivity and specificity. Depending on which of these is more important in clinical practice the thresholds would need to be altered accordingly. We have also assigned an equal score to each of the components which may oversimplify the complex nature of the disease process.

6.7 Conclusions

The rate of SMI in this low risk asymptomatic cohort of patients with type 2 diabetes was higher than expected (17%). No conventional risk factors other than

age were associated with SMI. Several simple clinical parameters including Q waves, EA ratio, GLS and NT-proBNP were associated with SMI. By combining them we were able to define a simple screening tool with good diagnostic accuracy for the detection of SMI.

7. Final Conclusions

There is increasing evidence that CMR can provide accurate quantification of subclinical cardiac change in both health and disease. Detection of subclinical change has both diagnostic and prognostic potential that until now primarily been used in research but in the coming years will likely be integrated into clinical practice.

In this thesis we have used tissue characterisation by both ECV and LGE to detect subclinical change in asymptomatic cohorts. We have also reported changes in strain and volumetric parameters that can be detected by CMR. We have applied these techniques to a wide range of subjects including patients with HCM, endurance athletes and asymptomatic patients with type 2 diabetes mellitus.

The main findings were:

7.1 Diagnosing HCM

i.   As LV hypertrophy increases ECV decreases in athletes but increases in HCM.

ii. Based on this divergent finding ECV can be used distinguish HCM and athletic remodelling with high diagnostic accuracy, in particular in subjects with indeterminate maximal segmental wall thickness.

iii. CMR using T1 mapping thus has a potential role in the exclusion of HCM in athletes presenting with left ventricular hypertrophy, but requires further validation in more varied patient populations.

iv. Regional strain impairment measured by feature tracking and tissue tagging is predominantly associated with the degree of hypertrophy and replacement fibrosis assessed by the presence of LGE.

v.   In non-hypertrophied segments strain is not significantly impaired by the presence of interstitial fibrosis. Therefore the presence of interstitial fibrosis (defined as ECV>30% in this cohort) may be a more useful method than impairment of strain of identifying HCM in subjects with borderline LV hypertrophy.

7.2 Cardiac Change in athletes

i. This cohort of endurance athletes had lower LV circumferential strain, LV torsion and biventricular diastolic strain rates than sedentary controls.

ii. There was a linear association between lactate threshold and LV torsion, which is secondary to decreased apical rotation in athletes with high lactate threshold.

iii. This association could be utilised to differentiate athletic remodelling from early dilated cardiomyopathy.

7.3 Subclinical Cardiac Change in diabetes

i. Patients with type 2 diabetes and persistent microalbuminuria, positive hs-cTnT and NT-proBNP have cardiac extracellular matrix expansion detected by CMR

ii. Therefore the increased risk of heart failure in these patients may be mediated by diffuse cardiac fibrosis.

iii. The rate of SMI in this low risk asymptomatic cohort of patients with type 2 diabetes was higher than expected (17%).

iv. No conventional risk factors other than age were associated with SMI. Several basic parameters including Q waves, EA ratio, GLS and NT-proBNP were associated with SMI.

v. By combining them we were able to propose a simple screening tool with good diagnostic accuracy for the detection of SMI.

8. References

Aaronson, K.D., Schwartz, J.S., Chen, T.M., Wong, K.L., Goin, J.E. and Mancini, D.M. 1997. Development and prospective validation of a clinical index to predict survival in ambulatory patients referred for cardiac transplant evaluation. *Circulation.* **95**(12), pp.2660-2667.

Abergel, E., Chatellier, G., Hagege, A.A., Oblak, A., Linhart, A., Ducardonnet, A. and Menard, J. 2004. Serial left ventricular adaptations in world-class professional cyclists: implications for disease screening and follow-up. *J Am Coll Cardiol.* **44**(1), pp.144-149.

Arbab-Zadeh, A., Perhonen, M., Howden, E., Peshock, R.M., Zhang, R., Adams-Huet, B., Haykowsky, M.J. and Levine, B.D. 2014. Cardiac remodeling in response to 1 year of intensive endurance training. *Circulation.* **130**(24), pp.2152-2161.

Arenja, N., Mueller, C., Ehl, N.F., Brinkert, M., Roost, K., Reichlin, T., Sou, S.M., Hochgruber, T., Osswald, S. and Zellweger, M.J. 2013. Prevalence, extent, and independent predictors of silent myocardial infarction. *Am J Med.* **126**(6), pp.515-522.

Baggish, A.L., Wang, F., Weiner, R.B., Elinoff, J.M., Tournoux, F., Boland, A., Picard, M.H., Hutter, A.M., Jr. and Wood, M.J. 2008. Training-specific changes in cardiac structure and function: a prospective and longitudinal assessment of competitive athletes. *J Appl Physiol (1985).* **104**(4), pp.1121-1128.

Balady, G.J., Arena, R., Sietsema, K., Myers, J., Coke, L., Fletcher, G.F., Forman, D., Franklin, B., Guazzi, M., Gulati, M., Keteyian, S.J., Lavie, C.J., Macko, R., Mancini, D. and Milani, R.V. 2010. Clinician's Guide to cardiopulmonary exercise testing in adults: a scientific statement from the American Heart Association. *Circulation.* **122**(2), pp.191-225.

Barison, A., Aquaro, G.D., Pugliese, N.R., Cappelli, F., Chiappino, S., Vergaro, G., Mirizzi, G., Todiere, G., Passino, C., Masci, P.G., Perfetto, F. and Emdin, M. 2015. Measurement of myocardial amyloid deposition in systemic amyloidosis: insights from cardiovascular magnetic resonance imaging. *J Intern Med.* **277**(5), pp.605-614.

Basavarajaiah, S., Wilson, M., Whyte, G., Shah, A., McKenna, W. and Sharma, S. 2008. Prevalence of hypertrophic cardiomyopathy in highly trained athletes: relevance to pre-participation screening. *J Am Coll Cardiol.* **51**(10), pp.1033-1039.

Bassett, D.R., Jr. and Howley, E.T. 2000. Limiting factors for maximum oxygen uptake and determinants of endurance performance. *Med Sci Sports Exerc.* **32**(1), pp.70-84.

Beaver, W.L., Wasserman, K. and Whipp, B.J. 1986. A new method for detecting anaerobic threshold by gas exchange. *J Appl Physiol (1985).* **60**(6), pp.2020-2027.

Bentley, D.J., Newell, J. and Bishop, D. 2007. Incremental exercise test design and analysis: implications for performance diagnostics in endurance athletes. *Sports Med.* **37**(7), pp.575-586.

Berger, J.S., Jordan, C.O., Lloyd-Jones, D. and Blumenthal, R.S. 2010. Screening for cardiovascular risk in asymptomatic patients. *J Am Coll Cardiol.* **55**(12), pp.1169-1177.

Biere, L., Donal, E., Terrien, G., Kervio, G., Willoteaux, S., Furber, A. and Prunier, F. 2014. Longitudinal strain is a marker of microvascular obstruction and infarct size in patients with acute ST-segment elevation myocardial infarction. *PLoS One.* **9**(1), pe86959.

Bluemke, D.A., Kronmal, R.A., Lima, J.A., Liu, K., Olson, J., Burke, G.L. and Folsom, A.R. 2008. The relationship of left ventricular mass and geometry to incident cardiovascular events: the MESA (Multi-Ethnic Study of Atherosclerosis) study. *J Am Coll Cardiol.* **52**(25), pp.2148-2155.

Bos, J.M., Towbin, J.A. and Ackerman, M.J. 2009. Diagnostic, prognostic, and therapeutic implications of genetic testing for hypertrophic cardiomyopathy. *J Am Coll Cardiol.* **54**(3), pp.201-211.

Boudina, S. and Abel, E.D. 2007. Diabetic cardiomyopathy revisited. *Circulation.* **115**(25), pp.3213-3223.

Bowen, T.S., Cannon, D.T., Begg, G., Baliga, V., Witte, K.K. and Rossiter, H.B. 2012. A novel cardiopulmonary exercise test protocol and criterion to determine maximal oxygen uptake in chronic heart failure. *J Appl Physiol (1985).* **113**(3), pp.451-458.

Boyer, J.K., Thanigaraj, S., Schechtman, K.B. and Perez, J.E. 2004. Prevalence of ventricular diastolic dysfunction in asymptomatic, normotensive patients with diabetes mellitus. *Am J Cardiol.* **93**(7), pp.870-875.

Brouwer, W.P., Germans, T., Head, M.C., van der Velden, J., Heymans, M.W., Christiaans, I., Houweling, A.C., Wilde, A.A. and van Rossum, A.C. 2012. Multiple myocardial crypts on modified long-axis view are a specific finding in pre-hypertrophic HCM mutation carriers. *Eur Heart J Cardiovasc Imaging.* **13**(4), pp.292-297.

Brownlee, M. 2005. The pathobiology of diabetic complications: a unifying mechanism. *Diabetes.* **54**(6), pp.1615-1625.

Buchfuhrer, M.J., Hansen, J.E., Robinson, T.E., Sue, D.Y., Wasserman, K. and Whipp, B.J. 1983. Optimizing the exercise protocol for cardiopulmonary assessment. *J Appl Physiol Respir Environ Exerc Physiol.* **55**(5), pp.1558-1564.

Burns, A.T., McDonald, I.G., Thomas, J.D., Macisaac, A. and Prior, D. 2008. Doin' the twist: new tools for an old concept of myocardial function. *Heart.* **94**(8), pp.978-983.

Carr, A.A., Kowey, P.R., Devereux, R.B., Brenner, B.M., Dahlof, B., Ibsen, H., Lindholm, L.H., Lyle, P.A., Snapinn, S.M., Zhang, Z., Edelman, J.M. and Shahinfar, S. 2005. Hospitalizations for new heart failure among subjects with diabetes mellitus in the RENAAL and LIFE studies. *Am J Cardiol.* **96**(11), pp.1530-1536.

Caselli, S., Maron, M.S., Urbano-Moral, J.A., Pandian, N.G., Maron, B.J. and Pelliccia, A. 2014. Differentiating left ventricular hypertrophy in athletes from that in patients with hypertrophic cardiomyopathy. *Am J Cardiol.* **114**(9), pp.1383-1389.

Caselli, S., Montesanti, D., Autore, C., Di Paolo, F.M., Pisicchio, C., Squeo, M.R., Musumeci, B., Spataro, A., Pandian, N.G. and Pelliccia, A. 2015. Patterns of left ventricular longitudinal strain and strain rate in Olympic athletes. *J Am Soc Echocardiogr.* **28**(2), pp.245-253.

Castagno, D., Baird-Gunning, J., Jhund, P.S., Biondi-Zoccai, G., MacDonald, M.R., Petrie, M.C., Gaita, F. and McMurray, J.J. 2011. Intensive glycemic control has no impact on the risk of heart failure in type 2 diabetic patients: evidence from a 37,229 patient meta-analysis. *Am Heart J.* **162**(5), pp.938-948 e932.

Cerqueira, M.D., Weissman, N.J., Dilsizian, V., Jacobs, A.K., Kaul, S., Laskey, W.K., Pennell, D.J., Rumberger, J.A., Ryan, T., Verani, M.S., American Heart Association Writing Group on Myocardial, S. and Registration for Cardiac, I. 2002. Standardized myocardial segmentation and nomenclature for tomographic imaging of the heart. A statement for healthcare professionals from the Cardiac Imaging Committee of the Council on Clinical Cardiology of the American Heart Association. *Circulation.* **105**(4), pp.539-542.

Chan, R.H., Maron, B.J., Olivotto, I., Pencina, M.J., Assenza, G.E., Haas, T., Lesser, J.R., Gruner, C., Crean, A.M., Rakowski, H., Udelson, J.E., Rowin, E., Lombardi, M., Cecchi, F., Tomberli, B., Spirito, P., Formisano, F., Biagini, E., Rapezzi, C., De Cecco, C.N., Autore, C., Cook, E.F., Hong, S.N., Gibson, C.M., Manning, W.J., Appelbaum, E. and Maron, M.S. 2014. Prognostic value of quantitative contrast-enhanced cardiovascular magnetic resonance for the evaluation of sudden death risk in patients with hypertrophic cardiomyopathy. *Circulation.* **130**(6), pp.484-495.

Choi, E.Y., Rosen, B.D., Fernandes, V.R., Yan, R.T., Yoneyama, K., Donekal, S., Opdahl, A., Almeida, A.L., Wu, C.O., Gomes, A.S., Bluemke, D.A. and Lima, J.A. 2013. Prognostic value of myocardial circumferential strain for incident heart failure and cardiovascular events in asymptomatic individuals: the Multi-Ethnic Study of Atherosclerosis. *Eur Heart J.* **34**(30), pp.2354-2361.

Choudhury, L., Mahrholdt, H., Wagner, A., Choi, K.M., Elliott, M.D., Klocke, F.J., Bonow, R.O., Judd, R.M. and Kim, R.J. 2002. Myocardial scarring in asymptomatic or mildly symptomatic patients with hypertrophic cardiomyopathy. *J Am Coll Cardiol.* **40**(12), pp.2156-2164.

Chung, J., Abraszewski, P., Yu, X., Liu, W., Krainik, A.J., Ashford, M., Caruthers, S.D., McGill, J.B. and Wickline, S.A. 2006. Paradoxical increase in ventricular torsion and systolic torsion rate in type I diabetic patients under tight glycemic control. *J Am Coll Cardiol.* **47**(2), pp.384-390.

Cortigiani, L., Rigo, F., Gherardi, S., Sicari, R., Galderisi, M., Bovenzi, F. and Picano, E. 2007. Additional prognostic value of coronary flow reserve in diabetic and nondiabetic patients with negative dipyridamole stress echocardiography by wall motion criteria. *J Am Coll Cardiol.* **50**(14), pp.1354-1361.

Cubbon, R.M., Adams, B., Rajwani, A., Mercer, B.N., Patel, P.A., Gherardi, G., Gale, C.P., Batin, P.D., Ajjan, R., Kearney, L., Wheatcroft, S.B., Sapsford, R.J., Witte, K.K. and Kearney, M.T. 2013. Diabetes mellitus is associated with adverse prognosis in chronic heart failure of ischaemic and non-ischaemic aetiology. *Diab Vasc Dis Res.*

Cury, R.C., Shash, K., Nagurney, J.T., Rosito, G., Shapiro, M.D., Nomura, C.H., Abbara, S., Bamberg, F., Ferencik, M., Schmidt, E.J., Brown, D.F., Hoffmann, U. and Brady, T.J. 2008. Cardiac magnetic resonance with T2-weighted imaging improves detection of patients with acute coronary syndrome in the emergency department. *Circulation.* **118**(8), pp.837-844.

Dabir, D., Child, N., Kalra, A., Rogers, T., Gebker, R., Jabbour, A., Plein, S., Yu, C.Y., Otton, J., Kidambi, A., McDiarmid, A., Broadbent, D., Higgins, D.M., Schnackenburg, B., Foote, L., Cummins, C., Nagel, E. and Puntmann, V.O. 2014. Reference values for healthy human myocardium using a T1 mapping methodology: results from the International T1 Multicenter cardiovascular magnetic resonance study. *J Cardiovasc Magn Reson.* **16**, p69.

Dass, S., Suttie, J.J., Piechnik, S.K., Ferreira, V.M., Holloway, C.J., Banerjee, R., Mahmod, M., Cochlin, L., Karamitsos, T.D., Robson, M.D., Watkins, H. and Neubauer, S. 2012. Myocardial tissue characterization using magnetic resonance noncontrast t1 mapping in hypertrophic and dilated cardiomyopathy. *Circ Cardiovasc Imaging.* **5**(6), pp.726-733.

Davis, T.M., Coleman, R.L. and Holman, R.R. 2013. Prognostic significance of silent myocardial infarction in newly diagnosed type 2 diabetes mellitus: United Kingdom Prospective Diabetes Study (UKPDS) 79. *Circulation.* **127**(9), pp.980-987.

Davis, T.M., Fortun, P., Mulder, J., Davis, W.A. and Bruce, D.G. 2004. Silent myocardial infarction and its prognosis in a community-based cohort of Type 2 diabetic patients: the Fremantle Diabetes Study. *Diabetologia.* **47**(3), pp.395-399.

de Simone, G., Gottdiener, J.S., Chinali, M. and Maurer, M.S. 2008. Left ventricular mass predicts heart failure not related to previous myocardial infarction: the Cardiovascular Health Study. *Eur Heart J.* **29**(6), pp.741-747.

de Zeeuw, D., Remuzzi, G., Parving, H.H., Keane, W.F., Zhang, Z., Shahinfar, S., Snapinn, S., Cooper, M.E., Mitch, W.E. and Brenner, B.M. 2004. Albuminuria, a therapeutic target for cardiovascular protection in type 2 diabetic patients with nephropathy. *Circulation.* **110**(8), pp.921-927.

DeLong, E.R., DeLong, D.M. and Clarke-Pearson, D.L. 1988. Comparing the areas under two or more correlated receiver operating characteristic curves: a nonparametric approach. *Biometrics.* **44**(3), pp.837-845.

Devereux, R.B., Roman, M.J., Paranicas, M., O'Grady, M.J., Lee, E.T., Welty, T.K., Fabsitz, R.R., Robbins, D., Rhoades, E.R. and Howard, B.V. 2000. Impact of diabetes on cardiac structure and function: the strong heart study. *Circulation.* **101**(19), pp.2271-2276.

Dhillon, A., Sweet, W., Popovic, Z.B., Smedira, N.G., Thamilarasan, M., Lytle, B.W., Tan, C., Starling, R.C., Lever, H.M., Moravec, C.S. and Desai, M.Y. 2014. Association of noninvasively measured left ventricular mechanics with in vitro muscle contractile performance: a prospective study in hypertrophic cardiomyopathy patients. *J Am Heart Assoc.* **3**(6), pe001269.

Dormandy, J.A., Charbonnel, B., Eckland, D.J., Erdmann, E., Massi-Benedetti, M., Moules, I.K., Skene, A.M., Tan, M.H., Lefebvre, P.J., Murray, G.D., Standl, E., Wilcox, R.G., Wilhelmsen, L., Betteridge, J., Birkeland, K., Golay, A., Heine, R.J., Koranyi, L., Laakso, M., Mokan, M., Norkus, A., Pirags, V., Podar, T.,

Scheen, A., Scherbaum, W., Schernthaner, G., Schmitz, O., Skrha, J., Smith, U., Taton, J. and investigators, P.R. 2005. Secondary prevention of macrovascular events in patients with type 2 diabetes in the PROactive Study (PROspective pioglitAzone Clinical Trial In macroVascular Events): a randomised controlled trial. *Lancet.* **366**(9493), pp.1279-1289.

Dweck, M.R., Chow, M.W., Joshi, N.V., Williams, M.C., Jones, C., Fletcher, A.M., Richardson, H., White, A., McKillop, G., van Beek, E.J., Boon, N.A., Rudd, J.H. and Newby, D.E. 2012. Coronary arterial 18F-sodium fluoride uptake: a novel marker of plaque biology. *J Am Coll Cardiol.* **59**(17), pp.1539-1548.

Elliott, P.M., Anastasakis, A., Borger, M.A., Borggrefe, M., Cecchi, F., Charron, P., Hagege, A.A., Lafont, A., Limongelli, G., Mahrholdt, H., McKenna, W.J., Mogensen, J., Nihoyannopoulos, P., Nistri, S., Pieper, P.G., Pieske, B., Rapezzi, C., Rutten, F.H., Tillmanns, C. and Watkins, H. 2014. 2014 ESC Guidelines on diagnosis and management of hypertrophic cardiomyopathy: The Task Force for the Diagnosis and Management of Hypertrophic Cardiomyopathy of the European Society of Cardiology (ESC). *Eur Heart J.* **35**(39), pp.2733-2779.

Esch, B.T., Scott, J.M., Haykowsky, M.J., Paterson, I., Warburton, D.E., Cheng-Baron, J., Chow, K. and Thompson, R.B. 2010. Changes in ventricular twist and untwisting with orthostatic stress: endurance athletes versus normally active individuals. *J Appl Physiol (1985).* **108**(5), pp.1259-1266.

Fang, L., Beale, A., Ellims, A.H., Moore, X.L., Ling, L.H., Taylor, A.J., Chin-Dusting, J. and Dart, A.M. 2013. Associations between fibrocytes and postcontrast myocardial T1 times in hypertrophic cardiomyopathy. *J Am Heart Assoc.* **2**(5), pe000270.

Flett, A.S., Hayward, M.P., Ashworth, M.T., Hansen, M.S., Taylor, A.M., Elliott, P.M., McGregor, C. and Moon, J.C. 2010. Equilibrium contrast cardiovascular magnetic resonance for the measurement of diffuse myocardial fibrosis: preliminary validation in humans. *Circulation.* **122**(2), pp.138-144.

Fonseca, C.G., Dissanayake, A.M., Doughty, R.N., Whalley, G.A., Gamble, G.D., Cowan, B.R., Occleshaw, C.J. and Young, A.A. 2004. Three-dimensional assessment of left ventricular systolic strain in patients with type 2 diabetes mellitus, diastolic dysfunction, and normal ejection fraction. *Am J Cardiol.* **94**(11), pp.1391-1395.

From, A.M., Scott, C.G. and Chen, H.H. 2010. The development of heart failure in patients with diabetes mellitus and pre-clinical diastolic dysfunction a population-based study. *J Am Coll Cardiol.* **55**(4), pp.300-305.

Galderisi, M., Anderson, K.M., Wilson, P.W. and Levy, D. 1991. Echocardiographic evidence for the existence of a distinct diabetic cardiomyopathy (the Framingham Heart Study). *Am J Cardiol.* **68**(1), pp.85-89.

Garcia-Alvarez, A., Sitges, M., Delgado, V., Ortiz, J., Vidal, B., Poyatos, S., de Caralt, T.M., Heras, M., Bosch, X., Azqueta, M., Pare, C. and Brugada, J. 2009. Relation of plasma brain natriuretic peptide levels on admission for ST-elevation myocardial infarction to left ventricular end-diastolic volume six months later measured by both echocardiography and cardiac magnetic resonance. *Am J Cardiol.* **104**(7), pp.878-882.

Garg, R., Rao, A.D., Baimas-George, M., Hurwitz, S., Foster, C., Shah, R.V., Jerosch-Herold, M., Kwong, R.Y., Di Carli, M.F. and Adler, G.K. 2015. Mineralocorticoid receptor blockade improves coronary microvascular function in individuals with type 2 diabetes. *Diabetes.* **64**(1), pp.236-242.

Germans, T., Wilde, A.A., Dijkmans, P.A., Chai, W., Kamp, O., Pinto, Y.M. and van Rossum, A.C. 2006. Structural abnormalities of the inferoseptal left ventricular wall detected by cardiac magnetic resonance imaging in carriers of hypertrophic cardiomyopathy mutations. *J Am Coll Cardiol.* **48**(12), pp.2518-2523.

Gersh, B.J., Maron, B.J., Bonow, R.O., Dearani, J.A., Fifer, M.A., Link, M.S., Naidu, S.S., Nishimura, R.A., Ommen, S.R., Rakowski, H., Seidman, C.E., Towbin, J.A., Udelson, J.E. and Yancy, C.W. 2011. 2011 ACCF/AHA guideline for the diagnosis and treatment of hypertrophic cardiomyopathy: executive summary: a report of the American College of Cardiology Foundation/American Heart Association Task Force on Practice Guidelines. *Circulation.* **124**(24), pp.2761-2796.

Giannetta, E., Isidori, A.M., Galea, N., Carbone, I., Mandosi, E., Vizza, C.D., Naro, F., Morano, S., Fedele, F. and Lenzi, A. 2012. Chronic Inhibition of cGMP phosphodiesterase 5A improves diabetic cardiomyopathy: a randomized, controlled clinical trial using magnetic resonance imaging with myocardial tagging. *Circulation.* **125**(19), pp.2323-2333.

Gottdiener, J.S., Arnold, A.M., Aurigemma, G.P., Polak, J.F., Tracy, R.P., Kitzman, D.W., Gardin, J.M., Rutledge, J.E. and Boineau, R.C. 2000. Predictors of congestive heart failure in the elderly: the Cardiovascular Health Study. *J Am Coll Cardiol.* **35**(6), pp.1628-1637.

Gradman, A., Deedwania, P., Cody, R., Massie, B., Packer, M., Pitt, B. and Goldstein, S. 1989. Predictors of total mortality and sudden death in mild to moderate heart failure. Captopril-Digoxin Study Group. *J Am Coll Cardiol.* **14**(3), pp.564-570; discussion 571-562.

Green, J.J., Berger, J.S., Kramer, C.M. and Salerno, M. 2012. Prognostic value of late gadolinium enhancement in clinical outcomes for hypertrophic cardiomyopathy. *JACC Cardiovasc Imaging.* **5**(4), pp.370-377.

Gregg, E.W., Li, Y., Wang, J., Burrows, N.R., Ali, M.K., Rolka, D., Williams, D.E. and Geiss, L. 2014. Changes in diabetes-related complications in the United States, 1990-2010. *N Engl J Med.* **370**(16), pp.1514-1523.

Grothues, F., Smith, G.C., Moon, J.C., Bellenger, N.G., Collins, P., Klein, H.U. and Pennell, D.J. 2002. Comparison of interstudy reproducibility of cardiovascular magnetic resonance with two-dimensional echocardiography in normal subjects and in patients with heart failure or left ventricular hypertrophy. *Am J Cardiol.* **90**(1), pp.29-34.

Gulati, A., Ismail, T.F., Jabbour, A., Ismail, N.A., Morarji, K., Ali, A., Raza, S., Khwaja, J., Brown, T.D., Liodakis, E., Baksi, A.J., Shakur, R., Guha, K., Roughton, M., Wage, R., Cook, S.A., Alpendurada, F., Assomull, R.G., Mohiaddin, R.H., Cowie, M.R., Pennell, D.J. and Prasad, S.K. 2013. Clinical utility and prognostic value of left atrial volume assessment by cardiovascular magnetic resonance in non-ischaemic dilated cardiomyopathy. *Eur J Heart Fail.* **15**(6), pp.660-670.

Hafstad, A.D., Boardman, N.T., Lund, J., Hagve, M., Khalid, A.M., Wisloff, U., Larsen, T.S. and Aasum, E. 2011. High intensity interval training alters substrate utilization and reduces oxygen consumption in the heart. *J Appl Physiol (1985).* **111**(5), pp.1235-1241.

Han, Y., Osborn, E.A., Maron, M.S., Manning, W.J. and Yeon, S.B. 2009. Impact of papillary and trabecular muscles on quantitative analyses of cardiac function in hypertrophic cardiomyopathy. *J Magn Reson Imaging.* **30**(5), pp.1197-1202.

Heckbert, S.R., Post, W., Pearson, G.D., Arnett, D.K., Gomes, A.S., Jerosch-Herold, M., Hundley, W.G., Lima, J.A. and Bluemke, D.A. 2006. Traditional cardiovascular risk factors in relation to left ventricular mass, volume, and systolic function by cardiac magnetic resonance imaging: the Multiethnic Study of Atherosclerosis. *J Am Coll Cardiol.* **48**(11), pp.2285-2292.

Ho, C.Y., Abbasi, S.A., Neilan, T.G., Shah, R.V., Chen, Y., Heydari, B., Cirino, A.L., Lakdawala, N.K., Orav, E.J., Gonzalez, A., Lopez, B., Diez, J., Jerosch-Herold, M. and Kwong, R.Y. 2013. T1 measurements identify extracellular volume expansion in hypertrophic cardiomyopathy sarcomere mutation carriers with and without left ventricular hypertrophy. *Circ Cardiovasc Imaging.* **6**(3), pp.415-422.

Ho, C.Y., Lopez, B., Coelho-Filho, O.R., Lakdawala, N.K., Cirino, A.L., Jarolim, P., Kwong, R., Gonzalez, A., Colan, S.D., Seidman, J.G., Diez, J. and Seidman, C.E. 2010. Myocardial fibrosis as an early manifestation of hypertrophic cardiomyopathy. *N Engl J Med.* **363**(6), pp.552-563.

Holland, D.J., Marwick, T.H., Haluska, B.A., Leano, R., Hordern, M.D., Hare, J.L., Fang, Z.Y., Prins, J.B. and Stanton, T. 2015. Subclinical LV dysfunction and 10-year outcomes in type 2 diabetes mellitus. *Heart.* **101**(13), pp.1061-1066.

Holman, R.R., Paul, S.K., Bethel, M.A., Matthews, D.R. and Neil, H.A. 2008. 10-year follow-up of intensive glucose control in type 2 diabetes. *N Engl J Med.* **359**(15), pp.1577-1589.

Hoshi, T., Sato, A., Akiyama, D., Hiraya, D., Sakai, S., Shindo, M., Mori, K., Minami, M. and Aonuma, K. 2015. Coronary high-intensity plaque on T1-weighted magnetic resonance imaging and its association with myocardial injury after percutaneous coronary intervention. *Eur Heart J.* **36**(29), pp.1913-1922.

Huelsmann, M., Neuhold, S., Strunk, G., Moertl, D., Berger, R., Prager, R., Abrahamian, H., Riedl, M., Pacher, R., Luger, A. and Clodi, M. 2008. NT-proBNP has a high negative predictive value to rule-out short-term cardiovascular events in patients with diabetes mellitus. *Eur Heart J.* **29**(18), pp.2259-2264.

Hughes, S.E. 2004. The pathology of hypertrophic cardiomyopathy. *Histopathology.* **44**(5), pp.412-427.

Hulten, E., Pickett, C., Bittencourt, M.S., Villines, T.C., Petrillo, S., Di Carli, M.F. and Blankstein, R. 2013. Outcomes after coronary computed tomography angiography in the emergency department: a systematic review and meta-analysis of randomized, controlled trials. *J Am Coll Cardiol.* **61**(8), pp.880-892.

Ibrahim el, S.H. 2011. Myocardial tagging by cardiovascular magnetic resonance: evolution of techniques--pulse sequences, analysis algorithms, and applications. *J Cardiovasc Magn Reson.* **13**, p36.

Ibrahim, T., Bulow, H.P., Hackl, T., Hornke, M., Nekolla, S.G., Breuer, M., Schomig, A. and Schwaiger, M. 2007. Diagnostic value of contrast-enhanced magnetic resonance imaging and single-photon emission computed tomography for detection of myocardial necrosis early after acute myocardial infarction. *J Am Coll Cardiol.* **49**(2), pp.208-216.

Ibrahim, T., Nekolla, S.G., Schreiber, K., Odaka, K., Volz, S., Mehilli, J., Guthlin, M., Delius, W. and Schwaiger, M. 2002. Assessment of coronary flow reserve: comparison between contrast-enhanced magnetic resonance imaging and positron emission tomography. *J Am Coll Cardiol.* **39**(5), pp.864-870.

Iles, L., Pfluger, H., Phrommintikul, A., Cherayath, J., Aksit, P., Gupta, S.N., Kaye, D.M. and Taylor, A.J. 2008. Evaluation of diffuse myocardial fibrosis in heart failure with cardiac magnetic resonance contrast-enhanced T1 mapping. *J Am Coll Cardiol.* **52**(19), pp.1574-1580.

Iles, L.M., Ellims, A.H., Llewellyn, H., Hare, J.L., Kaye, D.M., McLean, C.A. and Taylor, A.J. 2015. Histological validation of cardiac magnetic resonance analysis of regional and diffuse interstitial myocardial fibrosis. *Eur Heart J Cardiovasc Imaging.* **16**(1), pp.14-22.

Ingkanisorn, W.P., Rhoads, K.L., Aletras, A.H., Kellman, P. and Arai, A.E. 2004. Gadolinium delayed enhancement cardiovascular magnetic resonance correlates with clinical measures of myocardial infarction. *J Am Coll Cardiol.* **43**(12), pp.2253-2259.

Iribarren, C., Karter, A.J., Go, A.S., Ferrara, A., Liu, J.Y., Sidney, S. and Selby, J.V. 2001. Glycemic control and heart failure among adult patients with diabetes. *Circulation.* **103**(22), pp.2668-2673.

Ismail, T.F., Prasad, S.K. and Pennell, D.J. 2012. Prognostic importance of late gadolinium enhancement cardiovascular magnetic resonance in cardiomyopathy. *Heart.* **98**(6), pp.438-442.

Jaarsma, C., Bekkers, S.C., Haidari, Z., Smulders, M.W., Nelemans, P.J., Gorgels, A.P., Crijns, H.J., Wildberger, J.E. and Schalla, S. 2013. Comparison of different electrocardiographic scoring systems for detection of any previous myocardial infarction as assessed with cardiovascular magnetic resonance imaging. *Am J Cardiol.* **112**(8), pp.1069-1074.

Jellis, C., Wright, J., Kennedy, D., Sacre, J., Jenkins, C., Haluska, B., Martin, J., Fenwick, J. and Marwick, T.H. 2011. Association of imaging markers of myocardial fibrosis with metabolic and functional disturbances in early diabetic cardiomyopathy. *Circ Cardiovasc Imaging.* **4**(6), pp.693-702.

Jerosch-Herold M, Wilke, N. and Stillman, A. 1998. Magnetic resonance quantification of the myocardial perfusion reserve with a Fermi function model for constrained deconvolution. *Med Phys.* **25**(1), pp.73-84.

Joshi, N.V., Vesey, A.T., Williams, M.C., Shah, A.S., Calvert, P.A., Craighead, F.H., Yeoh, S.E., Wallace, W., Salter, D., Fletcher, A.M., van Beek, E.J., Flapan, A.D., Uren, N.G., Behan, M.W., Cruden, N.L., Mills, N.L., Fox, K.A., Rudd, J.H., Dweck, M.R. and Newby, D.E. 2014. 18F-fluoride positron emission tomography for identification of ruptured and high-risk coronary

atherosclerotic plaques: a prospective clinical trial. *Lancet.* **383**(9918), pp.705-713.

Kang, X., Berman, D.S., Lewin, H.C., Cohen, I., Friedman, J.D., Germano, G., Hachamovitch, R. and Shaw, L.J. 1999. Incremental prognostic value of myocardial perfusion single photon emission computed tomography in patients with diabetes mellitus. *Am Heart J.* **138**(6 Pt 1), pp.1025-1032.

Kannel, W.B. and McGee, D.L. 1979. Diabetes and cardiovascular disease. The Framingham study. *JAMA.* **241**(19), pp.2035-2038.

Kawasaki, T., Sakai, C., Harimoto, K., Yamano, M., Miki, S. and Kamitani, T. 2013. Usefulness of high-sensitivity cardiac troponin T and brain natriuretic peptide as biomarkers of myocardial fibrosis in patients with hypertrophic cardiomyopathy. *Am J Cardiol.* **112**(6), pp.867-872.

Kellman, P., Arai, A.E. and Xue, H. 2013. T1 and extracellular volume mapping in the heart: estimation of error maps and the influence of noise on precision. *J Cardiovasc Magn Reson.* **15**, p56.

Kellman, P., Wilson, J.R., Xue, H., Bandettini, W.P., Shanbhag, S.M., Druey, K.M., Ugander, M. and Arai, A.E. 2012. Extracellular volume fraction mapping in the myocardium, part 2: initial clinical experience. *J Cardiovasc Magn Reson.* **14**, p64.

Ketchum, E.S. and Levy, W.C. 2011. Establishing prognosis in heart failure: a multimarker approach. *Prog Cardiovasc Dis.* **54**(2), pp.86-96.

Kim, S.A., Shim, C.Y., Kim, J.M., Lee, H.J., Choi, D.H., Choi, E.Y., Jang, Y., Chung, N. and Ha, J.W. 2011. Impact of left ventricular longitudinal diastolic functional reserve on clinical outcome in patients with type 2 diabetes mellitus. *Heart.* **97**(15), pp.1233-1238.

Kim, Y.J., Choi, B.W., Hur, J., Lee, H.J., Seo, J.S., Kim, T.H., Choe, K.O. and Ha, J.W. 2008. Delayed enhancement in hypertrophic cardiomyopathy: comparison with myocardial tagging MRI. *J Magn Reson Imaging.* **27**(5), pp.1054-1060.

Klues, H.G., Schiffers, A. and Maron, B.J. 1995. Phenotypic spectrum and patterns of left ventricular hypertrophy in hypertrophic cardiomyopathy: morphologic observations and significance as assessed by two-dimensional echocardiography in 600 patients. *J Am Coll Cardiol.* **26**(7), pp.1699-1708.

Kosmala, W., Kucharski, W., Przewlocka-Kosmala, M. and Mazurek, W. 2004. Comparison of left ventricular function by tissue Doppler imaging in patients with diabetes mellitus without systemic hypertension versus diabetes mellitus with systemic hypertension. *Am J Cardiol.* **94**(3), pp.395-399.

Kramer, C.M., Reichek, N., Ferrari, V.A., Theobald, T., Dawson, J. and Axel, L. 1994. Regional heterogeneity of function in hypertrophic cardiomyopathy. *Circulation.* **90**(1), pp.186-194.

Kwon, D.H., Smedira, N.G., Rodriguez, E.R., Tan, C., Setser, R., Thamilarasan, M., Lytle, B.W., Lever, H.M. and Desai, M.Y. 2009. Cardiac magnetic resonance detection of myocardial scarring in hypertrophic cardiomyopathy: correlation with histopathology and prevalence of ventricular tachycardia. *J Am Coll Cardiol.* **54**(3), pp.242-249.

Kwong, R.Y., Chan, A.K., Brown, K.A., Chan, C.W., Reynolds, H.G., Tsang, S. and Davis, R.B. 2006. Impact of unrecognized myocardial scar detected by

cardiac magnetic resonance imaging on event-free survival in patients presenting with signs or symptoms of coronary artery disease. *Circulation.* **113**(23), pp.2733-2743.

La Gerche, A., Claessen, G., Dymarkowski, S., Voigt, J.U., De Buck, F., Vanhees, L., Droogne, W., Van Cleemput, J., Claus, P. and Heidbuchel, H. 2015. Exercise-induced right ventricular dysfunction is associated with ventricular arrhythmias in endurance athletes. *Eur Heart J.* **36**(30), pp.1998-2010.

Lamarra, N., Whipp, B.J., Ward, S.A. and Wasserman, K. 1987. Effect of interbreath fluctuations on characterizing exercise gas exchange kinetics. *J Appl Physiol (1985).* **62**(5), pp.2003-2012.

Langer, H.F., Haubner, R., Pichler, B.J. and Gawaz, M. 2008. Radionuclide imaging: a molecular key to the atherosclerotic plaque. *J Am Coll Cardiol.* **52**(1), pp.1-12.

Larghat, A.M., Swoboda, P.P., Biglands, J.D., Kearney, M.T., Greenwood, J.P. and Plein, S. 2014. The microvascular effects of insulin resistance and diabetes on cardiac structure, function, and perfusion: a cardiovascular magnetic resonance study. *Eur Heart J Cardiovasc Imaging.* **15**(12), pp.1368-1376.

Larkman, D.J. and Nunes, R.G. 2007. Parallel magnetic resonance imaging. *Phys Med Biol.* **52**(7), pp.R15-55.

Larose, E., Ganz, P., Reynolds, H.G., Dorbala, S., Di Carli, M.F., Brown, K.A. and Kwong, R.Y. 2007. Right ventricular dysfunction assessed by cardiovascular magnetic resonance imaging predicts poor prognosis late after myocardial infarction. *J Am Coll Cardiol.* **49**(8), pp.855-862.

Luijkx, T., Cramer, M.J., Buckens, C.F., Zaidi, A., Rienks, R., Mosterd, A., Prakken, N.H., Dijkman, B., Mali, W.P. and Velthuis, B.K. 2013. Unravelling the grey zone: cardiac MRI volume to wall mass ratio to differentiate hypertrophic cardiomyopathy and the athlete's heart. *Br J Sports Med.* **0**, pp.1-7.

MacDonald, M.R., Petrie, M.C., Varyani, F., Ostergren, J., Michelson, E.L., Young, J.B., Solomon, S.D., Granger, C.B., Swedberg, K., Yusuf, S., Pfeffer, M.A. and McMurray, J.J. 2008. Impact of diabetes on outcomes in patients with low and preserved ejection fraction heart failure: an analysis of the Candesartan in Heart failure: Assessment of Reduction in Mortality and morbidity (CHARM) programme. *Eur Heart J.* **29**(11), pp.1377-1385.

Maceira, A.M., Cosin-Sales, J., Roughton, M., Prasad, S.K. and Pennell, D.J. 2010. Reference left atrial dimensions and volumes by steady state free precession cardiovascular magnetic resonance. *J Cardiovasc Magn Reson.* **12**, p65.

Mahrholdt, H., Wagner, A., Judd, R.M., Sechtem, U. and Kim, R.J. 2005. Delayed enhancement cardiovascular magnetic resonance assessment of non-ischaemic cardiomyopathies. *Eur Heart J.* **26**(15), pp.1461-1474.

Mangold, S., Kramer, U., Franzen, E., Erz, G., Bretschneider, C., Seeger, A., Claussen, C.D., Niess, A.M. and Burgstahler, C. 2013. Detection of cardiovascular disease in elite athletes using cardiac magnetic resonance imaging. *Rofo.* **185**(12), pp.1167-1174.

Maron, B.J. 2003. Sudden death in young athletes. *N Engl J Med.* **349**(11), pp.1064-1075.

Maron, B.J., Doerer, J.J., Haas, T.S., Tierney, D.M. and Mueller, F.O. 2009a. Sudden deaths in young competitive athletes: analysis of 1866 deaths in the United States, 1980-2006. *Circulation.* **119**(8), pp.1085-1092.

Maron, B.J. and Pelliccia, A. 2006. The heart of trained athletes: cardiac remodeling and the risks of sports, including sudden death. *Circulation.* **114**(15), pp.1633-1644.

Maron, B.J., Wolfson, J.K., Epstein, S.E. and Roberts, W.C. 1986. Intramural ("small vessel") coronary artery disease in hypertrophic cardiomyopathy. *J Am Coll Cardiol.* **8**(3), pp.545-557.

Maron, B.J., Wolfson, J.K. and Roberts, W.C. 1992. Relation between extent of cardiac muscle cell disorganization and left ventricular wall thickness in hypertrophic cardiomyopathy. *Am J Cardiol.* **70**(7), pp.785-790.

Maron, M.S., Finley, J.J., Bos, J.M., Hauser, T.H., Manning, W.J., Haas, T.S., Lesser, J.R., Udelson, J.E., Ackerman, M.J. and Maron, B.J. 2008. Prevalence, clinical significance, and natural history of left ventricular apical aneurysms in hypertrophic cardiomyopathy. *Circulation.* **118**(15), pp.1541-1549.

Maron, M.S., Maron, B.J., Harrigan, C., Buros, J., Gibson, C.M., Olivotto, I., Biller, L., Lesser, J.R., Udelson, J.E., Manning, W.J. and Appelbaum, E. 2009b. Hypertrophic cardiomyopathy phenotype revisited after 50 years with cardiovascular magnetic resonance. *J Am Coll Cardiol.* **54**(3), pp.220-228.

McGavock, J.M., Lingvay, I., Zib, I., Tillery, T., Salas, N., Unger, R., Levine, B.D., Raskin, P., Victor, R.G. and Szczepaniak, L.S. 2007. Cardiac steatosis in diabetes mellitus: a 1H-magnetic resonance spectroscopy study. *Circulation.* **116**(10), pp.1170-1175.

McMurray, J.J., Adamopoulos, S., Anker, S.D., Auricchio, A., Bohm, M., Dickstein, K., Falk, V., Filippatos, G., Fonseca, C., Gomez-Sanchez, M.A., Jaarsma, T., Kober, L., Lip, G.Y., Maggioni, A.P., Parkhomenko, A., Pieske, B.M., Popescu, B.A., Ronnevik, P.K., Rutten, F.H., Schwitter, J., Seferovic, P., Stepinska, J., Trindade, P.T., Voors, A.A., Zannad, F., Zeiher, A., Bax, J.J., Baumgartner, H., Ceconi, C., Dean, V., Deaton, C., Fagard, R., Funck-Brentano, C., Hasdai, D., Hoes, A., Kirchhof, P., Knuuti, J., Kolh, P., McDonagh, T., Moulin, C., Reiner, Z., Sechtem, U., Sirnes, P.A., Tendera, M., Torbicki, A., Vahanian, A., Windecker, S., Bonet, L.A., Avraamides, P., Ben Lamin, H.A., Brignole, M., Coca, A., Cowburn, P., Dargie, H., Elliott, P., Flachskampf, F.A., Guida, G.F., Hardman, S., Iung, B., Merkely, B., Mueller, C., Nanas, J.N., Nielsen, O.W., Orn, S., Parissis, J.T. and Ponikowski, P. 2012. ESC guidelines for the diagnosis and treatment of acute and chronic heart failure 2012: The Task Force for the Diagnosis and Treatment of Acute and Chronic Heart Failure 2012 of the European Society of Cardiology. Developed in collaboration with the Heart Failure Association (HFA) of the ESC. *Eur J Heart Fail.* **14**(8), pp.803-869.

Messroghli, D.R., Bainbridge, G.J., Alfakih, K., Jones, T.R., Plein, S., Ridgway, J.P. and Sivananthan, M.U. 2005. Assessment of regional left ventricular function: accuracy and reproducibility of positioning standard short-axis sections in cardiac MR imaging. *Radiology.* **235**(1), pp.229-236.

Messroghli, D.R., Radjenovic, A., Kozerke, S., Higgins, D.M., Sivananthan, M.U. and Ridgway, J.P. 2004. Modified Look-Locker inversion recovery (MOLLI) for

high-resolution T1 mapping of the heart. *Magn Reson Med.* **52**(1), pp.141-146.

Milliken, M.C., Stray-Gundersen, J., Peshock, R.M., Katz, J. and Mitchell, J.H. 1988. Left ventricular mass as determined by magnetic resonance imaging in male endurance athletes. *Am J Cardiol.* **62**(4), pp.301-305.

Moody, W.E., Taylor, R.J., Edwards, N.C., Chue, C.D., Umar, F., Taylor, T.J., Ferro, C.J., Young, A.A., Townend, J.N., Leyva, F. and Steeds, R.P. 2015. Comparison of magnetic resonance feature tracking for systolic and diastolic strain and strain rate calculation with spatial modulation of magnetization imaging analysis. *J Magn Reson Imaging.* **41**(4), pp.1000-1012.

Moon, J.C., De Arenaza, D.P., Elkington, A.G., Taneja, A.K., John, A.S., Wang, D., Janardhanan, R., Senior, R., Lahiri, A., Poole-Wilson, P.A. and Pennell, D.J. 2004a. The pathologic basis of Q-wave and non-Q-wave myocardial infarction: a cardiovascular magnetic resonance study. *J Am Coll Cardiol.* **44**(3), pp.554-560.

Moon, J.C., Fisher, N.G., McKenna, W.J. and Pennell, D.J. 2004b. Detection of apical hypertrophic cardiomyopathy by cardiovascular magnetic resonance in patients with non-diagnostic echocardiography. *Heart.* **90**(6), pp.645-649.

Moon, J.C., McKenna, W.J., McCrohon, J.A., Elliott, P.M., Smith, G.C. and Pennell, D.J. 2003. Toward clinical risk assessment in hypertrophic cardiomyopathy with gadolinium cardiovascular magnetic resonance. *J Am Coll Cardiol.* **41**(9), pp.1561-1567.

Moon, J.C., Messroghli, D.R., Kellman, P., Piechnik, S.K., Robson, M.D., Ugander, M., Gatehouse, P.D., Arai, A.E., Friedrich, M.G., Neubauer, S., Schulz-Menger, J., Schelbert, E.B., Society for Cardiovascular Magnetic Resonance, I. and Cardiovascular Magnetic Resonance Working Group of the European Society of, C. 2013. Myocardial T1 mapping and extracellular volume quantification: a Society for Cardiovascular Magnetic Resonance (SCMR) and CMR Working Group of the European Society of Cardiology consensus statement. *J Cardiovasc Magn Reson.* **15**, p92.

Moon, J.C., Mogensen, J., Elliott, P.M., Smith, G.C., Elkington, A.G., Prasad, S.K., Pennell, D.J. and McKenna, W.J. 2005. Myocardial late gadolinium enhancement cardiovascular magnetic resonance in hypertrophic cardiomyopathy caused by mutations in troponin I. *Heart.* **91**(8), pp.1036-1040.

Moon, J.C., Reed, E., Sheppard, M.N., Elkington, A.G., Ho, S.Y., Burke, M., Petrou, M. and Pennell, D.J. 2004c. The histologic basis of late gadolinium enhancement cardiovascular magnetic resonance in hypertrophic cardiomyopathy. *J Am Coll Cardiol.* **43**(12), pp.2260-2264.

Morrish, N.J., Wang, S.L., Stevens, L.K., Fuller, J.H. and Keen, H. 2001. Mortality and causes of death in the WHO Multinational Study of Vascular Disease in Diabetes. *Diabetologia.* **44 Suppl 2**, pp.S14-21.

Mortality, G.B.D. and Causes of Death, C. 2015. Global, regional, and national age-sex specific all-cause and cause-specific mortality for 240 causes of death, 1990-2013: a systematic analysis for the Global Burden of Disease Study 2013. *Lancet.* **385**(9963), pp.117-171.

Motoyama, S., Ito, H., Sarai, M., Kondo, T., Kawai, H., Nagahara, Y., Harigaya, H., Kan, S., Anno, H., Takahashi, H., Naruse, H., Ishii, J., Hecht, H., Shaw, L.J., Ozaki, Y. and Narula, J. 2015. Plaque Characterization by Coronary Computed Tomography Angiography and the Likelihood of Acute Coronary Events in Mid-Term Follow-Up. *J Am Coll Cardiol.* **66**(4), pp.337-346.

Muhlestein, J.B., Lappe, D.L., Lima, J.A., Rosen, B.D., May, H.T., Knight, S., Bluemke, D.A., Towner, S.R., Le, V., Bair, T.L., Vavere, A.L. and Anderson, J.L. 2014. Effect of screening for coronary artery disease using CT angiography on mortality and cardiac events in high-risk patients with diabetes: the FACTOR-64 randomized clinical trial. *JAMA.* **312**(21), pp.2234-2243.

Murthy, V.L., Naya, M., Foster, C.R., Gaber, M., Hainer, J., Klein, J., Dorbala, S., Blankstein, R. and Di Carli, M.F. 2012. Association between coronary vascular dysfunction and cardiac mortality in patients with and without diabetes mellitus. *Circulation.* **126**(15), pp.1858-1868.

Nagueh, S.F., Appleton, C.P., Gillebert, T.C., Marino, P.N., Oh, J.K., Smiseth, O.A., Waggoner, A.D., Flachskampf, F.A., Pellikka, P.A. and Evangelisa, A. 2009. Recommendations for the evaluation of left ventricular diastolic function by echocardiography. *Eur J Echocardiogr.* **10**(2), pp.165-193.

Nahser, P.J., Jr., Brown, R.E., Oskarsson, H., Winniford, M.D. and Rossen, J.D. 1995. Maximal coronary flow reserve and metabolic coronary vasodilation in patients with diabetes mellitus. *Circulation.* **91**(3), pp.635-640.

Naoumova, R.P., Kindler, H., Leccisotti, L., Mongillo, M., Khan, M.T., Neuwirth, C., Seed, M., Holvoet, P., Betteridge, J. and Camici, P.G. 2007. Pioglitazone improves myocardial blood flow and glucose utilization in nondiabetic patients with combined hyperlipidemia: a randomized, double-blind, placebo-controlled study. *J Am Coll Cardiol.* **50**(21), pp.2051-2058.

Naqvi, T.Z., Padmanabhan, S., Rafii, F., Hyuhn, H.K. and Mirocha, J. 2006. Comparison of usefulness of left ventricular diastolic versus systolic function as a predictor of outcome following primary percutaneous coronary angioplasty for acute myocardial infarction. *Am J Cardiol.* **97**(2), pp.160-166.

Ng, A.C., Auger, D., Delgado, V., van Elderen, S.G., Bertini, M., Siebelink, H.M., van der Geest, R.J., Bonetti, C., van der Velde, E.T., de Roos, A., Smit, J.W., Leung, D.Y., Bax, J.J. and Lamb, H.J. 2012. Association between diffuse myocardial fibrosis by cardiac magnetic resonance contrast-enhanced T(1) mapping and subclinical myocardial dysfunction in diabetic patients: a pilot study. *Circ Cardiovasc Imaging.* **5**(1), pp.51-59.

Ng, A.C., Delgado, V., Bertini, M., van der Meer, R.W., Rijzewijk, L.J., Hooi Ewe, S., Siebelink, H.M., Smit, J.W., Diamant, M., Romijn, J.A., de Roos, A., Leung, D.Y., Lamb, H.J. and Bax, J.J. 2010. Myocardial steatosis and biventricular strain and strain rate imaging in patients with type 2 diabetes mellitus. *Circulation.* **122**(24), pp.2538-2544.

Ng, A.C., Delgado, V., Bertini, M., van der Meer, R.W., Rijzewijk, L.J., Shanks, M., Nucifora, G., Smit, J.W., Diamant, M., Romijn, J.A., de Roos, A., Leung, D.Y., Lamb, H.J. and Bax, J.J. 2009. Findings from left ventricular strain and strain rate imaging in asymptomatic patients with type 2 diabetes mellitus. *Am J Cardiol.* **104**(10), pp.1398-1401.

Nguyen, T.L., Phan, J.A., Hee, L., Moses, D.A., Otton, J., Terreblanche, O.D., Xiong, J., Premawardhana, U., Rajaratnam, R., Juergens, C.P., Dimitri, H.R., French, J.K., Richards, D.A. and Thomas, L. 2015. High-sensitivity troponin T predicts infarct scar characteristics and adverse left ventricular function by cardiac magnetic resonance imaging early after reperfused acute myocardial infarction. *Am Heart J.* **170**(4), pp.715-725 e712.

Nijland, F., Kamp, O., Karreman, A.J., van Eenige, M.J. and Visser, C.A. 1997. Prognostic implications of restrictive left ventricular filling in acute myocardial infarction: a serial Doppler echocardiographic study. *J Am Coll Cardiol.* **30**(7), pp.1618-1624.

Nistri, S., Olivotto, I., Betocchi, S., Losi, M.A., Valsecchi, G., Pinamonti, B., Conte, M.R., Casazza, F., Galderisi, M., Maron, B.J. and Cecchi, F. 2006. Prognostic significance of left atrial size in patients with hypertrophic cardiomyopathy (from the Italian Registry for Hypertrophic Cardiomyopathy). *Am J Cardiol.* **98**(7), pp.960-965.

Noguchi, T., Tanaka, A., Kawasaki, T., Goto, Y., Morita, Y., Asaumi, Y., Nakao, K., Fujiwara, R., Nishimura, K., Miyamoto, Y., Ishihara, M., Ogawa, H., Koga, N., Narula, J. and Yasuda, S. 2015. Effect of Intensive Statin Therapy on Coronary High-Intensity Plaques Detected by Noncontrast T1-Weighted Imaging: The AQUAMARINE Pilot Study. *J Am Coll Cardiol.* **66**(3), pp.245-256.

Nottin, S., Doucende, G., Schuster-Beck, I., Dauzat, M. and Obert, P. 2008. Alteration in left ventricular normal and shear strains evaluated by 2D-strain echocardiography in the athlete's heart. *J Physiol.* **586**(Pt 19), pp.4721-4733.

Obokata, M., Nagata, Y., Wu, V.C., Kado, Y., Kurabayashi, M., Otsuji, Y. and Takeuchi, M. 2015. Direct comparison of cardiac magnetic resonance feature tracking and 2D/3D echocardiography speckle tracking for evaluation of global left ventricular strain. *Eur Heart J Cardiovasc Imaging.*

Ofstad, A.P., Johansen, O.E., Gullestad, L., Birkeland, K.I., Orvik, E., Fagerland, M.W., Urheim, S. and Aakhus, S. 2014. Neutral impact on systolic and diastolic cardiac function of 2 years of intensified multi-intervention in type 2 diabetes: the randomized controlled Asker and Baerum Cardiovascular Diabetes (ABCD) study. *Am Heart J.* **168**(3), pp.280-288 e282.

Olivotto, I., Maron, M.S., Autore, C., Lesser, J.R., Rega, L., Casolo, G., De Santis, M., Quarta, G., Nistri, S., Cecchi, F., Salton, C.J., Udelson, J.E., Manning, W.J. and Maron, B.J. 2008. Assessment and significance of left ventricular mass by cardiovascular magnetic resonance in hypertrophic cardiomyopathy. *J Am Coll Cardiol.* **52**(7), pp.559-566.

Ommen, S.R., Nishimura, R.A., Appleton, C.P., Miller, F.A., Oh, J.K., Redfield, M.M. and Tajik, A.J. 2000. Clinical utility of Doppler echocardiography and tissue Doppler imaging in the estimation of left ventricular filling pressures: A comparative simultaneous Doppler-catheterization study. *Circulation.* **102**(15), pp.1788-1794.

Onishi, T., Saha, S.K., Delgado-Montero, A., Ludwig, D.R., Onishi, T., Schelbert, E.B., Schwartzman, D. and Gorcsan, J., 3rd. 2015. Global longitudinal strain and global circumferential strain by speckle-tracking echocardiography and

feature-tracking cardiac magnetic resonance imaging: comparison with left ventricular ejection fraction. *J Am Soc Echocardiogr.* **28**(5), pp.587-596.

Osborne, G., Wolfe, L.A., Burggraf, G.W. and Norman, R. 1992. Relationships between cardiac dimensions, anthropometric characteristics and maximal aerobic power (VO2max) in young men. *Int J Sports Med.* **13**(3), pp.219-224.

Pelliccia, A., Maron, B.J., De Luca, R., Di Paolo, F.M., Spataro, A. and Culasso, F. 2002. Remodeling of left ventricular hypertrophy in elite athletes after long-term deconditioning. *Circulation.* **105**(8), pp.944-949.

Pelliccia, A., Maron, B.J., Di Paolo, F.M., Biffi, A., Quattrini, F.M., Pisicchio, C., Roselli, A., Caselli, S. and Culasso, F. 2005. Prevalence and clinical significance of left atrial remodeling in competitive athletes. *J Am Coll Cardiol.* **46**(4), pp.690-696.

Pelliccia, A., Maron, B.J., Spataro, A., Proschan, M.A. and Spirito, P. 1991. The upper limit of physiologic cardiac hypertrophy in highly trained elite athletes. *N Engl J Med.* **324**(5), pp.295-301.

Pelliccia, A., Maron, M.S. and Maron, B.J. 2012. Assessment of left ventricular hypertrophy in a trained athlete: differential diagnosis of physiologic athlete's heart from pathologic hypertrophy. *Prog Cardiovasc Dis.* **54**(5), pp.387-396.

Pencina, M.J., D'Agostino, R.B., Sr., D'Agostino, R.B., Jr. and Vasan, R.S. 2008. Evaluating the added predictive ability of a new marker: from area under the ROC curve to reclassification and beyond. *Stat Med.* **27**(2), pp.157-172; discussion 207-112.

Pereira, F., de Moraes, R., Tibirica, E. and Nobrega, A.C. 2013. Interval and continuous exercise training produce similar increases in skeletal muscle and left ventricle microvascular density in rats. *Biomed Res Int.* **2013**, p752817.

Perrone-Filardi, P., Achenbach, S., Mohlenkamp, S., Reiner, Z., Sambuceti, G., Schuijf, J.D., Van der Wall, E., Kaufmann, P.A., Knuuti, J., Schroeder, S. and Zellweger, M.J. 2011. Cardiac computed tomography and myocardial perfusion scintigraphy for risk stratification in asymptomatic individuals without known cardiovascular disease: a position statement of the Working Group on Nuclear Cardiology and Cardiac CT of the European Society of Cardiology. *Eur Heart J.* **32**(16), pp.1986-1993, 1993a, 1993b.

Pluim, B.M., Zwinderman, A.H., van der Laarse, A. and van der Wall, E.E. 2000. The athlete's heart. A meta-analysis of cardiac structure and function. *Circulation.* **101**(3), pp.336-344.

Poirier, P., Bogaty, P., Garneau, C., Marois, L. and Dumesnil, J.G. 2001. Diastolic dysfunction in normotensive men with well-controlled type 2 diabetes: importance of maneuvers in echocardiographic screening for preclinical diabetic cardiomyopathy. *Diabetes Care.* **24**(1), pp.5-10.

Popovic, Z.B., Kwon, D.H., Mishra, M., Buakhamsri, A., Greenberg, N.L., Thamilarasan, M., Flamm, S.D., Thomas, J.D., Lever, H.M. and Desai, M.Y. 2008. Association between regional ventricular function and myocardial fibrosis in hypertrophic cardiomyopathy assessed by speckle tracking echocardiography and delayed hyperenhancement magnetic resonance imaging. *J Am Soc Echocardiogr.* **21**(12), pp.1299-1305.

Poulsen, M.K., Dahl, J.S., Henriksen, J.E., Hey, T.M., Hoilund-Carlsen, P.F., Beck-Nielsen, H. and Moller, J.E. 2013. Left atrial volume index: relation to long-term clinical outcome in type 2 diabetes. *J Am Coll Cardiol.* **62**(25), pp.2416-2421.

Price, D.A., Porter, L.E., Gordon, M., Fisher, N.D., De'Oliveira, J.M., Laffel, L.M., Passan, D.R., Williams, G.H. and Hollenberg, N.K. 1999. The paradox of the low-renin state in diabetic nephropathy. *J Am Soc Nephrol.* **10**(11), pp.2382-2391.

Puntmann, V.O., Voigt, T., Chen, Z., Mayr, M., Karim, R., Rhode, K., Pastor, A., Carr-White, G., Razavi, R., Schaeffter, T. and Nagel, E. 2013. Native T1 mapping in differentiation of normal myocardium from diffuse disease in hypertrophic and dilated cardiomyopathy. *JACC Cardiovasc Imaging.* **6**(4), pp.475-484.

Raman, F.S., Kawel-Boehm, N., Gai, N., Freed, M., Han, J., Liu, C.Y., Lima, J.A., Bluemke, D.A. and Liu, S. 2013. Modified look-locker inversion recovery T1 mapping indices: assessment of accuracy and reproducibility between magnetic resonance scanners. *J Cardiovasc Magn Reson.* **15**, p64.

Rana, B.S., Davies, J.I., Band, M.M., Pringle, S.D., Morris, A. and Struthers, A.D. 2006. B-type natriuretic peptide can detect silent myocardial ischaemia in asymptomatic type 2 diabetes. *Heart.* **92**(7), pp.916-920.

Rao, A.D., Shah, R.V., Garg, R., Abbasi, S.A., Neilan, T.G., Perlstein, T.S., Di Carli, M.F., Jerosch-Herold, M., Kwong, R.Y. and Adler, G.K. 2013. Aldosterone and myocardial extracellular matrix expansion in type 2 diabetes mellitus. *Am J Cardiol.* **112**(1), pp.73-78.

Rawlins, J., Carre, F., Kervio, G., Papadakis, M., Chandra, N., Edwards, C., Whyte, G.P. and Sharma, S. 2010. Ethnic differences in physiological cardiac adaptation to intense physical exercise in highly trained female athletes. *Circulation.* **121**(9), pp.1078-1085.

Rijzewijk, L.J., van der Meer, R.W., Smit, J.W., Diamant, M., Bax, J.J., Hammer, S., Romijn, J.A., de Roos, A. and Lamb, H.J. 2008. Myocardial steatosis is an independent predictor of diastolic dysfunction in type 2 diabetes mellitus. *J Am Coll Cardiol.* **52**(22), pp.1793-1799.

Rossiter, H.B., Kowalchuk, J.M. and Whipp, B.J. 2006. A test to establish maximum O2 uptake despite no plateau in the O2 uptake response to ramp incremental exercise. *J Appl Physiol (1985).* **100**(3), pp.764-770.

Roth, G.A., Nguyen, G., Forouzanfar, M.H., Mokdad, A.H., Naghavi, M. and Murray, C.J. 2015. Estimates of Global and Regional Premature Cardiovascular Mortality in 2025. *Circulation.* **132**(13), pp.1270-1282.

Rudolph, A., Abdel-Aty, H., Bohl, S., Boye, P., Zagrosek, A., Dietz, R. and Schulz-Menger, J. 2009. Noninvasive detection of fibrosis applying contrast-enhanced cardiac magnetic resonance in different forms of left ventricular hypertrophy relation to remodeling. *J Am Coll Cardiol.* **53**(3), pp.284-291.

Sado, D.M., Flett, A.S., Banypersad, S.M., White, S.K., Maestrini, V., Quarta, G., Lachmann, R.H., Murphy, E., Mehta, A., Hughes, D.A., McKenna, W.J., Taylor, A.M., Hausenloy, D.J., Hawkins, P.N., Elliott, P.M. and Moon, J.C. 2012. Cardiovascular magnetic resonance measurement of myocardial extracellular volume in health and disease. *Heart.* **98**(19), pp.1436-1441.

Scharhag, J., Schneider, G., Urhausen, A., Rochette, V., Kramann, B. and Kindermann, W. 2002. Athlete's heart: right and left ventricular mass and function in male endurance athletes and untrained individuals determined by magnetic resonance imaging. *J Am Coll Cardiol.* **40**(10), pp.1856-1863.

Schelbert, E.B., Cao, J.J., Sigurdsson, S., Aspelund, T., Kellman, P., Aletras, A.H., Dyke, C.K., Thorgeirsson, G., Eiriksdottir, G., Launer, L.J., Gudnason, V., Harris, T.B. and Arai, A.E. 2012. Prevalence and prognosis of unrecognized myocardial infarction determined by cardiac magnetic resonance in older adults. *JAMA.* **308**(9), pp.890-896.

Schnell, F., Claessen, G., La Gerche, A., Bogaert, J., Lentz, P.A., Claus, P., Mabo, P., Carre, F. and Heidbuchel, H. 2015. Subepicardial delayed gadolinium enhancement in asymptomatic athletes: let sleeping dogs lie? *Br J Sports Med.*

Scott, J.M., Esch, B.T., Haykowsky, M.J., Paterson, I., Warburton, D.E., Chow, K., Cheng Baron, J., Lopaschuk, G.D. and Thompson, R.B. 2010. Effects of high intensity exercise on biventricular function assessed by cardiac magnetic resonance imaging in endurance trained and normally active individuals. *Am J Cardiol.* **106**(2), pp.278-283.

Seferovic, P.M. and Paulus, W.J. 2015. Clinical diabetic cardiomyopathy: a two-faced disease with restrictive and dilated phenotypes. *Eur Heart J.* **36**(27), pp.1718-1727.

Selvin, E., Lazo, M., Chen, Y., Shen, L., Rubin, J., McEvoy, J.W., Hoogeveen, R.C., Sharrett, A.R., Ballantyne, C.M. and Coresh, J. 2014. Diabetes mellitus, prediabetes, and incidence of subclinical myocardial damage. *Circulation.* **130**(16), pp.1374-1382.

Shah, B.N., Balaji, G., Alhajiri, A., Ramzy, I.S., Ahmadvazir, S. and Senior, R. 2013. Incremental diagnostic and prognostic value of contemporary stress echocardiography in a chest pain unit: mortality and morbidity outcomes from a real-world setting. *Circ Cardiovasc Imaging.* **6**(2), pp.202-209.

Sharma, S., Elliott, P.M., Whyte, G., Mahon, N., Virdee, M.S., Mist, B. and McKenna, W.J. 2000. Utility of metabolic exercise testing in distinguishing hypertrophic cardiomyopathy from physiologic left ventricular hypertrophy in athletes. *J Am Coll Cardiol.* **36**(3), pp.864-870.

Shehata, M.L., Cheng, S., Osman, N.F., Bluemke, D.A. and Lima, J.A. 2009. Myocardial tissue tagging with cardiovascular magnetic resonance. *J Cardiovasc Magn Reson.* **11**, p55.

Sheppard, M.N. 2012. Aetiology of sudden cardiac death in sport: a histopathologist's perspective. *Br J Sports Med.* **46 Suppl 1**, pp.i15-21.

Sibal, L. and Home, P.D. 2009. Management of type 2 diabetes: NICE guidelines. *Clin Med.* **9**(4), pp.353-357.

Smith, B.M., Dorfman, A.L., Yu, S., Russell, M.W., Agarwal, P.P., Mahani, M.G. and Lu, J.C. 2014. Clinical significance of late gadolinium enhancement in patients<20 years of age with hypertrophic cardiomyopathy. *Am J Cardiol.* **113**(7), pp.1234-1239.

Solomon, S.D., Anavekar, N., Skali, H., McMurray, J.J., Swedberg, K., Yusuf, S., Granger, C.B., Michelson, E.L., Wang, D., Pocock, S. and Pfeffer, M.A. 2005.

Influence of ejection fraction on cardiovascular outcomes in a broad spectrum of heart failure patients. *Circulation.* **112**(24), pp.3738-3744.

Stewart, G.M., Yamada, A., Haseler, L.J., Kavanagh, J.J., Koerbin, G., Chan, J. and Sabapathy, S. 2015. Altered ventricular mechanics after 60 min of high-intensity endurance exercise: insights from exercise speckle-tracking echocardiography. *Am J Physiol Heart Circ Physiol.* **308**(8), pp.H875-883.

Stohr, E.J., McDonnell, B., Thompson, J., Stone, K., Bull, T., Houston, R., Cockcroft, J. and Shave, R. 2012. Left ventricular mechanics in humans with high aerobic fitness: adaptation independent of structural remodelling, arterial haemodynamics and heart rate. *J Physiol.* **590**(Pt 9), pp.2107-2119.

Stratton, I.M., Adler, A.I., Neil, H.A., Matthews, D.R., Manley, S.E., Cull, C.A., Hadden, D., Turner, R.C. and Holman, R.R. 2000. Association of glycaemia with macrovascular and microvascular complications of type 2 diabetes (UKPDS 35): prospective observational study. *BMJ.* **321**(7258), pp.405-412.

Stuber, M., Scheidegger, M.B., Fischer, S.E., Nagel, E., Steinemann, F., Hess, O.M. and Boesiger, P. 1999. Alterations in the local myocardial motion pattern in patients suffering from pressure overload due to aortic stenosis. *Circulation.* **100**(4), pp.361-368.

Swoboda, P.P., Larghat, A., Zaman, A., Fairbairn, T.A., Motwani, M., Greenwood, J.P. and Plein, S. 2013. Reproducibility of myocardial strain and left ventricular twist measured using complementary spatial modulation of magnetization. *J Magn Reson Imaging.*

Tervaert, T.W., Mooyaart, A.L., Amann, K., Cohen, A.H., Cook, H.T., Drachenberg, C.B., Ferrario, F., Fogo, A.B., Haas, M., de Heer, E., Joh, K., Noel, L.H., Radhakrishnan, J., Seshan, S.V., Bajema, I.M., Bruijn, J.A. and Renal Pathology, S. 2010. Pathologic classification of diabetic nephropathy. *J Am Soc Nephrol.* **21**(4), pp.556-563.

Thygesen, K., Alpert, J.S., Jaffe, A.S., Simoons, M.L., Chaitman, B.R., White, H.D., Katus, H.A., Apple, F.S., Lindahl, B., Morrow, D.A., Clemmensen, P.M., Johanson, P., Hod, H., Underwood, R., Bax, J.J., Bonow, J.J., Pinto, F., Gibbons, R.J., Fox, K.A., Atar, D., Newby, L.K., Galvani, M., Hamm, C.W., Uretsky, B.F., Steg, P.G., Wijns, W., Bassand, J.P., Menasche, P., Ravkilde, J., Ohman, E.M., Antman, E.M., Wallentin, L.C., Armstrong, P.W., Januzzi, J.L., Nieminen, M.S., Gheorghiade, M., Filippatos, G., Luepker, R.V., Fortmann, S.P., Rosamond, W.D., Levy, D., Wood, D., Smith, S.C., Hu, D., Lopez-Sendon, J.L., Robertson, R.M., Weaver, D., Tendera, M., Bove, A.A., Parkhomenko, A.N., Vasilieva, E.J., Mendis, S., Baumgartner, H., Ceconi, C., Dean, V., Deaton, C., Fagard, R., Funck-Brentano, C., Hasdai, D., Hoes, A., Kirchhof, P., Knuuti, J., Kolh, P., McDonagh, T., Moulin, C., Popescu, B.A., Reiner, Z., Sechtem, U., Sirnes, P.A., Torbicki, A., Vahanian, A., Windecker, S., Morais, J., Aguiar, C., Almahmeed, W., Arnar, D.O., Barili, F., Bloch, K.D., Bolger, A.F., Botker, H.E., Bozkurt, B., Bugiardini, R., Cannon, C., de Lemos, J., Eberli, F.R., Escobar, E., Hlatky, M., James, S., Kern, K.B., Moliterno, D.J., Mueller, C., Neskovic, A.N., Pieske, B.M., Schulman, S.P., Storey, R.F., Taubert, K.A., Vranckx, P. and Wagner, D.R. 2012. Third universal definition of myocardial infarction. *J Am Coll Cardiol.* **60**(16), pp.1581-1598.

Todiere, G., Aquaro, G.D., Piaggi, P., Formisano, F., Barison, A., Masci, P.G., Strata, E., Bacigalupo, L., Marzilli, M., Pingitore, A. and Lombardi, M. 2012. Progression of myocardial fibrosis assessed with cardiac magnetic resonance in hypertrophic cardiomyopathy. *J Am Coll Cardiol.* **60**(10), pp.922-929.

Udelson, J.E., Beshansky, J.R., Ballin, D.S., Feldman, J.A., Griffith, J.L., Handler, J., Heller, G.V., Hendel, R.C., Pope, J.H., Ruthazer, R., Spiegler, E.J., Woolard, R.H. and Selker, H.P. 2002. Myocardial perfusion imaging for evaluation and triage of patients with suspected acute cardiac ischemia: a randomized controlled trial. *JAMA.* **288**(21), pp.2693-2700.

Ugander, M., Oki, A.J., Hsu, L.Y., Kellman, P., Greiser, A., Aletras, A.H., Sibley, C.T., Chen, M.Y., Bandettini, W.P. and Arai, A.E. 2012. Extracellular volume imaging by magnetic resonance imaging provides insights into overt and sub-clinical myocardial pathology. *Eur Heart J.* **33**(10), pp.1268-1278.

Unverferth, D.V., Magorien, R.D., Moeschberger, M.L., Baker, P.B., Fetters, J.K. and Leier, C.V. 1984. Factors influencing the one-year mortality of dilated cardiomyopathy. *Am J Cardiol.* **54**(1), pp.147-152.

Urbano-Moral, J.A., Rowin, E.J., Maron, M.S., Crean, A. and Pandian, N.G. 2014. Investigation of global and regional myocardial mechanics with 3-dimensional speckle tracking echocardiography and relations to hypertrophy and fibrosis in hypertrophic cardiomyopathy. *Circ Cardiovasc Imaging.* **7**(1), pp.11-19.

Utomi, V., Oxborough, D., Whyte, G.P., Somauroo, J., Sharma, S., Shave, R., Atkinson, G. and George, K. 2013. Systematic review and meta-analysis of training mode, imaging modality and body size influences on the morphology and function of the male athlete's heart. *Heart.* **99**(23), pp.1727-1733.

Utz, J.A., Herfkens, R.J., Heinsimer, J.A., Bashore, T., Califf, R., Glover, G., Pelc, N. and Shimakawa, A. 1987. Cine MR determination of left ventricular ejection fraction. *AJR Am J Roentgenol.* **148**(5), pp.839-843.

Valente, A.M., Lakdawala, N.K., Powell, A.J., Evans, S.P., Cirino, A.L., Orav, E.J., MacRae, C.A., Colan, S.D. and Ho, C.Y. 2013. Comparison of echocardiographic and cardiac magnetic resonance imaging in hypertrophic cardiomyopathy sarcomere mutation carriers without left ventricular hypertrophy. *Circ Cardiovasc Genet.* **6**(3), pp.230-237.

Valsangiacomo Buechel, E.R. and Mertens, L.L. 2012. Imaging the right heart: the use of integrated multimodality imaging. *Eur Heart J.* **33**(8), pp.949-960.

van Dalen, B.M., Kauer, F., Vletter, W.B., Soliman, O.I., van der Zwaan, H.B., Ten Cate, F.J. and Geleijnse, M.L. 2010. Influence of cardiac shape on left ventricular twist. *J Appl Physiol (1985).* **108**(1), pp.146-151.

van der Meer, R.W., Rijzewijk, L.J., de Jong, H.W., Lamb, H.J., Lubberink, M., Romijn, J.A., Bax, J.J., de Roos, A., Kamp, O., Paulus, W.J., Heine, R.J., Lammertsma, A.A., Smit, J.W. and Diamant, M. 2009. Pioglitazone improves cardiac function and alters myocardial substrate metabolism without affecting cardiac triglyceride accumulation and high-energy phosphate metabolism in patients with well-controlled type 2 diabetes mellitus. *Circulation.* **119**(15), pp.2069-2077.

van Heerebeek, L., Hamdani, N., Handoko, M.L., Falcao-Pires, I., Musters, R.J., Kupreishvili, K., Ijsselmuiden, A.J., Schalkwijk, C.G., Bronzwaer, J.G., Diamant, M., Borbely, A., van der Velden, J., Stienen, G.J., Laarman, G.J., Niessen, H.W. and Paulus, W.J. 2008. Diastolic stiffness of the failing diabetic heart: importance of fibrosis, advanced glycation end products, and myocyte resting tension. *Circulation.* **117**(1), pp.43-51.

Varnava, A.M., Elliott, P.M., Baboonian, C., Davison, F., Davies, M.J. and McKenna, W.J. 2001. Hypertrophic cardiomyopathy: histopathological features of sudden death in cardiac troponin T disease. *Circulation.* **104**(12), pp.1380-1384.

Varnava, A.M., Elliott, P.M., Sharma, S., McKenna, W.J. and Davies, M.J. 2000. Hypertrophic cardiomyopathy: the interrelation of disarray, fibrosis, and small vessel disease. *Heart.* **84**(5), pp.476-482.

Velagaleti, R.S., Gona, P., Chuang, M.L., Salton, C.J., Fox, C.S., Blease, S.J., Yeon, S.B., Manning, W.J. and O'Donnell, C.J. 2010. Relations of insulin resistance and glycemic abnormalities to cardiovascular magnetic resonance measures of cardiac structure and function: the Framingham Heart Study. *Circ Cardiovasc Imaging.* **3**(3), pp.257-263.

Verhaert, D., Thavendiranathan, P., Giri, S., Mihai, G., Rajagopalan, S., Simonetti, O.P. and Raman, S.V. 2011. Direct T2 quantification of myocardial edema in acute ischemic injury. *JACC Cardiovasc Imaging.* **4**(3), pp.269-278.

Vermes, E., Childs, H., Carbone, I., Barckow, P. and Friedrich, M.G. 2013. Auto-threshold quantification of late gadolinium enhancement in patients with acute heart disease. *J Magn Reson Imaging.* **37**(2), pp.382-390.

Vinereanu, D., Florescu, N., Sculthorpe, N., Tweddel, A.C., Stephens, M.R. and Fraser, A.G. 2001. Differentiation between pathologic and physiologic left ventricular hypertrophy by tissue Doppler assessment of long-axis function in patients with hypertrophic cardiomyopathy or systemic hypertension and in athletes. *Am J Cardiol.* **88**(1), pp.53-58.

Wackers, F.J., Young, L.H., Inzucchi, S.E., Chyun, D.A., Davey, J.A., Barrett, E.J., Taillefer, R., Wittlin, S.D., Heller, G.V., Filipchuk, N., Engel, S., Ratner, R.E., Iskandrian, A.E. and Detection of Ischemia in Asymptomatic Diabetics, I. 2004. Detection of silent myocardial ischemia in asymptomatic diabetic subjects: the DIAD study. *Diabetes Care.* **27**(8), pp.1954-1961.

Weiner, R.B., Hutter, A.M., Jr., Wang, F., Kim, J., Weyman, A.E., Wood, M.J., Picard, M.H. and Baggish, A.L. 2010. The impact of endurance exercise training on left ventricular torsion. *JACC Cardiovasc Imaging.* **3**(10), pp.1001-1009.

Wendt, T.M., Tanji, N., Guo, J., Kislinger, T.R., Qu, W., Lu, Y., Bucciarelli, L.G., Rong, L.L., Moser, B., Markowitz, G.S., Stein, G., Bierhaus, A., Liliensiek, B., Arnold, B., Nawroth, P.P., Stern, D.M., D'Agati, V.D. and Schmidt, A.M. 2003. RAGE drives the development of glomerulosclerosis and implicates podocyte activation in the pathogenesis of diabetic nephropathy. *Am J Pathol.* **162**(4), pp.1123-1137.

Whipp, B.J., Ward, S.A. and Wasserman, K. 1986. Respiratory markers of the anaerobic threshold. *Adv Cardiol.* **35**, pp.47-64.

White, S.K., Sado, D.M., Fontana, M., Banypersad, S.M., Maestrini, V., Flett, A.S., Piechnik, S.K., Robson, M.D., Hausenloy, D.J., Sheikh, A.M., Hawkins, P.N.

and Moon, J.C. 2013. T1 mapping for myocardial extracellular volume measurement by CMR: bolus only versus primed infusion technique. *JACC Cardiovasc Imaging.* **6**(9), pp.955-962.

Wilson, J.M.G. and Jungner, G. 1968. Principles and Practice of Screening for Disease. *Who Chronicle.* **22**(11), pp.473-&.

Wilson, M., O'Hanlon, R., Prasad, S., Deighan, A., Macmillan, P., Oxborough, D., Godfrey, R., Smith, G., Maceira, A., Sharma, S., George, K. and Whyte, G. 2011. Diverse patterns of myocardial fibrosis in lifelong, veteran endurance athletes. *J Appl Physiol (1985).* **110**(6), pp.1622-1626.

Wong, T.C., Piehler, K., Meier, C.G., Testa, S.M., Klock, A.M., Aneizi, A.A., Shakesprere, J., Kellman, P., Shroff, S.G., Schwartzman, D.S., Mulukutla, S.R., Simon, M.A. and Schelbert, E.B. 2012. Association between extracellular matrix expansion quantified by cardiovascular magnetic resonance and short-term mortality. *Circulation.* **126**(10), pp.1206-1216.

Wong, T.C., Piehler, K.M., Kang, I.A., Kadakkal, A., Kellman, P., Schwartzman, D.S., Mulukutla, S.R., Simon, M.A., Shroff, S.G., Kuller, L.H. and Schelbert, E.B. 2013. Myocardial extracellular volume fraction quantified by cardiovascular magnetic resonance is increased in diabetes and associated with mortality and incident heart failure admission. *Eur Heart J.*

Yancy, C.W., Jessup, M., Bozkurt, B., Butler, J., Casey, D.E., Jr., Drazner, M.H., Fonarow, G.C., Geraci, S.A., Horwich, T., Januzzi, J.L., Johnson, M.R., Kasper, E.K., Levy, W.C., Masoudi, F.A., McBride, P.E., McMurray, J.J., Mitchell, J.E., Peterson, P.N., Riegel, B., Sam, F., Stevenson, L.W., Tang, W.H., Tsai, E.J. and Wilkoff, B.L. 2013. 2013 ACCF/AHA Guideline for the Management of Heart Failure: A Report of the American College of Cardiology Foundation/American Heart Association Task Force on Practice Guidelines. *Circulation.*

Yokoyama, I., Ohtake, T., Momomura, S., Yonekura, K., Woo-Soo, S., Nishikawa, J., Sasaki, Y. and Omata, M. 1998. Hyperglycemia rather than insulin resistance is related to reduced coronary flow reserve in NIDDM. *Diabetes.* **47**(1), pp.119-124.

Young, A.A. and Cowan, B.R. 2012. Evaluation of left ventricular torsion by cardiovascular magnetic resonance. *J Cardiovasc Magn Reson.* **14**, p49.

Young, L.H., Wackers, F.J., Chyun, D.A., Davey, J.A., Barrett, E.J., Taillefer, R., Heller, G.V., Iskandrian, A.E., Wittlin, S.D., Filipchuk, N., Ratner, R.E., Inzucchi, S.E. and Investigators, D. 2009. Cardiac outcomes after screening for asymptomatic coronary artery disease in patients with type 2 diabetes: the DIAD study: a randomized controlled trial. *JAMA.* **301**(15), pp.1547-1555.

Zellweger, M.J., Dubois, E.A., Lai, S., Shaw, L.J., Amanullah, A.M., Lewin, H.C., Friedman, J.D., Kang, X., Germano, G. and Berman, D.S. 2002. Risk stratification in patients with remote prior myocardial infarction using rest-stress myocardial perfusion SPECT: prognostic value and impact on referral to early catheterization. *J Nucl Cardiol.* **9**(1), pp.23-32.

Zellweger, M.J., Hachamovitch, R., Kang, X., Hayes, S.W., Friedman, J.D., Germano, G., Pfisterer, M.E. and Berman, D.S. 2004. Prognostic relevance of symptoms versus objective evidence of coronary artery disease in diabetic patients. *Eur Heart J.* **25**(7), pp.543-550.

Zinman, B., Wanner, C., Lachin, J.M., Fitchett, D., Bluhmki, E., Hantel, S., Mattheus, M., Devins, T., Johansen, O.E., Woerle, H.J., Broedl, U.C., Inzucchi, S.E. and Investigators, E.-R.O. 2015. Empagliflozin, Cardiovascular Outcomes, and Mortality in Type 2 Diabetes. *N Engl J Med.*

9. Appendix

9.1 Ethical approval for studies 1, 2 and 3

NHS
Health Research Authority

NRES Committee Yorkshire & The Humber - Leeds West

Room 002, Jarrow Business Centre
Rolling Mill Road
Jarrow
Tyne and Wear
NE32 3DT

Telephone: 0191 428 3387

30 May 2014

Prof Sven Plein
Consultant Cardiologist, British Heart Foundation Senior Clinical Research Fellow
University of Leeds
Department of Cardiology
Sunshine Corridor
Leeds General Infirmary
LS1 3EX

Dear Prof Plein

Study title:	**The Athletes Heart Study: Multi-modality assessment of athletic cardiac adaptation**
REC reference:	**14/YH/0126**
IRAS project ID:	**151213**

Thank you for your email of 30 May 2014, responding to the Committee's request for further information on the above research and submitting revised documentation.

The further information has been considered on behalf of the Committee by the Chair.

We plan to publish your research summary wording for the above study on the HRA website, together with your contact details. Publication will be no earlier than three months from the date of this opinion letter. Should you wish to provide a substitute contact point, require further information, or wish to make a request to postpone publication, please contact the REC Manager, Miss Sarah Grimshaw, nrescommittee.yorkandhumber-leedswest@nhs.net.

Confirmation of ethical opinion

On behalf of the Committee, I am pleased to confirm a favourable ethical opinion for the above research on the basis described in the application form, protocol and supporting documentation as revised, subject to the conditions specified below.

Conditions of the favourable opinion

The favourable opinion is subject to the following conditions being met prior to the start of the study.

Management permission or approval must be obtained from each host organisation prior to the start of the study at the site concerned.

Management permission ("R&D approval") should be sought from all NHS organisations involved in the study in accordance with NHS research governance arrangements.

Guidance on applying for NHS permission for research is available in the Integrated Research

Application System or at http://www.rdforum.nhs.uk.

Where a NHS organisation's role in the study is limited to identifying and referring potential participants to research sites ("participant identification centre"), guidance should be sought from the R&D office on the information it requires to give permission for this activity.

For non-NHS sites, site management permission should be obtained in accordance with the procedures of the relevant host organisation.

Sponsors are not required to notify the Committee of approvals from host organisations

Registration of Clinical Trials

All clinical trials (defined as the first four categories on the IRAS filter page) must be registered on a publicly accessible database within 6 weeks of recruitment of the first participant (for medical device studies, within the timeline determined by the current registration and publication trees).

There is no requirement to separately notify the REC but you should do so at the earliest opportunity e.g. when submitting an amendment. We will audit the registration details as part of the annual progress reporting process.

To ensure transparency in research, we strongly recommend that all research is registered but for non-clinical trials this is not currently mandatory.

If a sponsor wishes to contest the need for registration they should contact Catherine Blewett (catherineblewett@nhs.net), the HRA does not, however, expect exceptions to be made. Guidance on where to register is provided within IRAS.

It is the responsibility of the sponsor to ensure that all the conditions are complied with before the start of the study or its initiation at a particular site (as applicable).

Ethical review of research sites

NHS sites

The favourable opinion applies to all NHS sites taking part in the study, subject to management permission being obtained from the NHS/HSC R&D office prior to the start of the study (see "Conditions of the favourable opinion" below).

Approved documents

The final list of documents reviewed and approved by the Committee is as follows:

Document	Version	Date
Evidence of Sponsor insurance or indemnity (non NHS Sponsors only)	Henderson Insurance Brokers	18 September 2013
GP/consultant information sheets or letters	1.0	25 February 2014
Letters of invitation to participant	v1.0	30 May 2014
Other [Email Confirming Database Registration]	Peter Swoboda	30 May 2014
Participant consent form	1.0	28 February 2014
Participant information sheet (PIS)	v1.1	30 May 2014
REC Application Form	IRAS Version 3.5, 151213/597221/1/872	
Research protocol or project proposal	1.0	28 February 2014
Summary CV for Chief Investigator (CI)	Sven Plein	

Statement of compliance

The Committee is constituted in accordance with the Governance Arrangements for Research Ethics Committees and complies fully with the Standard Operating Procedures for Research Ethics Committees in the UK.

After ethical review

<u>Reporting requirements</u>

The attached document *"After ethical review – guidance for researchers"* gives detailed guidance on reporting requirements for studies with a favourable opinion, including:

- Notifying substantial amendments
- Adding new sites and investigators
- Notification of serious breaches of the protocol
- Progress and safety reports
- Notifying the end of the study

The HRA website also provides guidance on these topics, which is updated in the light of changes in reporting requirements or procedures.

<u>Feedback</u>

You are invited to give your view of the service that you have received from the National Research Ethics Service and the application procedure. If you wish to make your views known please use the feedback form available on the HRA website: http://www.hra.nhs.uk/about-the-hra/governance/quality-assurance/

We are pleased to welcome researchers and R & D staff at our NRES committee members' training days – see details at http://www.hra.nhs.uk/hra-training/

14/YH/0126	Please quote this number on all correspondence

With the Committee's best wishes for the success of this project.

Yours sincerely

S. Grimshaw

pp
Dr Rhona Bratt
Chair

Email: nrescommittee.yorkandhumber-leedswest@nhs.net

Enclosures: "After ethical review – guidance for researchers" *SL-AR2*

Copy to: *Dr Peter Swoboda, University of Leeds*
Mrs Anne Gowing, Leeds Teaching Hospitals NHS Trust
Ms Clare Skinner, University of Leeds

9.2 Ethical approval for studies 4 and 5

NHS
Health Research Authority

NRES Committee Yorkshire & The Humber - Leeds East

North East REC Centre
Room 002
TEDCO Business Centre
Viking Industrial Park
Rolling Mill Road
Jarrow
NE32 3DT

Telephone: 0191 4283545

16 April 2013

Dr Peter Swoboda
BHF Clinical Research Fellow in Cardiac MRI
B Floor, Clarendon Wing
Leeds General Infirmary
Leeds
LS1 3EX

Dear Dr Swoboda

Study title:	**Mechanisms and Reversibility of Heart Failure associated with Diabetes: A Cardiac Magnetic Resonance Study**
REC reference:	**13/YH/0098**
IRAS project ID:	**112396**

Thank you for your letter of 15th April 2013 responding to the Committee's request for further information on the above research and submitting revised documentation.

The further information has been considered on behalf of the Committee by the Chair.

We plan to publish your research summary wording for the above study on the NRES website, together with your contact details, unless you expressly withhold permission to do so. Publication will be no earlier than three months from the date of this favourable opinion letter. Should you wish to provide a substitute contact point, require further information, or wish to withhold permission to publish, please contact the Co-ordinator Hayley Jeffries, hayley.jeffries@nhs.net.

Confirmation of ethical opinion

On behalf of the Committee, I am pleased to confirm a favourable ethical opinion for the above research on the basis described in the application form, protocol and supporting documentation as revised, subject to the conditions specified below.

A Research Ethics Committee established by the Health Research Authority

Ethical review of research sites

NHS sites

The favourable opinion applies to all NHS sites taking part in the study, subject to management permission being obtained from the NHS/HSC R&D office prior to the start of the study (see "Conditions of the favourable opinion" below).

Approved documents

The final list of documents reviewed and approved by the Committee is as follows:

Document	Version	Date
Covering Letter		15 April 2013
Evidence of insurance or indemnity		21 September 2012
GP/Consultant Information Sheets	1.2	13 February 2013
Investigator CV	CI CV	13 February 2013
Investigator CV	Dr Greenwood & Prof Plein	11 March 2013
Letter of invitation to participant	1.2	13 March 2013
Other: Letter from funder		29 October 2012
Participant Consent Form	1.0 Dec 2012	
Participant Information Sheet	1.3, April 2013	
Protocol	1.2	13 February 2013
REC application	1.0	12 March 2013
Referees or other scientific critique report		29 October 2012
Response to Request for Further Information		

Statement of compliance

The Committee is constituted in accordance with the Governance Arrangements for Research Ethics Committees and complies fully with the Standard Operating Procedures for Research Ethics Committees in the UK.

After ethical review

Reporting requirements

The attached document *"After ethical review – guidance for researchers"* gives detailed guidance on reporting requirements for studies with a favourable opinion, including:

- Notifying substantial amendments
- Adding new sites and investigators
- Notification of serious breaches of the protocol
- Progress and safety reports
- Notifying the end of the study

A Research Ethics Committee established by the Health Research Authority

The NRES website also provides guidance on these topics, which is updated in the light of changes in reporting requirements or procedures.

<u>Feedback</u>

You are invited to give your view of the service that you have received from the National Research Ethics Service and the application procedure. If you wish to make your views known please use the feedback form available on the website.

Further information is available at National Research Ethics Service website > After Review

13/YH/0098	**Please quote this number on all correspondence**

We are pleased to welcome researchers and R & D staff at our NRES committee members' training days – see details at http://www.hra.nhs.uk/hra-training/

With the Committee's best wishes for the success of this project.

Yours sincerely

pp   H Jp

Dr C E Chu
Chair

Email:hayley.jeffries@nhs.net

Enclosures: "After ethical review – guidance for researchers" *[SL-AR2]*

Copy to: Mrs Anne Gowing, Leeds Teaching Hospitals NHS Trust